Optimized Production and Purification of LCC DNA Minivectors for Applications in Gene Therapy and Vaccine Development

by

Chi Hong Sum

A thesis
presented to the University of Waterloo
in fulfillment of the
thesis requirement for the degree of
Master of Science
in
Pharmacy

Waterloo, Ontario, Canada, 2014

AUTHOR'S DECLARATION

I hereby declare that I am the sole author of this thesis. This is a true copy of the thesis, including any required final revisions, as accepted by my examiners.

I understand that my thesis may be made electronically available to the public.

Abstract

Linear covalently closed (LCC) DNA minivectors serve to be superior to conventional circular covalently closed (CCC) plasmid DNA (pDNA) vectors due to enhancements to both transfection efficiency and safety. Specifically, LCC DNA minivectors have a heightened safety profile as insertional mutagenesis is inhibited by covalently closed terminal ends conferring double-strand breaks that cause chromosomal disruption and cell death in the low frequency event of chromosomal integration. The development of a one-step, *E. coli* based *in vivo* LCC DNA minivector production system enables facile and efficient production of LCC DNA minivectors referred to as DNA ministrings. This novel *in vivo* system demonstrates high versatility, generating DNA ministrings catered to numerous potential applications in gene therapy and vaccine development.

In the present study, numerous aspects pertaining to the generation of gene therapeutics with LCC DNA ministrings have been explored with relevance to both industry and clinical settings. Through systematic assessment of induction duration, cultivation strategy, and genetic/chemical modifications, the novel *in vivo* system was optimized to produce high yields of DNA ministrings at ~90% production efficiency. Purification of LCC DNA ministrings using anion exchange membrane chromatography demonstrated rapid, scalable purification of DNA vectors as well as its potential in the separation of different DNA isoforms. The application of a hydrogel-based strong Q-anion exchange membrane, with manipulations to salt gradient, constituted effective separation of parental supercoiled CCC precursor pDNA and LCC DNA. The resulting DNA ministrings were employed for the generation of 16-3-16 gemini surfactant based synthetic vectors and comparative analysis,

through physical characterization and *in vitro* transfection assays, was conducted between DNA ministring derived and CCC pDNA derived lipoplexes. Differences in DNA topology were observed to induce differences in particle size and DNA protection/encapsulation upon lipoplex formation. Lastly, the *in vivo* DNA minivector production system successfully generated *gagV3*(BCE) LCC DNA ministrings for downstream development of a HIV DNA-VLP (Virus-like particle) vaccine, thus highlighting the capacity of such system to produce DNA ministrings with numerous potential applications.

Acknowledgements

I would like to first and foremost express my deepest gratitude and appreciation to Dr. Roderick Slavcev and Dr. Shawn Wettig for their continuing support and guidance that has gotten me through all the highs and lows I encountered during my graduate studies. I would not be here without their expertise and creative input which continues to fuel my curiosity and drive as a student and as an aspiring scientist. It has been an amazing experience and an honour to have such supervisors/mentors that I can rely on for advice and support now and, hopefully, in the future to come.

I would like to thank my committee members: Dr. Bernard Duncker and Dr. Mike Beazely for all their input into my research. As well, I would like to take the opportunity to thank Dr. Jonathan Blay for making graduate studies at the school of pharmacy a welcoming environment that all of us can enjoy.

Being co-supervised has enriched my experience as I had the opportunity to work with many of my fellow colleagues in both the Slavcev (Nafiseh, Farah, Jessica, Heba, Shirley, Judy, Peter, & Teresa) and Wettig (Lizzie, Amany, Festo, Sam, Aula, Mehrnoosh, Osama, Shahid, Taksim, Jason, & Shanon) group. I would like to specifically thank Judy and Jane for all their tremendous help with my project. Special shout-out to Tarek, Wes, Gary, Anil, Rabiya, Roger, Samih, Eric, Leonard, Sarah, and Haley for making school fun and for making those long hours in the lab a lot more bearable.

I am grateful for the continuing support from my parents and my family. Their love throughout all these years has gotten me through numerous tough and stressful times. I would not be here without them.

Lastly, I am grateful that my journey through grad school has led me to Judy who has been there for me through all the good times and the tough times in the lab and at home. She has been there supporting and encouraging me to read when I could no longer read, to work harder when I feel lazy, and to eat when I can no longer eat (chicken wings …. mMmmmm). My journey would not be complete without her. Thank you!!

Dedication

To Judy, my parents, my family and of course….. to science!

To Science!!!!

Table of Contents

AUTHOR'S DECLARATION ii
Abstract iii
Acknowledgements v
Dedication vii
Table of Contents viii
List of Figures xii
List of Tables xiv
List of Abbreviations xv
Chapter 1 General Introduction 1
1.1 Introduction to Gene Therapy 1
1.1.1 Current Advances in Gene Therapy 1
1.1.2 Safety Limitations of GT Viral Vectors 2
1.2 Non-Viral Gene Delivery 4
1.2.1 Barriers of Gene Delivery 4
1.3 Non-Viral Delivery Systems 7
1.3.1 Naked pDNA Vectors 7
1.3.2 Physical Delivery Systems: Microinjection, Gene Gun, Electroporation 8
1.3.3 Emerging Delivery Systems: Sonoporation, Optical Transfection, Magnetofection 8
1.3.4 Chemical Delivery Systems: Synthetic Vectors 11
1.3.4.1 Polymer-based Vectors 12
1.3.4.1.1 Poly-L-Lysine (PLL) 14
1.3.4.1.2 Polyethylenimine (PEI) 14
1.3.4.1.3 Chitosan 16
1.3.4.1.4 Poly(amidoamine) (PAMAM) Dendrimers 17
1.3.4.2 Cationic Peptide Vectors 17
1.3.4.3 Cationic Lipids 19
1.3.4.3.1 Lipoplex Formation, Packing Structures and Influences of Helper Lipids 22
1.3.4.3.2 Overcoming barriers with cationic lipid based synthetic vectors. 26
1.3.4.4 Gemini Surfactants 32

1.3.4.4.1 Lipoplex formation and gene transfection using m-s-m gemini surfactants 34
1.4 Recombinant Plasmid DNA (pDNA) Vectors 38
1.4.1 Novel DNA Vectors: DNA Minicircles and LCC DNA Minivectors 41
1.4.1.1 DNA Minicircles 42
1.4.1.2 LCC DNA Minivectors 44
1.4.1.3 Impact of Vector Size and Topology on Gene Delivery 47
1.5 One-Step *in vivo* Linear Covalently Closed (LCC) DNA Minivector Production System 49
1.5.1 Incorporation of Multiple DNA-targeting sequences (DTS) for Improved Nuclear Entry . 52
1.5.2 DNA Ministrings: A DNA Vector with a Heightened Safety Profile 52
1.6 Summary & Thesis Objectives 54
1.6.1 Objectives 55
Chapter 2 Optimization of a One-Step Heat Inducible *in vivo* LCC DNA Minivector Production System 57
2.1 Introduction 57
2.2 Materials and Methods 64
2.2.1 Strains and Plasmids 64
2.2.2 Assessing Effects of Volume and Culturing Conditions on DNA Ministring Production .. 64
2.2.3 Assessing the Introduction of Protease-specific and Associated Gene Deletions to Enhance LCC DNA Processing 66
2.2.4 Assessing Effects of Ciprofloxacin on Plasmid Replication and DNA Ministring Production 67
2.2.5 Assessing the Introduction of DnaB Helicase Mutations on DNA Ministring Production . 68
2.2.6 Statistical Analysis 69
2.3 Results 71
2.3.1 Comparative Analysis of DNA Ministring Production between Tel and TelN 71
2.3.2 A Two Stage Continuous Cultivation Improved LCC DNA Ministring Production Efficiency and Scalability 72
2.3.3 LCC DNA Ministring Production was Enhanced in a Δ*hflX* Host Mutation Background . 75
2.3.4 Ciprofloxacin Enhanced DNA Ministring Production 78
2.3.5 Effects of DnaB Helicase Mutations on DNA Ministring Production 80
2.4 Discussion 84
2.5 Conclusion 92

Chapter 3 Separation and Purification of Linear Covalently Closed (LCC) DNA by Q-Anion Exchange Membrane Chromatography 93
3.1 Introduction 93
3.2 Material and Methods 97
3.2.1 Production of LCC DNA products 97
3.2.2 DNA Separation by Anion Exchange Membrane Chromatography 97
3.2.2.1 Buffers 97
3.2.2.2 Membrane material, pre-treatment, loading, and elution 97
3.2.3 DNA Analysis 98
3.3 Results and Discussion 99
3.4 Conclusions 106
Chapter 4 Transfection and Physical Characterization of DNA/16-3-16/DOPE Gemini Surfactant Based Vectors for the Delivery of LCC DNA Ministrings 107
4.1 Introduction 107
4.2 Materials and Methods 109
4.2.1 Production of CCC pDNA, LCC DNA products, and LCC DNA ministrings 109
4.2.2 Generation of CCC/16-3-16/DOPE and LCC/16-3-16/DOPE Transfection Lipoplexes. . 110
4.2.3 Characterization of 16-3-16 Gemini Based Lipoplexes 111
4.2.3.1 Particle Size and Zeta Potential 111
4.2.3.2 DNase Sensitivity Assay 111
4.2.3.3 Transfection of OVCAR-3 Cells 112
4.3 Results 113
4.3.1 Particle Size and Zeta Potential (ζ) 113
4.3.2 DNase Sensitivity 116
4.3.3 Preliminary Investigation of the Transfection Efficiency of pNN9 (CCC) and DNA ministring (LCC) Derived Lipoplexes 118
4.4 Discussion 120
4.5 Conclusion 123
Chapter 5 Application of DNA Ministrings to the Development of an HIV DNA VLP Vaccine 124
5.1 Introduction 124
5.2 Materials and Methods 132
5.2.1 Construction of pGagV3(BCE) Vector 132

5.2.2 Production of *gagV3(BCE)* LCC DNA Ministrings 133
5.2.3 Transfection of K562 Cells 133
5.3 Results 135
5.3.1 Production of *gagV3(BCE)* LCC DNA Ministrings 135
5.3.2 Preliminary Investigation into Optimal K562 Transfections with Lipofectamine 136
5.4 Discussion 138
5.5 Conclusion 144
Chapter 6 Summary 146
6.1 Summary 146
6.2 Future Directions 148
6.2.1 Further Optimization of LCC DNA Minivector Production System for Complete pDNA Processing 148
6.2.2 Targeted Delivery into K562-αvβ3 with RGD-Functionalized Synthetic Vectors 148
6.2.3 Targeted Delivery into Dendritic Cells and VLP Formation 149
Bibliography 150

List of Figures

Figure 1.1 Extracellular and intracellular barriers to gene delivery 6
Figure 1.2 Structures of commonly used polymers in synthetic vectors for gene delivery. 13
Figure 1.3 Structures of commonly used cationic lipids in synthetic vectors for gene delivery. 21
Figure 1.4 Lipoplex phase structures 24
Figure 1.5 Packing parameter and expected aggregate structures. 24
Figure 1.6 Neutral lipids in lipoplex formation. 26
Figure 1.7 Endocytic pathways in the cellular uptake of lipoplexes 28
Figure 1.8 Mechanisms of endosomal escape in lamellar lipoplexes 29
Figure 1.9 Mechanism of endosomal escape in fusogenic, DOPE containing lipoplexes 31
Figure 1.10 Structural schematic of conventional (A) and gemini (B) surfactants. 33
Figure 1.11 Chemical Structure of m-s-m gemini surfactants. 36
Figure 1.12 Recombinant plasmid DNA (pDNA) vectors. 38
Figure 1.13 Schematic of plasmid DNA (pDNA) vectors, DNA minicircles, and Linear Covalently Closed (LCC) DNA minivectors. 41
Figure 1.14 *In vitro* production of LCC DNA minivectors. 44
Figure 1.15 Schematic of the one-step *in vivo* LCC DNA minivector production system 50
Figure 1.16 Parental pDNA vector substrate (pNN9) for the production of LCC DNA ministrings 51
Figure 1.17 Flow chart of progression from production and purification to application of LCC DNA ministrings. 56
Figure 2.1 LCC DNA ministring production using the one-step *in vivo* LCC DNA minivector production system 58
Figure 2.2 Protease mutants cannot generate DNA ministrings in absence of *tel/telN* expression 68
Figure 2.3 Comparative analysis of TelN and Tel protelomerase-mediated processing 72
Figure 2.4 Effects of culturing technique and volume on DNA ministring production 73
Figure 2.5 Gel analysis of LCC DNA ministring production between batch and two stage continuous cultivations 74
Figure 2.6 Effects of protease-specific and associated deletions on Tel-mediated DNA ministring production 76
Figure 2.7 Effects of protease-specific and associated deletions on TelN-mediated DNA ministring production 77

Figure 2.8 LCC DNA ministring production efficiency upon the introduction of ciprofloxacin at various concentrations 79
Figure 2.9 LCC DNA ministring production after the introduction of ciprofloxacin 80
Figure 2.10 Tel and TelN-mediated DNA ministring production efficiency in *dnaB*[Ts] mutants 82
Figure 2.11 LCC DNA ministring production in *dnaB*[Ts] mutants 83
Figure 3.1 Separation of DNA isoforms by anion exchange membrane chromatography 102
Figure 3.2 Analysis of LCC pDNA species in late elutions from anion exchange membrane chromatography 103
Figure 4.1 Particle size variations for DNA/16-3-16/DOPE lipoplexes with increasing N^+/P^- charge ratios 116
Figure 4.2 DNase sensitivity assay for DNA/16-3-16 and DNA/16-3-16/DOPE lipoplexes 117
Figure 4.3 DNase sensitivity assay for A) CCC/16-3-16/DOPE lipoplexes and B) LCC/16-3-16/DOPE lipoplexes 118
Figure 4.4 Preliminary analysis of transfection efficiencies for CCC/16-3-16/DOPE and LCC/16-3-16/DOPE lipoplexes in OVCAR-3 cells. 119
Figure 5.1 Schematic of pGagV3(BCE) Vector 132
Figure 5.2 Tel-mediated processing of precursor plasmids into *egfp* and *gagV3(BCE)* LCC DNA ministrings 136
Figure 5.3 Preliminary analysis of transfection efficiencies attained from variations to cell seeding and post transfection incubation using Lipofectamine 137
Figure 5.4 Preliminary analysis of transfection efficiencies using DNA/16-3-16/DOPE lipoplexes. 139
Figure 5.5 Schematic for targeted delivery of *gagV3*(BCE) DNA ministring into dendritic cells 144

List of Tables

Table 1-1 Integrase involved in DNA minicircle production. 43
Table 2-1 Strains used in this study. 70
Table 4-1 Particle size & zeta potential of CCC pNN9, LCC DNA ministring, 16-3-16, and DOPE. 114
Table 4-2 Particle size and zeta potential of DNA/16-3-16 and DNA/16-3-16/DOPE lipoplexes. ... 115

List of Abbreviations

Δ*clpP*	ClpP protease *E. coli* K-12 single-gene knockout
Δ*lon*	Lon protease *E. coli* K-12 single-gene knockout
Δ*hflx*	HflX *E. coli* K-12 single-gene knockout
Δ*hflk*	HflK *E. coli* K-12 single-gene knockout
λ	Lambda bacteriophage
σ^{32}	Heat shock sigma factor
σ^{38}	Stationary phase sigma factor
ζ	Zeta potential
° C	Degrees Celsius
A_{600}	Absorbance at 600 nm
a.a.	Amino acid
AAA+	**A**TPase-**A**ssociated with diverse cellular **A**ctivities
Ad5	Adenovirus serotype 5
ADCC	Antibody-dependent cell-mediated cytotoxicity
ADCVI	Antibody-dependent cell-mediated virus inhibition
AEC	Anion exchange chromatography
AGE	Agarose gel electrophoresis
AIDS	Acquired immunodeficiency syndrome
Ap	Ampicillin antibiotic
APC	Antigen presenting cells
ATP	Adenosine triphosphate
bp	base pair
CCC	Circular covalently closed
CD	Cluster of differentiation
Cm	Chloramphenicol antibiotic
CMC	Critical micelle concentration
CMV	Cytomegalovirus

CpG	Unmethylated CpG dinucleotides
CPP	Cell penetrating peptide
ctDNA	Calf thymus DNA
CTL	Cytotoxic T lymphocyte
DC-Chol	3β-[N-(N',N'-dimethylaminoethyl) carbamoyl] cholesterol
DC_SIGN	Dendritic cell specific intercellular adhesion molecule-3-grabbing non-integrin
DNA	Deoxyribonucleic acid
dnaB8	DnaB helicase temperature sensitive fast stop mutation
dnaB252	DnaB helicase temperature sensitive slow stop mutation
DOGS	Di-octadecyl-amido-glycyl-spermine
DOPE	1,2-dioleoyl-sn-glycero-3-phosphatidylethanolamine
DOSPA	2,3-dioleyloxy-N-[2(sperminecarboxamido)ethyl]-N,N-dimethyl-1-propanaminium trifluoroacetate
DOSPER	1,3-dioleoyloxy-2-(6-carboxyspermyl)-propylamide)
DOTAP	N-[1-(2,3-dioleoyloxy)propyl]-N,N,N-trimethylammonium methyl sulfate
DOTMA	N-[1-(2,3-dioleyloxy)propyl]-N,N,N-trimethylammonium chloride
DTS	DNA nuclear targeting sequences
E. coli	*Escherichia coli*
EGFP	Enhanced green fluorescent protein
EGTA	Ethylene glycol tetraacetic acid
EU	Endotoxin unit
FACS	Fluorescence activated cell sorting
FBS	Fetal bovine serum
G418	Geneticin
gp	Glycoprotein
GT	Gene therapy
GTP	Guanosine triphosphate

H_I	Hexagonal phase structure
H^C_{II}	Inverted hexagonal phase structure
HAART	Highly active antiretroviral therapy
HIC	Hydrophobic interaction chromatography
HIV	Human immunodeficiency virus
HSPs	Heat shock proteins
HSPGs	Heparin sulfate proteoglycans
HSR	Heat shock response
IFN-γ	Interferon-γ
IL12	Interleukin 12
IL2RG	Interleukin 2 receptor-γ
IMDM	Iscove's Modified Dulbecco's Medium
IPTG	Isopropyl β-D-1-thiogalactopyranoside
K562	Immortalized myelogenous leukemia cell line
L^C_α	Lamellar phase structure
LCC	Linear covalently closed
LISW	Laser induced stress waves
Kan	Kanamycin antibiotic
kb	kilobase
kDa	kilodalton
LB	Luria-Bertani
LMO2	LIM domain only 2
LO	Linear open DNA
MDDC	Myeloid derived dendritic cell
MHC	Major histocompatibility complex
MIDGE	Minimalistic immunogenic defined gene expression
MiLV	Micro-linear vector
miRNA	Micro RNA
MPG	An amphipathic peptide (CPP)

mRNA	Messenger RNA
m-s-m	N,N-bis(dimethylalkyl)-α,ω-alkanediammonium surfactants
MTOC	Microtubule organizing centre
N^+/P^-	Nitrogen to phosphate charge ratio
Nd:YAG	Neodymium-doped yttrium aluminum garnet ($Nd:Y_3Al_5O_{12}$)
NFκB	Nuclear factor kappa-light-chain-enhancer of activated B cells
NK	Natural killer cells
NLS	Nuclear localization signal
NPC	Nuclear pore complex
OC	Open circular DNA
oriC	*E. coli* origin of replication
OTC	Ornithine transcarbamylase
OVCAR-3	Ovarian cancer cell line
P	Packing parameter
P1	P1 temperate bacteriophage
pal	Tel protelomerase recognition site
PAMAM	Poly(amidoamine)
PAMPs	Pathogen associated molecular patterns
PBS	Phosphate buffer saline
PCR	Polymerase chain reaction
PDI	Polydispersity index
pDNA	Plasmid DNA
PEG	Polyethylene glycol
PEI	Polyethylenimine
pL/pR	Lambda bacteriophage leftward/rightward promoters
PLL	Poly-L-lysine
RBPS	Recombination based plasmid separation
R cells	TelN and Tel recombinase expressing cells
rAd	Recombinant adenoviral vector

RGD	Arg-Gly-Asp
rRNA	Ribosomal RNA
RNA	Ribonucleic acid
RPM	Rounds per minute
SCID-XI	X-linked severe combined immunodeficiency
SEC	Size exclusion chromatography
siRNA	Small interfering RNA
SPIONs	Superparamagnetic iron oxide nanoparticles
ssRNA	Single strand RNA
SV40	Simian virus 40
TAT	Trans-activating transcriptional activator
TCA	Tricarboxylic acid
Tel	Bacteriophage PY54 derived protelomerase
TelN	Bacteriophage N15 derived protelomerase
telRL	TelN protelomerase recognition site
TLR	Toll-like receptors
TN	Tris-HCl/NaCl
tos	Telomere occupancy site
Ts	Temperature sensitive
VLP	Virus-like particle
W2NN	$TelN^+$ wild type cells
W3NN	Tel^+ wild type cells

Chapter 1
General Introduction

1.1 Introduction to Gene Therapy

Gene therapy (GT) involves the administration of nucleic acids for the purpose of treating diseases associated with the absence, abnormal expression, or overexpression of specific genes or genetic elements. Such therapies often entail the delivery of specific gene expression cassettes catered to the expression of a deficient protein product. Delivery of such expression cassettes can be achieved through recombinant viruses, referred to as viral vectors, or through non viral means using bacteria derived recombinant plasmid DNA (pDNA) vectors [1].

1.1.1 Current Advances in Gene Therapy

Globally, there are over 1,800 approved GT clinical trials with viral vectors accounting approximately two-thirds of all trials [2]. Adenoviral vectors are the most commonly used viral vector due mainly to their high transfection efficiency, high expression, and infection of non-dividing cells [2]; each of which are features commonly shared amongst many different viral vectors. The prominence of such vectors is exemplified by the Chinese approval of *Gendicine* (SiBiono GeneTech Co.), a non-replicative recombinant adenoviral vector (rAd-p53) for the treatment of head and neck squamous cell carcinoma, and *Onocorine* (Sunway Biotech Co. Ltd), a conditionally replicative recombinant adenoviral vector for the treatment of late stage refractory nasopharyngeal cancer, in 2003 and 2005 respectively [3]. In 2008, *Cerepro* (Ark Therapeutics Group plc) became the first and only adenoviral vector to have

completed a phase III clinical trial [3]. More recently, *Glybera* (UniQure), an adeno-associated viral vector delivering human lipoprotein lipase gene in muscle tissue for the treatment of lipoprotein lipase deficiency, received approval in 2012 as the first gene therapeutic from the European Commission [3-5]. The successful development of such therapeutics highlights the effectiveness of viral vectors for gene delivery and the potential of gene therapy in the treatment of many different diseases.

1.1.2 Safety Limitations of GT Viral Vectors

Despite the high usage of viral vectors to gene delivery application, the employment of viral vectors poses important safety concerns due to potential induction of undesired immunostimulatory responses and/or insertional mutagenesis. Among the five main classes of viral vectors (oncoretroviruses, lentiviruses, adeno-associated viruses, adenoviruses, and herpes simplex viruses), adenoviral vectors are considered the most immunogenic as they may induce cytotoxic T-lymphocyte (CTL), neutralizing antibody, and cytokine-mediated inflammatory responses [6]. Inflammatory responses imparted by the adenoviral capsid have been shown to linearly correlate with increasing vector dose and a "threshold effect", whereby limited symptoms are observed before severe cellular damage occurs at dosages above the threshold; this effect has also been implicated in dose-escalation studies [6]. In conjunction with the promiscuity of viral vectors, the systemic delivery of these vectors may also lead to severe complications from inflammatory responses. Such complications are represented by the tragic death of Jesse Gelsinger, a patient in phase I gene therapy clinical trial for an adenoviral vector based therapeutic treating ornithine transcarbamylase (OTC) deficiency [6-8]. OTC is a metabolic enzyme required for the breakdown of ammonia and

intermediate phenotypes have been observed in males with genetic mutations contributing to partially defective enzyme. The genetic nature of the disease prompted a GT approach and the use of adenoviral vectors as a viable option. However, intra-hepatic administration of the vectors led to systemic inflammation, multi-organ failure, and the eventual death of the subject. Autopsy reports later attributed vector induced activation of innate immunity as the main cause of death [8].

Safety concerns associated with insertional mutagenesis have also been documented in an *ex vivo* GT strategy to treat X-linked severe combined immunodeficiency (SCID-XI) using a γ-retroviral vector [2, 7, 9]. SCID-XI is caused by genetic mutations in the gene encoding interleukin 2 receptor-γ (*IL2RG)* leading to the faulty development of T cells and natural killer (NK) cells and subsequent complications from infections due to a lack of lymphocytes in the blood. From 1999 to 2009, a total of 20 patients suffering from SCID-XI were treated with a γ-retroviral vector to correct the genetic defect, achieving an impressive 85% success rate. However, a quarter of these patients were later found to have developed T-cell leukemia, with one patient succumbing to the cancer [9]. Development of T cell leukemia was attributed to the uncontrolled proliferation of T-cells due to vector integration near the *LMO2* proto-oncogene promoter and subsequent deregulated expression of oncogenes [2]. In conjunction with the enhancer activity of the viral long terminal repeats, the vector was identified to integrate in a semi random manner, targeting promoter and gene regions of actively transcribed genes at higher frequencies [9]. Similarly, the development of acute T cell leukemia was also found in a patient enrolled in a GT clinical trial for treating Wiscott-Aldrich syndrome using a γ-retroviral vector possessing viral long terminal repeats [2].

1.2 Non-Viral Gene Delivery

Aside from serious safety concerns, the application of viral vectors is hindered by limited repeat administrations due to pre-existing immunity, size of delivered gene construct, scale-up, as well as high production costs, contamination during production, and lack of desired tissue selectivity [6, 10-12]. Such drawbacks continue to drive the exploration of non-viral means of gene delivery. Non-viral delivery systems are generally advantageous over viral vector systems with respect to: 1) safety (immunocompatibility); 2) production costs; 3) scalability; 4) the ability to transfect larger sized pDNA; and 5) adaptability for different delivery options (e.g. targeted delivery, time-dependent release, enhanced circulation times, repeat administrations) [10, 11, 13-15]. However, while preferential from a safety perspective, non-viral delivery systems generally suffer from low transfection efficiencies [16], an important obstacle that must be addressed in order for such systems to be recognized as effective vehicles for gene delivery.

1.2.1 Barriers of Gene Delivery

The low transfection efficiencies associated with non-viral delivery systems are directly attributed to the various barriers encountered during the process of gene delivery (Figure 1.1). There are numerous extracellular barriers that must be bypassed prior to reaching the target tissue/cells. Unprotected pDNA vectors are rapidly degraded by nucleases upon systemic delivery. Although the packaging of DNA cargo into synthetic vectors may offer protection from nuclease degradation, the net positive charges of these vectors gives rise to several additional problems: 1) non-specific interactions with negatively charged cellular blood components, vessel endothelia, and serum proteins; and 2) extravasation across the

endothelial barrier and extracellular matrices. Interactions with negatively charged serum proteins results in the formation of ternary complexes and large aggregates. In severe cases, vessel obstruction and risks of pulmonary embolism may arise from significant aggregation with other blood components like erythrocytes [17, 18]. The highly charged particles may prompt interactions with complement components leading to opsonization and subsequent complement activation that results in their removal by the reticuloendothelial system [19, 20]. The above mentioned interactions compromise systemic delivery of vectors contributing to rapid removal and short half-life *in vivo*.

Upon reaching the target cells, the cell membrane is the next significant barrier due to repulsive forces between negatively charged DNA and the negatively charged membranes. Net positive charges of synthetic vectors promote effective electrostatic interactions with cell membranes, enabling cellular uptake by endocytosis. However, without appropriate mechanisms of endosomal escape, the endocytosed vectors are subjected to lysosomal degradation. Intracellular trafficking of released DNA cargo is hampered by cytoskeletal elements rendering passive diffusion ineffective. The limited mobility of DNA elevates the risk of degradation by intracellular nucleases prior to reaching the nuclear membrane. Finally, the nuclear membrane poses yet another barrier as passive diffusion through the nuclear pore complex (NPC) is restricted to small molecules (ions, metabolites, and smaller proteins) less than 60 kDa or 9-11 nm in diameter [1, 12]. The dissociation and reorganization of nuclear membrane during mitosis facilitates nuclear entry as a 50-3000 fold increase in gene product was previously observed in transfection of cells at G2 or G2/M

stages compared to cells at G1 [21]. However, nuclear entry remains problematic for gene delivery in non-dividing cells.

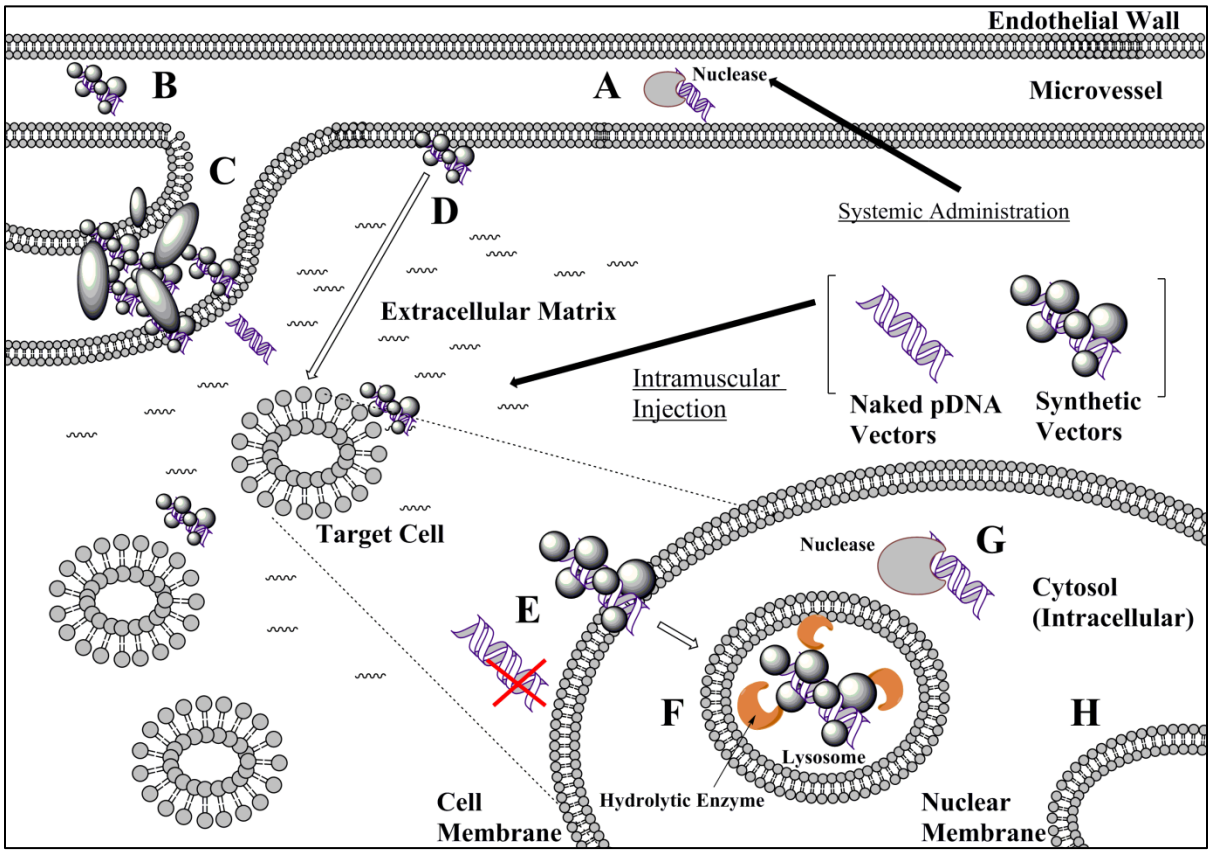

Figure 1.1 Extracellular and intracellular barriers to gene delivery: A) Degradation of unprotected, naked pDNA vectors by nucleases upon systemic delivery; **B)** Removal of synthetic vectors by the reticuloendothelial system; **C)** Significant aggregation with blood components leading to vessel obstruction; **D)** Extravasation of naked pDNA and synthetic vectors across the endothelial wall and extracellular matrix; **E)** Repulsive forces between naked pDNA vectors and cell membrane inhibit effective cellular uptake and internalization; **F)** Lysosomal degradation of synthetic vectors and DNA cargo in absence of endosomal escape; **G)** Degradation of released DNA cargo by intracellular nucleases; **H)** Nuclear membrane obstructing nuclear entry and transgene expression.

1.3 Non-Viral Delivery Systems

Non-viral gene delivery systems can be divided into three major categories: naked pDNA vectors, physical delivery, and chemical delivery via synthetic vectors. The basis of physical delivery systems stems from disruptions to cell membranes for pDNA vectors to bypass this barrier. Established methods such as microinjection, gene gun, and electroporation are examples of physical gene delivery that have been previously explored, each with its own inherent advantages and disadvantages. In addition, sonoporation, optical transfection, and magnetofection are three examples of emerging techniques, pointing to the ongoing exploration of suitable methods of physical gene delivery. Chemical delivery systems involve the packaging of pDNA into synthetic vectors. The design of these synthetic vectors involves a bottom-up approach where different components pertinent to transfection (DNA compaction and encapsulation, targeted delivery, cellular uptake and internalization, endosomal escape, and nuclear localization) are combined together to form a self-assembling nanoparticle. Each gene delivery system is described in greater detail below.

1.3.1 Naked pDNA Vectors

Direct injections of naked pDNA vectors have been explored *in vivo* with low success rates and they often require high doses of pDNA due to the large size and hydrophilic nature of the plasmid, which severely hampers the ability to bypass several physical barriers including blood endothelium, extracellular matrix, and cell membrane [22]. In particular, negatively charged DNA is subjected to repulsive forces from the negatively charge cell membrane which diminishes the close interactions required for successful uptake. The unprotected pDNA vector is also subjected to intra and extracellular nuclease degradation during the

delivery process, further limiting successful internalization and expression of intact functional pDNA vectors [22].

1.3.2 Physical Delivery Systems: Microinjection, Gene Gun, Electroporation

Microinjection involves direct targeted injection of pDNA vectors into the cell nucleus for efficient gene delivery. Unfortunately, low throughput and the requirement of high precision and accuracy render this method ineffective in any practical (i.e. clinical) setting. The gene gun, also known as ballistic gene delivery, is a needle free method involving the discharge of accelerated pDNA-coated gold or tungsten particles of various sizes directly into cell cytoplasm. Despite efficient gene delivery, there are several disadvantages associated with gene gun including: low throughput; non-specific, non-uniform, and variable delivery; limited tissue depth; and potential for substantial inflammation/damage to the administered area [23]. Similarly, electroporation, which involves the application of an electrical field for localized transient changes in cellular membrane permeability, has documented high throughput gene delivery across a variety of cells and tissues *in vitro* and *in vivo* [24]. However, they are notorious for inducing substantial cell death leading to low cell viabilities [23]. Although the above mentioned methods are able to overcome some issues contributing to low transfection efficiencies hampering non-viral gene delivery, they have yet to become widely accepted systems for gene delivery as they are difficult to standardize in clinical trials and their application is considered to be laborious and impractical [25].

1.3.3 Emerging Delivery Systems: Sonoporation, Optical Transfection, Magnetofection

Sonoporation employs low intensity ultrasound to induce modifications to the endothelial layer, along with increases in membrane permeability and transient pore formation. The

process is often accompanied by the addition of microbubbles, contrast agents used in ultrasound imaging, to improve pore formation through controlled bubble collapse referred to as cavitation [26]. The application of sonoporation in gene delivery provides several advantages over other physical methods: 1) ultrasound is commonly applied as a non-invasive diagnostic medical imaging technique using clinically approved microbubbles; 2) site specific delivery may be achieved through effective image-guided spatial and temporal control over ultrasound; and 3) sonoporation is highly suitable for repeat administrations [26, 27]. In addition, sonoporation may work in tandem with chemical delivery systems by coupling synthetic vectors (eg. lipoplexes and polyplexes) to microbubbles for enhanced delivery [26, 28] or act as a release mechanism for controlled cytoplasmic release of DNA cargo within cells [29]. Further evaluation is required to ascertain the optimal acoustic parameters capable of uniform cavitation and DNA entry into different tissues.

In optical transfection, femtosecond-pulsed lasers providing near infrared (700-1100 nm) multiphoton pulses have been used for single cell transfections yielding high transfection efficiency and low cytotoxicity. Direct single target irradiation induces photon absorption and free electron excitation that contributes to localized changes in membrane permeability including transient pore formation [30-32]. However, the high transfection efficiencies achieved using femtosecond pulsed lasers are overshadowed by low throughput, limited loading concentrations, and the requirement of expensive equipment [31]. Alternatively, nanosecond-pulsed lasers have been applied to generate photomechanical stress waves, referred to as laser-induced stress waves (LISW), that create shear forces for transient increase in membrane permeability and entry of exogenous pDNA vectors by passive

diffusion [31]. LISW in GT was previously demonstrated in NIH/3T3 murine fibroblast [33] *in vitro* as well as rat skin/muscle [34, 35] and mouse central nervous system [36] *in vivo*. In particular, the application of LISW in combination with polyethylenimine (PEI)/DNA synthetic vectors yielded efficient and widespread expression of the gene of interest (*egfp*) in mouse central nervous system with penetration depth of 1.5 mm and 3.5 mm into the cortex surface of adult and newborn mice respectively [36]. Further exploration of *Q*-switched Nd:YAG lasers for LISW mediated gene therapy may be warranted as they are commercially available, cost effective, easy to operate, safe, and approved for use in head and neck surgeries [35].

Magnetofection refers to gene delivery mediated by the application of magnetic fields acting on magnetic vectors typically comprising superparamagnetic iron oxide nanoparticles (SPIONs). These systems are generating significant interest as GT vectors due to their superparamagnetic properties, high biocompatibility, low toxicity, biodegradability *in vivo*, and concurrent applications in magnetic resonance imaging [37-39]. The formation of these magnetic vectors involve association of magnetic nanoparticles with lipid or polymer based synthetic vectors predominantly through electrostatic interactions [40]. Magnetofection serves to enhance gene delivery through rapid sedimentation overcoming the diffusion barrier which limits vector accumulation and lowers vector concentrations at target tissues. The introduction of magnetic fields rapidly sequesters magnetic vectors to target tissues which contribute to improved vector delivery despite lower administered doses. Magnetofection offers several significant advantages: 1) rapid vector internalization, 2) high transfection efficiencies at lower vector doses, and 3) lower cytotoxicity [37, 41]. In addition

to enhancing transfection efficiency by magnetofection, the application of an external magnetic field allows for localized and guided targeting in regions specifically exposed to the magnetic field. This feature is highlighted by Song et al. [42] where moving the external magnetic field down the spinal cord of adult male Wistar rats changed the regional distribution pattern of transgene expression. Despite the advantages of magnetofection *in vitro* [37] and *in vivo* [43-45], it is limited by low penetration depth of the external magnetic field, high field strengths required to overcome hydrodynamic forces for magnetic vector localization, and insufficient biodistribution analysis demonstrating the effects of magnetic targeting [46].

1.3.4 Chemical Delivery Systems: Synthetic Vectors

Enhanced transfection efficiencies exhibited in the above mentioned emerging techniques share a common theme of using synthetic vectors in combination with physical methods of gene delivery. Synthetic vectors offer advantages of: 1) complexation and compaction of pDNA vectors into discrete particles facilitating extravasation and delivery to target cells; 2) improved cellular uptake by promoting effective electrostatic interactions with cell membrane; 3) protection against extra and intracellular nucleases upon effective DNA encapsulation; 4) improved cytoplasmic release; and 5) intracellular trafficking to perinuclear regions for optimal nuclear localization. Synthetic vectors are classified according to their basic composition with cationic lipids (lipoplex), cationic polymers (polyplex), and cationic peptides as three major variations.

1.3.4.1 Polymer-based Vectors

Polymer-based vectors employ cationic polymers, containing a large number of primary, secondary, tertiary, and/or quaternary amine groups, for complexation and encapsulation of negatively charged DNA by electrostatic interactions. Strong DNA interactions with the high density of amine groups result in the formation of polyplexes that are typically more stable than cationic lipid derived lipoplexes [11]. Polyplex formation also protects the DNA cargo from degradation by nucleases during the delivery process. The net positive charges of these polyplexes prompt efficient cellular uptake through electrostatic interactions with negatively charged cell membranes, allowing polyplex internalization by endocytosis. Depending on the nature of the cationic polymer, polyplexes may also possess inherent abilities to promote endosomal escape, through the proton sponge effect, for cytoplasmic release and nuclear localization of DNA cargo. Generally, polymers of high molecular weight constitute higher charge density, leading to better DNA complexation and improved transfection efficiencies; however, this comes at a cost of greater cytotoxicity. Hence, an intricate balance between transfection efficiency and cytotoxicity is critical in the design of effective polymer-based vectors. Numerous variations of cationic polymers have been previously applied to GT, with poly-L-lysine (PLL), polyethylenimine (PEI), chitosan, and poly(amidoamine) (PAMAM) dendrimers as four commonly used polymers in synthetic vectors for gene delivery (Figure 1.2).

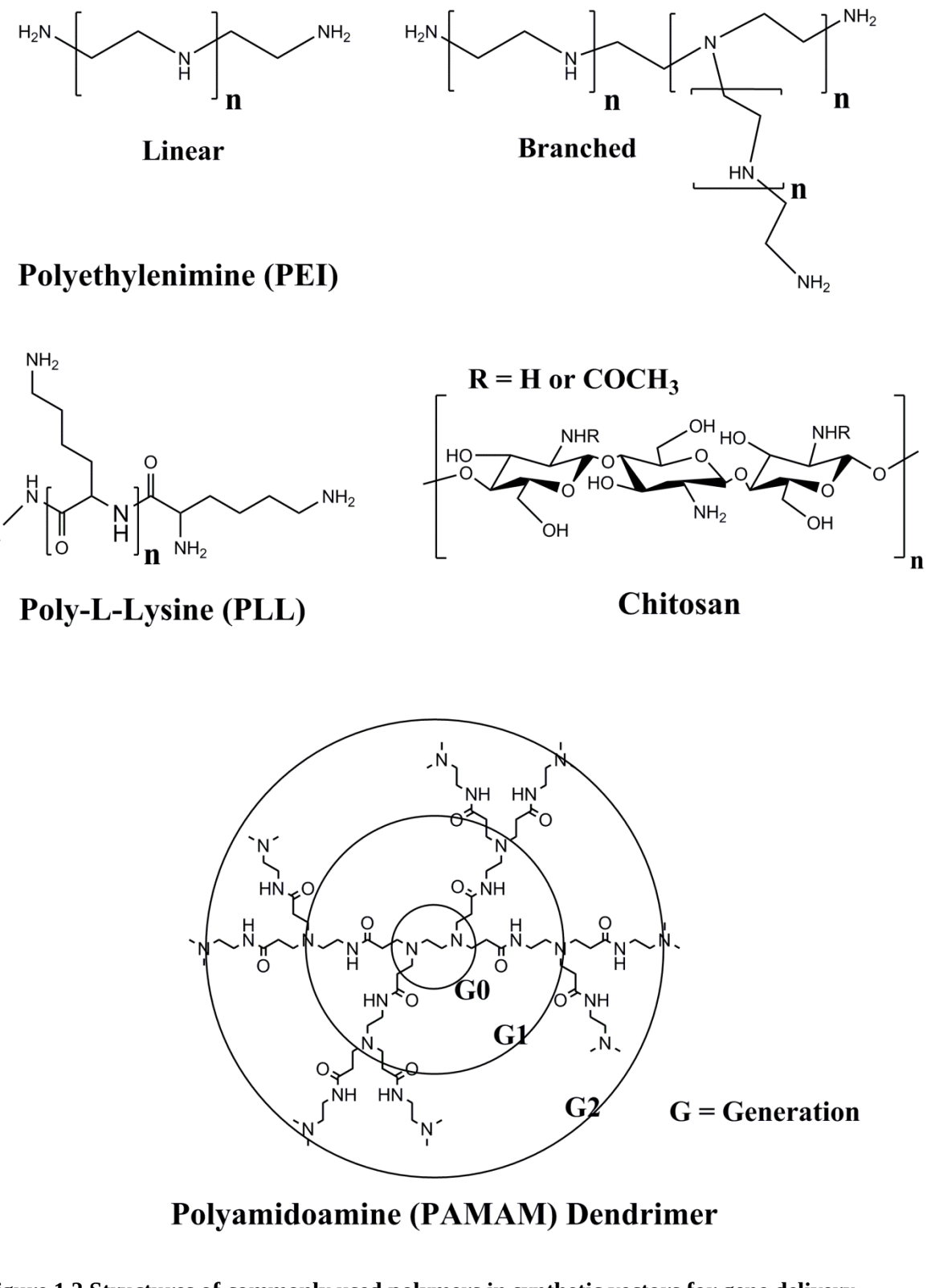

Figure 1.2 Structures of commonly used polymers in synthetic vectors for gene delivery.

1.3.4.1.1 Poly-L-Lysine (PLL)

Poly-L-Lysine (PLL)/DNA vectors consist of PLL, a synthetic repeat of the amino acid (a.a.) lysine with varying degrees of polymerization ranging from 90-450 residues, and such vectors are suitable for *in vivo* administrations as they are highly biodegradable [47]. The polymer length of PLL has significant influences over the extent of polymer-DNA interactions, complex stability, polyplex size, transfection efficiency, and cytotoxicity. Increasing polymer length contributes to greater net positive charge, tighter binding with DNA, and better protection from DNA degradation. PLL/DNA polyplexes with higher molecular weight were previously shown to exhibit prolonged circulation and reduced interactions with erythrocytes when compared to low molecular weight PLL/DNA polyplexes [47]. However, increasing the molecular weight of the polymer contributes to increasing cytotoxicity. By itself, PLL/DNA polyplexes elicit sub-optimal transfection efficiencies and require the co-application of endoosmotropic agents (eg. chloroquine) for raising endosomal pH to inhibit degradation by hydrolytic enzymes; or modifications with imidazole structures/fusogenic peptides for effective endosomal escape and improved delivery [17].

1.3.4.1.2 Polyethylenimine (PEI)

Currently considered to be the standard of polymer based vectors, linear and branched polyethylenimine (PEI) ranging from 800 to 25kDa have been applied for DNA complexation and transfection with 25 kDa branched and 22 kDa linear PEI being commonly used for gene delivery [48, 49]. Transfection efficiencies of PEI/DNA polyplexes are dependent on molecular weight, degree of branching, zeta potential, and particle size.

PEI/DNA polyplexes form homogeneous nanoparticles around 100 nm and exhibit enhanced transfection over PLL based vectors due to high density of primary, secondary, and tertiary amines promoting effective complexation [17]. Concurrently, the high density of amines, with compatible pKa values, confers significant buffering capacities over a wide range of pH; thus promoting effective endosomal escape according to the "proton sponge effect" [11, 12, 50]. Under physiological pH conditions within the early endosome, the majority of amines in PEI remain unprotonated. During the transition from early to late endosome, the endosome becomes progressively acidified through an ATPase enzyme that actively shuttles protons from the cytosol. A buffer effect ensues as protonation of the unprotonated amines in PEI causes more protons to be shuttled in order for the progressive drop in pH to occur. Increased proton shuttling is balanced by increasing concentrations of chloride counterions within the endosome, both of which contribute to raising osmotic pressure that causes osmotic swelling and eventual rupture of the endosome [17, 22]. Previous studies supporting the proton sponge effect indicated delayed endosomal acidification, enhanced chloride ion accumulation, and significant increases in relative endosome volume for PEI and poly(amidoamine) polyplexes, but not in non-buffering PLL polyplexes [51]. The removal of protonable amines by N-quaternization was shown to result in the abrogation of buffering capacities and an approximately 50 fold reduction in transfection efficiency when compared to parental PEI/DNA polyplexes [52]. Clinical studies have been conducted using linear 22 kDa PEI due to high transfection with acceptable biocompatibility. Of particular interest, linear 22 kDa PEI modified with mannose and dextrose was previously applied for transfection of pDNA encoding HIV proteins into target antigen presenting cells (APC) [49]. Despite enhanced

transfection efficiencies exhibited by PEI/DNA polyplexes, further modifications must be explored to overcome the issues relating high cytotoxicity, from the highly dense positive charges, and non-biodegradability of the polymer.

1.3.4.1.3 Chitosan

Chitosan is composed of linear polysaccharide with randomly distributed D-glucosamine (2-amino-2-deoxy-glucose) and N-acetyl-D-glucosamine (2-(acetylamino)-2-deoxy-D-glucose) joined by β-1,4 linkages. Chitosans are sought after as suitable synthetic vectors as they are biodegradable, biocompatible, and non-allergenic while possessing strong DNA affinity, mucoadhesive properties, and low cytotoxicity [53]. DNA complexation and encapsulation is influenced by both molecular weight and the degree of deacetylation as chitosan vectors with inherent low molecular weights and deacetylation resulted in inefficient DNA condensation and protection from degradation [54]. Presence of primary amines with pKa of 6.5 grants chitosan/DNA polyplexes buffering capacity but at a restricted pH range of 5-7 and at reduced capacities when compared to PEI based polyplexes [53]. Differences in buffering capacities between PEI and chitosan based polyplexes was illustrated through image based quantification [55] as DNA degradation was observed for chitosan/DNA polyplexes due to unpacking within the endolysosomes. In contrast, the high buffering capacity of PEI/DNA polyplexes led to rapid endosomal escape, allowing the polyplexes to attain comparable stabilities in endolysosomes and cytosol. The relatively lower transfection efficiencies for chitosan/DNA polyplexes was also attributed to reduced cellular uptake, due to less efficient DNA compaction, and limited nuclear transport of the DNA cargo [53].

1.3.4.1.4 Poly(amidoamine) (PAMAM) Dendrimers

Dendrimers are highly branched, highly symmetrical polymers with well defined 3D spherical structures and numerous terminal groups. They are comprised of three main domains: 1) a central core; 2) branches of repeating units forming a series of radially concentric layers referred to as generations; and 3) identical terminal functional groups for multiple interactions [56]. The structural nature of dendrimers constitutes features of monodispersity, high density of peripheral functional groups, defined globular shape, and multivalency. Poly(amidoamine) (PAMAM) dendrimers are composed of a central core of tertiary amines, an amide backbone, and primary amines as functional groups presented on the surface [53]. The surface primary amines (pKa ~7-9) permit effective DNA binding and cellular uptake while the interior tertiary amines (pKa ~3-6) provide buffering capacity critical to endosomal escape. Dendrimer charge ratio and dendrimer generation are two parameters critical to optimal transfection efficiency [57] with higher generations, G5 to G10, enabling better DNA complexation [17, 56, 58]. PAMAM dendrimers exhibit no significant cytotoxicity *in vitro* or *in vivo*, but their biocompatibility is dependent on size/generation, surface charge, and concentration. As dendrimers enable precise control over size, shape, and terminal groups, specific modifications may serve to improve transfection efficiency while limiting cytotoxicity.

1.3.4.2 Cationic Peptide Vectors

Peptide-assisted gene delivery offers improved gene delivery while attaining biodegradability with reduced cytotoxicity and immunogenicity. Various peptides have been incorporated into different synthetic vectors in overcoming numerous barriers during the delivery process: 1)

cell targeting peptides (eg. RGD peptide) for targeted delivery; 2) cell penetrating peptides (CPP) for cellular uptake; 3) endoosmolytic peptides including histidine rich and fusogenic peptides for endosomal escape; and 4) nuclear localization signal (NLS) peptides for nuclear localization. By themselves, highly positive charge peptides, like oligolysine and oligoarginine peptides, can act as standalone vectors as they can effectively bind and compact DNA. In comparison to polymers (PLL), oligolysine peptides have inherit advantages of specified peptide lengths, lower toxicity, and site specific modifications for improved delivery [47]. Oligolysine peptides of 13 or more a.a. residues were determined to achieve effective DNA compaction, forming complexes ranging from 53 to 231 nm [59]. A subsequent study reported the ability of oligolysine peptides, with 18 lysine residues, to protect DNA from degradation by endonuclease [60]. Similarly, oligoarginine peptides 4 to 16 residues long with modification by N-stearylation were shown to transfect cells with a 100 fold improvement in transfection efficiency [61]. MPG and trans-activating transcriptional activator (Tat) derived peptides are two variations of CPPs previously demonstrated to achieve successful nucleic acid/gene delivery. CPPs are short cationic or amphipathic peptides, 5-30 a.a. in length, with a net positive charge and improved cellular uptake through direct penetration and endocytosis. MPG is an amphipathic peptide comprised of a lysine rich SV40 nuclear localization signal (NLS) hydrophilic domain for DNA binding and a hydrophobic domain, derived from HIV gp41 fusion sequence, for protection from DNA degradation. This peptide was first to demonstrate peptide based siRNA delivery through non-covalent, electrostatic interactions [24]. Tat peptide, an arginine rich peptide derived from the 48-60 a.a. sequence of HIV trans-activating transcriptional activator (Tat) protein,

was shown to compact DNA and enhance transfection efficiency by six to eight fold over control peptides [47]. The above mentioned peptides, along with many peptide variations, have been applied to the delivery of pDNA, oligonucleotides, siRNA, and miRNA [62, 63]. However, transfection efficiencies remain insufficient as they are hindered by a lack of endosomal escape. Tat peptides, modified with the addition of 10 histidine residues for endoosmolytic capabilities, were reported to achieve a 7000 fold increase in transfection efficiency over the native peptide and the incorporation of 2 additional cysteine residues, for DNA protection, was indicated to further improve transfection [64]. Exploration of different peptide derivatives with similar modifications may enable effective gene delivery by cationic peptide vectors.

1.3.4.3 Cationic Lipids

Cationic lipids are composed of a cationic hydrophilic head group and a hydrophobic domain connected together by a linker. The hydrophilic head group commonly consists of a combination of phosphate and amine groups while the hydrophobic domain consists two types of hydrophobic moieties including aliphatic chains, cholesterol, and/or other variations of steroid rings [11]. The linker - commonly consisting of ether, ester, carbamate, or amide bonds - determines the flexibility, stability, and biodegradability of the cationic lipid [65]. DOTMA (N-[1-(2,3-dioleyloxy)propyl]-N,N,N-trimethylammonium chloride), a double chain monovalent quaternary ammonium lipid developed by Felgner et al. [66], was the first generation of cationic lipids that led to the development of the first commercialized reagent, Lipofectin (Invitrogen), applied for lipid-based transfection or lipofection. This spawned further modifications for subsequent generations of cationic lipids (Figure 1.3) which are still

commonly used for transfection today. DOTAP (N-[1-(2,3-dioleoyloxy)propyl]-N,N,N-trimethylammonium methyl sulfate) is a DOTMA derivative comprised of ester bonds, in place of ether bonds, for higher biodegradability and corresponding lower cytotoxicity [17]. DOSPER (1,3-dioleoyloxy-2-(6-carboxyspermyl)-propyl amide), DOGS (Di-octadecyl-amido-glycyl-spermine), and DOSPA (2,3-dioleyloxy-N-[2(sperminecarboxamido)ethyl]-N,N-dimethyl-1-propanaminium trifluoroacetate) are three examples of cationic lipids with modified head groups derived from polyamine spermine. The increased cationic groups in these multivalent lipids promote stronger DNA interaction for enhanced delivery. Lipofectamine^{TM} 2000 (Invitrogen), a commonly used commercialized transfection reagent composed of DOSPA and a neutral lipid, 1,2-dioleoyl-sn-glycero-3-phosphatidylethanolamine (DOPE), at 3:1 ratios, is an example of such multivalent lipids. Modifications to the length of aliphatic chain was shown to influence gene delivery capacity of monovalent lipids, like DOTMA and DOTAP, as transfection efficiency increases with decreasing chain length ($C_{14} > C_{16} > C_{18}$); however, such relationship was not observed with respect to lipospermine derivatives [12]. In place of aliphatic chains, the application of cholesterol derived cationic lipids, DC-Chol (3β-[N-(N',N'-dimethylaminoethyl) carbamoyl] cholesterol), was shown to promote better stability and reduced cytotoxicity for improved transfection efficiencies *in vitro* [12, 67]. As numerous variations can be applied to each of the three primary components, the high number of possible permutations contributes to over hundreds of different cationic lipids that have been explored and successfully applied to develop synthetic vectors for gene delivery.

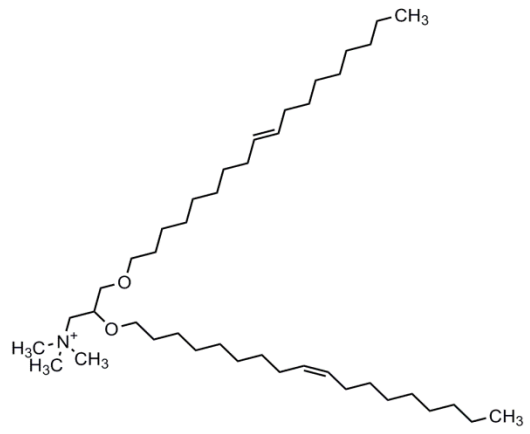

N-[1-(2, 3-dioleyloxy)propyl]-N,N,N-trimethylammonium chloride (DOTMA)

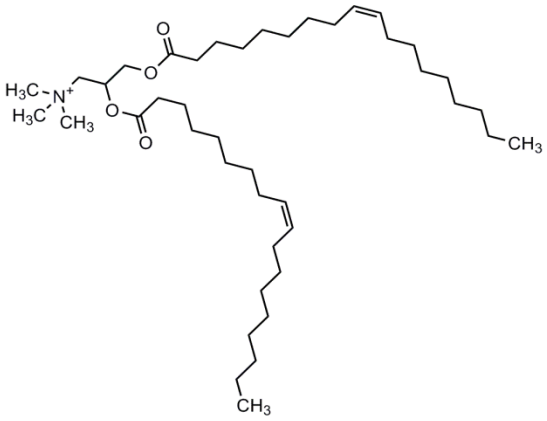

N-[1-(2,3-dioleoyloxy)propyl]-N,N,N-trimethylammonium methyl sulfate (DOTAP)

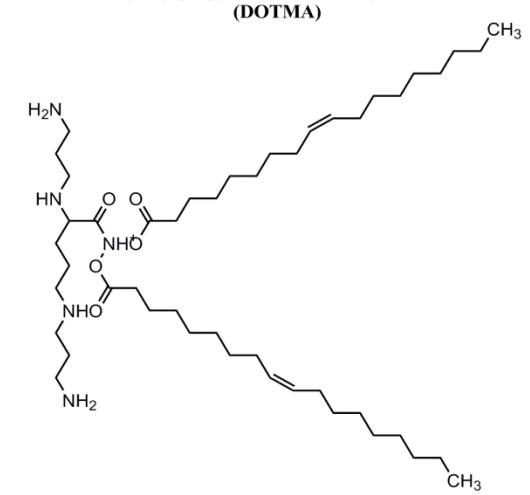

1,3-dioleoyloxy-2-(6-carboxyspermyl)-propyl amide (DOSPER)

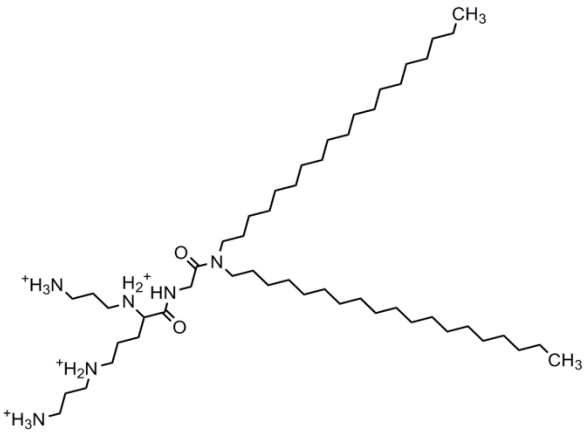

Di-octadecyl-amido-glycyl-spermine (DOGS)

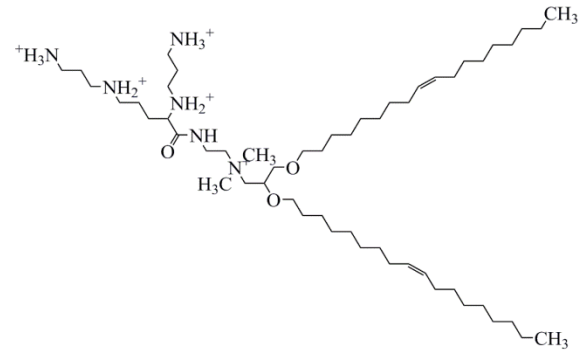

2,3-dioleyloxy-N-[2(sperminecarboxamido)ethyl]-N,N-dimethyl-1-propanaminium trifluoroacetate (DOSPA)

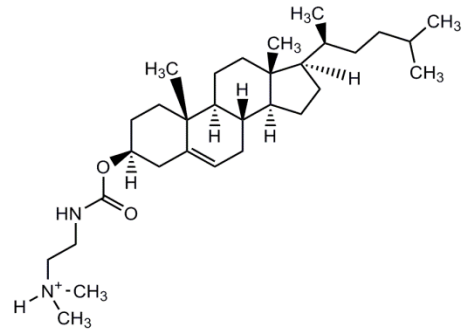

3â-[N-(N',N'-dimethylaminoethyl) carbamoyl] cholesterol (DC-Chol)

Figure 1.3 Structures of commonly used cationic lipids in synthetic vectors for gene delivery.

1.3.4.3.1 Lipoplex Formation, Packing Structures and Influences of Helper Lipids

The formation of lipoplexes stems from favorable electrostatic interactions between negatively charged DNA and positively charge cationic lipids. This is an entropy driven process arising from rapid lipid mixing/reorganization and subsequent release of tightly bound counterions from both DNA and lipid bilayers [68-72]. Distinct phases of lipoplex formation have been observed depending on the nitrogen to phosphate (N^+/P^-) charge ratios between cationic lipids and DNA [68]. At low N^+/P^- charge ratios of <1, DNA-DNA repulsion predominates leading to the formation of discrete lipoplex particles with excessive amounts of uncomplexed DNA. At neutral (N^+/P^- =1) or slightly positive charge ratios, charge neutralization prevents effective DNA encapsulation and prompts significant aggregations that prevent the generation of discrete lipoplexes [50]. The addition of excess lipid, conferring charge ratios >1, allows for effective DNA complexation and encapsulation leading to the formation of discrete lipoplex particles that are separated by electrostatic repulsion. Increasing charge ratios favors DNA compaction into small discrete lipoplex particles while instilling a positive surface charge for efficient cellular uptake upon optimal interactions with negatively charged cell membranes. However, this comes at a cost as cytotoxicity increases with greater cationic lipid content and surface charge [69].

Depending on the lipid composition, lipoplexes adopt a variety of phase structures including: 1) lamellar L^C_α, 2) hexagonal $H_{I,}$ and 3) inverted hexagonal H^C_{II} (Figure 1.4). Lamellar structures are characterized as DNA monolayers sandwiched between cationic membrane bilayers. Higher ordered hexagonal structures are characterized as DNA "rods" intercalated between spherical micelles arranged in a hexagonal lattice whereas inverted

hexagonal structures are characterized as DNA "rods" coated with a lipid monolayer arranged in a hexagonal lattice [70, 71]. The formation of the different phase structures is dependent on the curvature of the lipid system. The lipid components influencing the spontaneous curvature of the membrane, $C_o = 1/R_o$, will determine the actual curvature, $C = 1/R$, where R_o is the spontaneous radius of curvature of the lipid monolayer and R is the actual radius of the lipid system; the actual curvature describes the dominant structure of the self assembled lipoplexes as follows: lamellar ($C = 0$), hexagonal ($C_o > 0$), and inverted hexagonal ($C_o < 0$) [69, 73]. Spontaneous curvatures and corresponding phase structures relate to the concept of molecular packing parameter (P) defined as $P = V/la_0$ where V and l are the volume and length of hydrophobic tails, and a_0 is the surface area of the head group [74]. Different packing parameters are associated with different expected aggregate shapes: $P < 1/3$ for spheres, $1/3 < P < 1/2$ for cylinders, $1/2 < P < 1$ for vesicles and flexible bilayers (lamellar), $P = 1$ for planar bilayers (lamellar), and $P > 1$ for inverted structures (inverted hexagonal) (Figure 1.5) [69, 74]. The packing parameter is not always constant and modifications to the solution conditions (eg. temperature, pH, salts) can have drastic influences over the resulting phase structures [74].

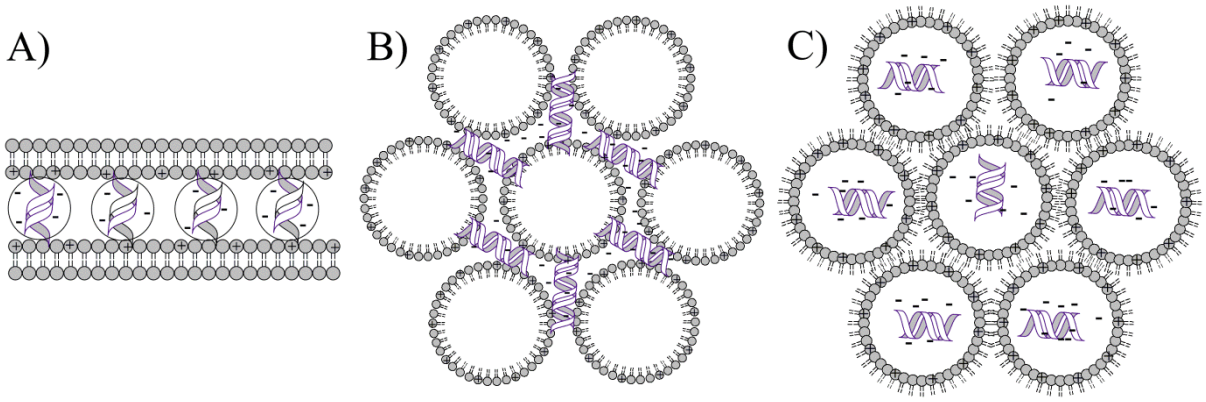

Figure 1.4 Lipoplex phase structures: A) Lamellar**; B)** Hexagonal H_I; **C)** Inverted hexagonal H^C_{II}.

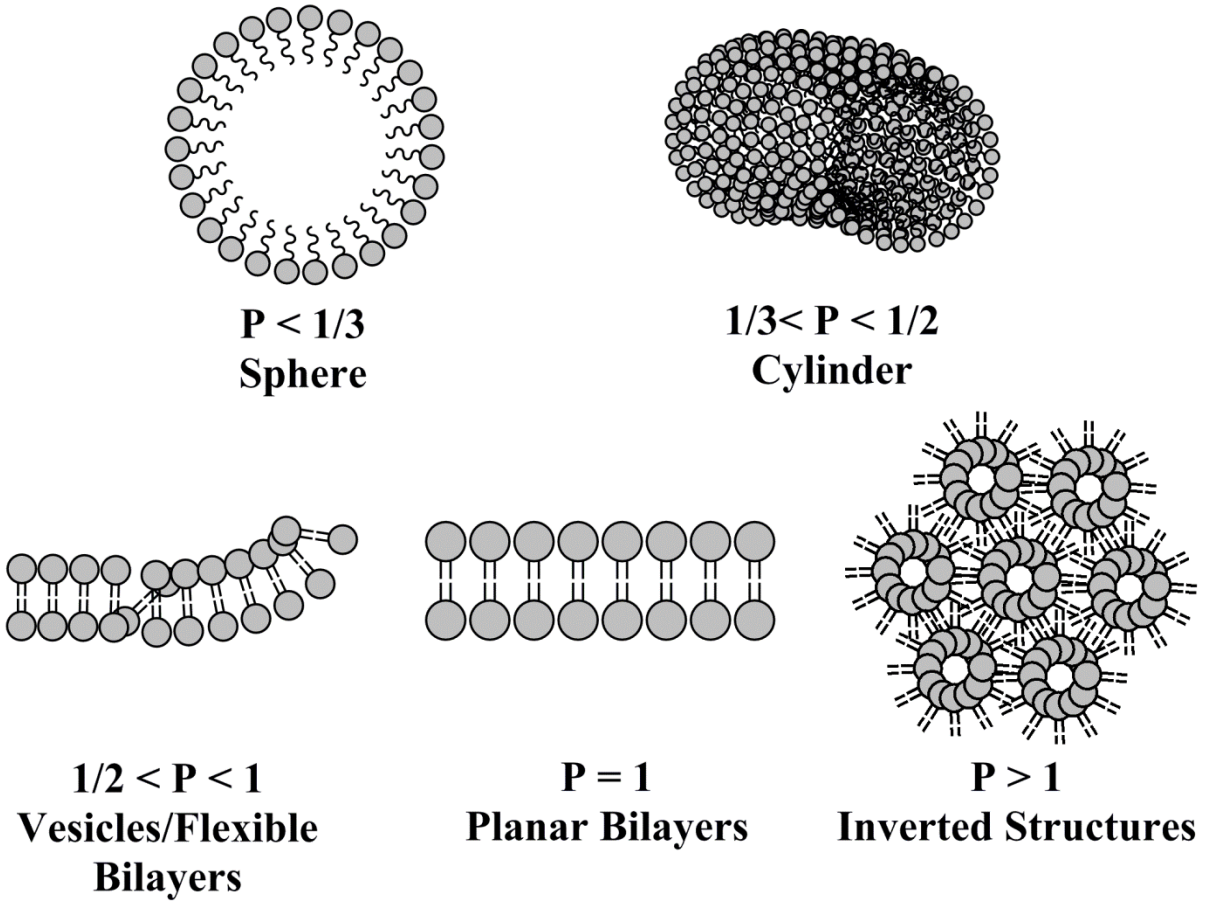

Figure 1.5 Packing parameter and expected aggregate structures.

The incorporation of neutral helper lipids DOPE or cholesterol (Figure 1.6) is capable of mediating the transition from lamellar to inverted hexagonal phase structures, a feature often considered critical to successful endosomal escape of lipoplexes [75]. DOPE has been previously demonstrated to exhibit pH dependent phase behaviors. At pH of 9 and above, DOPE is negatively charged and exists as spherical micelles; however, at physiological pH and temperatures above 10-15° C, the zwitterionic head groups of DOPE abolishes repulsion between head groups which leads to transitions into inverted hexagonal packing structures [76, 77]. The addition of pH responsive DOPE, possessing a packing parameter of $P > 1$, results in alterations to the actual curvature of the lipid system in accordance to the proportion of DOPE being incorporated. Greater fractions of DOPE contribute to a more negative actual curvature which increases the propensity for lamellar to inverted hexagonal phase transitions [73]. The relative ratio of DOPE to cationic lipid serves to determine the transition pH of DOPE from lamellar to inverted hexagonal as mixed systems of cationic lipid, with ethylenediamine head group, and DOPE decreased the transition pH of DOPE [77]. Hence, by controlling the DOPE composition within the lipid system, the overall phase structure of lipoplexes and pH induced phase transitions can be effectively regulated.

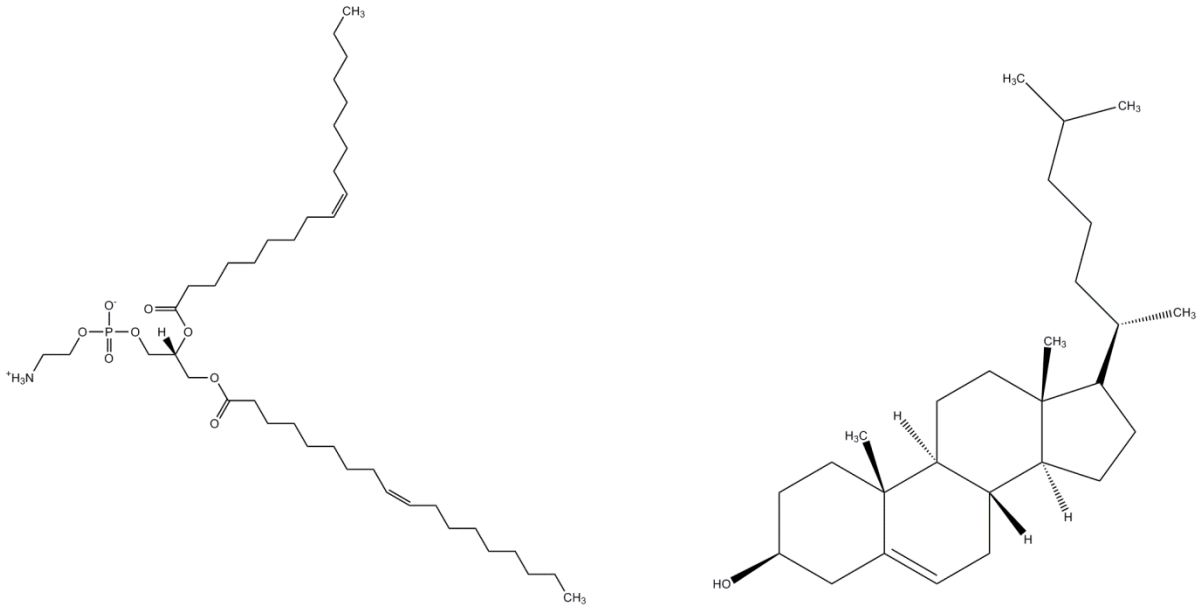

1,2-Dioleoyl-sn-glycero-3-phosphatidylethanolamine (DOPE)

Cholesterol

Figure 1.6 Neutral lipids in lipoplex formation.

1.3.4.3.2 Overcoming barriers with cationic lipid based synthetic vectors.

A substantial amount of research effort has been focused on the development of novel cationic lipids for gene delivery in part due to the ability of such synthetic vectors to bypass the numerous barriers described above. Effective DNA compaction and encapsulation by cationic lipids results in protection from nuclease mediated DNA degradation as well as the formation of discrete, small lipoplexes capable of cellular uptake by endocytosis (Figure 1.7). With the incorporation of ligands for targeted delivery, such lipoplexes are internalized by receptor mediated endocytosis. In absence of targeting ligands, lipoplexes undergo non-specific electrostatic interactions with anionic cell surface heparin sulfate proteoglycans (HSPGs) and may be internalized by various endocytic pathways including: phagocytosis,

macropinocytosis, clathrin mediated endocytosis, caveolae mediated endocytosis, and non-clathrin/non-caveolae mediated endocytosis [14, 78, 79]. These pathways differ with respect to vesicle size, embedded endosomal proteins, preferential uptake of specific particle sizes, and the ultimate fate of internalized particles [1, 79]. Due to the resulting polydispersities upon lipoplex formation, multiple pathways may be involved with clathrin mediated endocytosis being the predominant pathway due to preferential uptake of particles $\leq$ 200 nm. Particles ranging from 200-500 nm in size may undergo caveolae mediated endocytosis [80], while particles >500 nm may undergo phagocytosis or macropinocytosis; however, direct correlations between particle sizes and endocytic pathway have yet to be clearly elucidated. Upon clathrin mediated endocytosis, the early endosome, carrying the endocytosed vesicles, transitions to late endosome as they are subjected to microtubule assisted intracellular trafficking towards the microtubule organizing centre (MTOC) situated in the perinuclear region [14]. Progressive acidification during the transition from early to late endosome results in lysosomal degradation upon fusion with lysosomes. In caveolae mediated endocytosis, the endocytosed vesicles may fuse with the early endosome or caveosome, an endosomal compartment of neutral pH that is not subjected to lysosomal degradation [81]. Microtubule assisted transport of endocytosed lipoplexes towards MTOC drives rapid intracellular trafficking to the perinuclear region. However, suitable mechanisms of endosomal escape must be in place in order to prevent degradation of the DNA cargo.

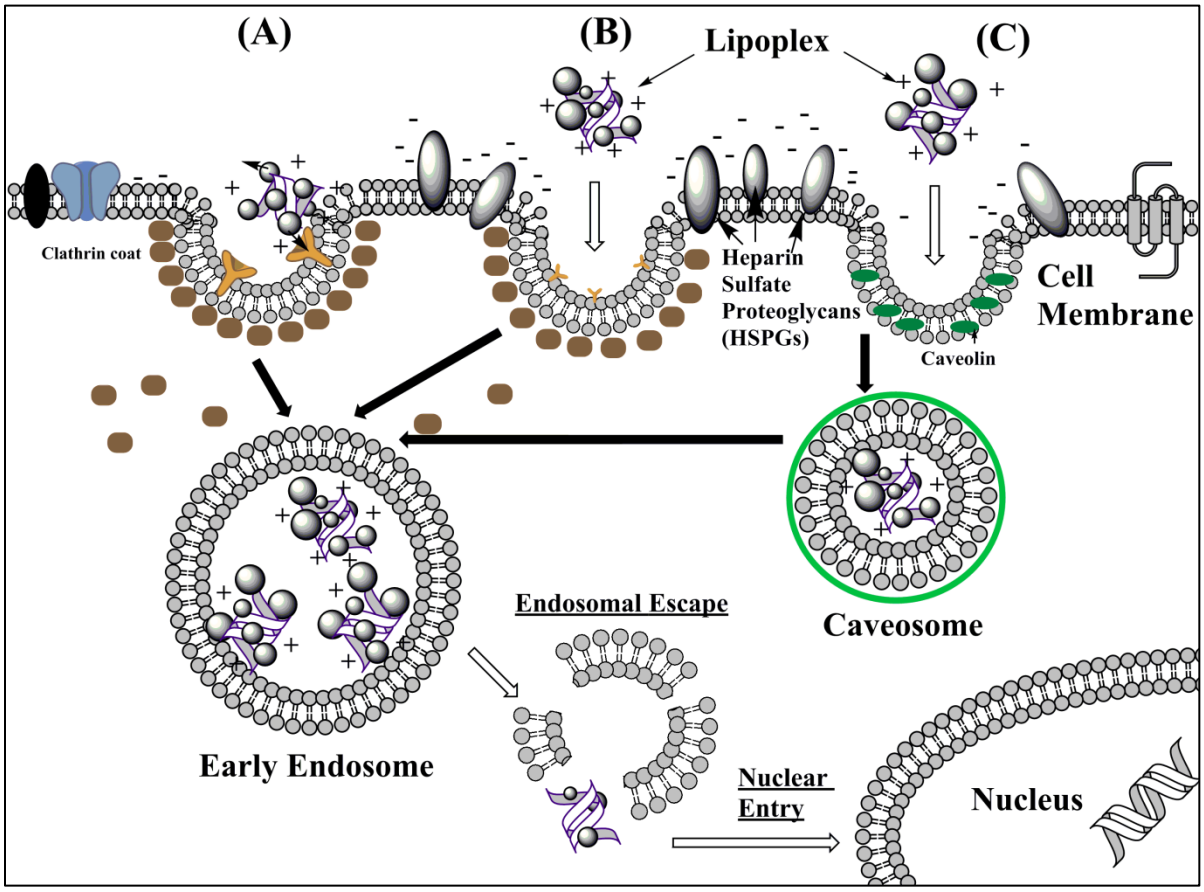

Figure 1.7 Endocytic pathways in the cellular uptake of lipoplexes: A) Receptor mediated endocytosis; **B)** Clathrin mediated endocytosis; **C)** Caveolae mediated endocytosis. The incorporation of targeting ligands permits cellular uptake of lipoplexes by receptor mediated endocytosis. Non-specific electrostatic interactions with anionic heparin sulfate proteoglycans (HSPGs) enable internalization by clathrin and caveolae mediated endocytosis. For clathrin mediated endocytosis, the internalized vesicle fuses with early endosomes for intracellular trafficking and transition into late endosomes. Endocytosed vesicles from caveolae mediated endocytosis may fuse with early endosome or caveosome. Subsequent endosomal escape and nuclear entry are both required for successful gene delivery after cellular uptake.

A number of mechanisms have been proposed regarding endosomal escape of lipoplexes with pre-dominant lamellar phase structures (Figure 1.8) and with DOPE containing lipoplexes possessing pH dependent fusogenic properties (Figure 1.9). Membrane charge density, the average charge per unit area of membrane, has been previously determined to be

the universal parameter for successful endosomal escape of lamellar lipoplexes [70, 71, 76, 82]. Lamellar lipoplexes with high membrane charge density were shown to elicit better endosomal escape via “flip-flop” fusion. In flip-flop fusion, lipoplexes with high membrane charge densities prompt close proximity interactions with anionic lipids of the endosomal membrane, flipping of anionic lipids from the cytoplasmic leaflet to the inner leaflet facing the endosomal lumen. Charge neutralization with anionic lipids induces higher ordered inverted hexagonal phase structures, displacing DNA upon endosomal escape [83].

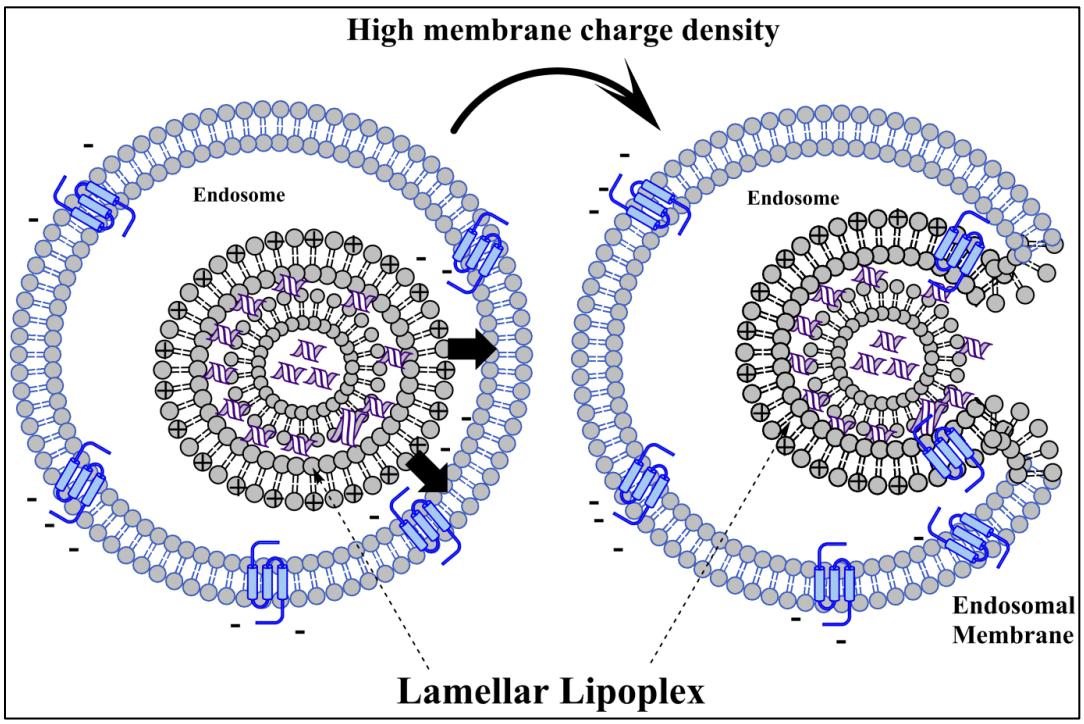

Figure 1.8 Mechanisms of endosomal escape in lamellar lipoplexes. Positively charged lipoplexes undergo close proximity electrostatic interactions with negatively charged anionic lipids of the endosomal membrane. "Flip-flop" fusion incurs as lipoplexes with high membrane charge densities causes anionic lipids to flip from the cytoplasmic leaflet towards to inner leaflet facing the endosomal lumen. This promotes charge neutralization and the induction of higher ordered structures critical to endosomal escape. Adapted from [73].

Exponential increases in transfection efficiency have been previously observed to correspond with increases in charge density. However, the inherently more stable and onion-like nature of lamellar lipoplexes render gradual endosomal escape due to slow electrostatic interactions between cationic lipids and anionic membrane components [82]. Lipoplexes from 200-400 nm with a cationic lipid to DNA charge of ≥ 2 have been observed to be most effective for *in vitro* transfections as their size stretches the limits of clathrin mediated endocytosis, allowing substantial membrane interactions and rapid lipid exchange [76].

Endosomal escape by DOPE containing lipoplexes employs a mechanism that is independent of membrane charge density. A drop in pH, as seen during the progression from early endosome to late endosome, triggers lamellar to inverted hexagonal phase transitions. The negative curvature of inverted hexagonal lipoplexes results in an elastically frustrated state with the outer lipid monolayer, possessing a positive curvature, that surrounds the lipoplexes; this constitutes the driving force for rapid fusion with cell and endosomal membranes (Figure 1.9) [70, 82]. The ability of DOPE containing lipoplexes to adopt inverted hexagonal phase structures for rapid fusion and endosomal escape is a significant contributing factor to higher transfection efficiency when compared to lipoplexes with lamellar phase structures.

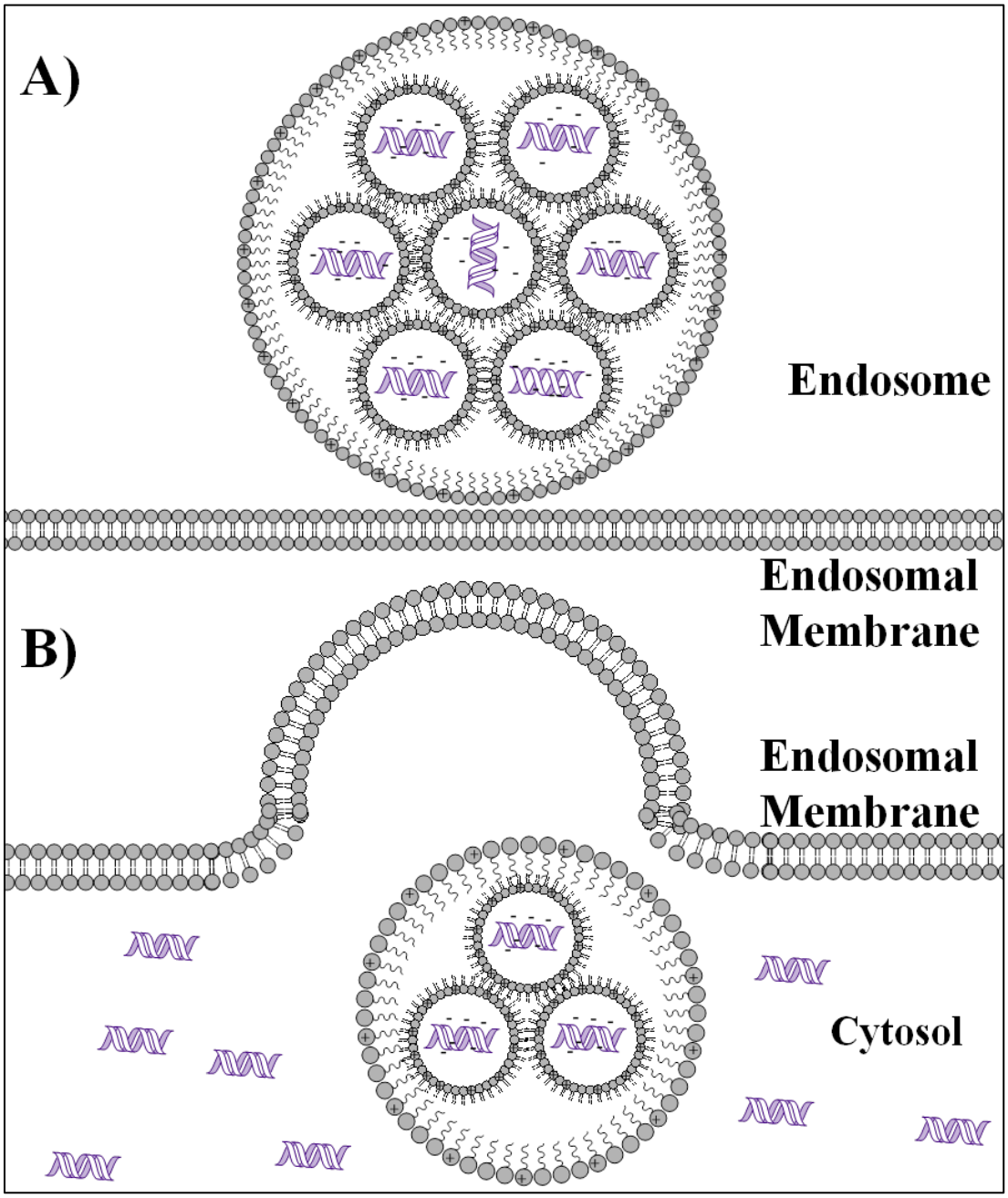

Figure 1.9 Mechanism of endosomal escape in fusogenic, DOPE containing lipoplexes. Progressive drops in pH trigger lamellar to inverted hexagonal phase transitions **(A)**, prompting an elastically frustrated state that drives rapid fusion with endosomal membrane and endosomal escape **(B)**. Adapted from [73].

Upon successful endosomal escape, lipoplexes and free DNA vectors are required to translocate across the nuclear membrane for transgene expression. Previous studies had indicated the potential of lipoplexes to undergo fusion with nuclear membranes, as visual evidence suggests the extension of DNA across the nuclear membrane while in aggregate forms larger than the NPC [84]. However, successful nuclear delivery, in absence of cell mitosis, generally occurs through the NPC. Nuclear localization signals (NLS), short amino acid sequences functioning as tags for nuclear transport, and DNA nuclear targeting sequences (DTS) may be incorporated to facilitate nuclear entry.

With considerations to *in vivo* administration, interactions with serum proteins and high clearance rate are detrimental particularly due to inverted hexagonal phase structures of DOPE containing lipoplexes [69]. The incorporation of polyethylene glycol (PEG) to lipoplexes can circumvent such issues as it masks surface charge, reduces aggregation, minimizes serum protein interactions, and prevents opsonin adsorption [10, 16].

1.3.4.4 Gemini Surfactants

Gemini surfactants are amphiphilic molecules composed of two surfactant monomers (cationic, anionic, or neutral) chemically linked by a spacer (Figure 1.10). Gemini surfactants possess higher charge per mass ratio than cationic lipids and have a critical micelle concentration (CMC), the concentration of surfactants at which micelles begin to form, that is one to two orders of magnitude lower than their monomer counterparts [15, 85, 86]. As such, gemini surfactants confer advantages of reduced toxicities and cost effectiveness over conventional surfactants. At low concentrations, gemini surfactants self-assemble into a variety of higher order assemblies (spherical micelles, bilayers, and inverted micelles)

depending on the nature of the head group, hydrophobic tails, and spacer [87]. Gemini surfactant derived synthetic vectors provide numerous advantages including: 1) high positive charge for effective DNA complexation at low concentrations; 2) efficient DNA compaction generating smaller complexes than their monomeric counterparts; 3) effective endosomal escape alone or in combination with DOPE; and 4) suitability for long term storage, over two months at ambient temperatures, in lyophilized formulations without losing functionality [88, 89]. Similar to cationic lipids, the numerous variations to the head group, hydrophobic tails, and spacer contribute to the high number of permutations allowing the modulation of their physicochemical properties and biological activity for efficient gene delivery. Different formulations of gemini surfactants, from traditional cationic m-s-m or N,N-bis(dimethylalkyl)-α,ω-alkanediammonium surfactants (where m and s represent the number of carbon atoms in the alkyl tails and in the polymethylene spacer group) to peptide or carbohydrate based compounds, have been previously studied for applications in gene therapy [15].

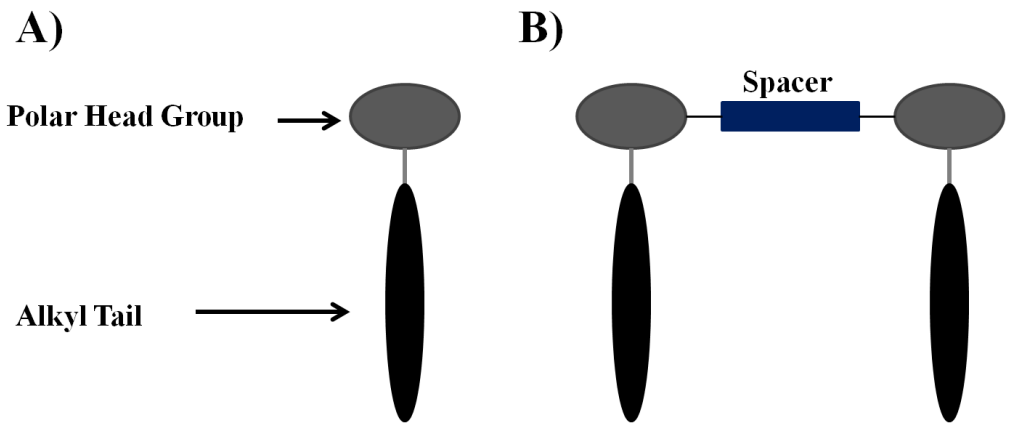

Figure 1.10 Structural schematic of conventional (A) and gemini (B) surfactants.

1.3.4.4.1 Lipoplex formation and gene transfection using m-s-m gemini surfactants

Similar to cationic lipids, lipoplex formation stems from electrostatic interactions between DNA and cationic gemini surfactants in an entropy driven process arising from the release of counterions from micelles and DNA [15]. Hence, gemini surfactants with a higher degree of micelle ionization, an indicator of counterion dissociation, are more efficient in DNA complexation [85]. DNA complexation is influenced by a number of contributing factors including the length and nature of hydrophobic tails as well as changes to the head group through modifications to spacer lengths and the inclusion of functional substitutions. Increasing alkyl tail length of m-s-m gemini surfactants serves to improve DNA compaction as result of greater hydrophobicity promoting stronger DNA interactions [90]. Alkyl tail lengths have profound effects on CMC as increasing alkyl tail lengths, with a fixed spacer, linearly decrease the natural log of CMC [15]. Such changes in CMC may alter DNA complexation and complex stability. Control of the CMC is critical as high CMC maintains a greater monomer concentration for DNA complexation while low CMC prompts better complex stability [91]. With respect to the nature of hydrophobic tails, increasing asymmetry between alkyl tails leads to an overall increase in hydrophobicity contributing to efficient DNA complexation [15]. The head group areas of m-s-m gemini surfactants are related to the polymethylene spacer lengths as head group areas increase with corresponding increases in spacer length up to a maximum at s = 10-12. Subsequent increases beyond the maximum results in the folding of the hydrophobic spacer causing the quaternary ammonium head groups to be in closer proximity [92]. As such, spacer lengths are able to modulate the degree of interaction between the nitrogen centres of m-s-m gemini surfactants and the phosphate

groups in DNA. Through manipulation to the spacer lengths of the 12-s-12 series of gemini surfactants, Karlsson et al. [90] have shown effective DNA complexation using gemini surfactants of short (s = 2-3) and long (s > 10) spacer lengths with intermediate spacer length being the least effective. Gemini surfactants with spacer lengths of 3 were confirmed to have compatible head group distances (~0.49 nm) that matched well with the spacing of phosphate groups (0.34 nm) in DNA [91]. Building on the findings from the impact of spacer lengths, amine substituted m-s-m surfactants, comprising of aza ($N\text{-}CH_3$) or imino (N-H) substituent(s) two or three methylene units apart, have been developed for the generation of multivalent gemini surfactants (m-5N-m, m-8N-m, m-7N-m, m-7NH-m) with better DNA binding and complexation (Figure 1.11) [87, 93, 94]. Similar to m-3-m surfactants, the distances for trimethylene spacers between the nitrogen centres in 12-7N-12 and 12-7NH-12 gemini surfactants were calculated to be ~0.51 nm [15].

As expected, gemini surfactants conferring improved DNA complexation were found to elicit enhanced transfection efficiencies. Increasing alkyl tail lengths corresponded to increases in transfection efficiencies with 16-3-16 and 18:1-3:18:1 gemini surfactants demonstrating higher transfection efficiencies over 12-3-12 gemini surfactant, with and without DOPE [95]. Asymmetric phytanyl-gemini surfactants (phy-3-m), possessing bulky hydrophobic tails, were previously demonstrated to achieve better transfection efficiencies over 16-3-16 gemini surfactants [85, 96]. Gemini surfactants with spacer lengths s = 3-12 were able to compact DNA into discrete 100-200 nm positively charged particles, but transfection efficiencies were highest using gemini surfactants with a trimethylene spacer (s =3) [87]. Increasing transfection efficiencies with spacers >12 was observed in correlation

with improved DNA complexation upon folding of the flexible spacer [91]. With respect to amine substituted gemini surfactants, 12-7NH-12 exhibited significantly greater transfection efficiencies over 12-3-12, 12-5N-12, 12-8N-12, and 12-7N-12 ($P < 0.01$); the dimethylene spacing in 12-5N-12 and 12-8N-12 gemini surfactants were found to be too short to facilitate binding with adjacent phosphate groups of DNA [93].

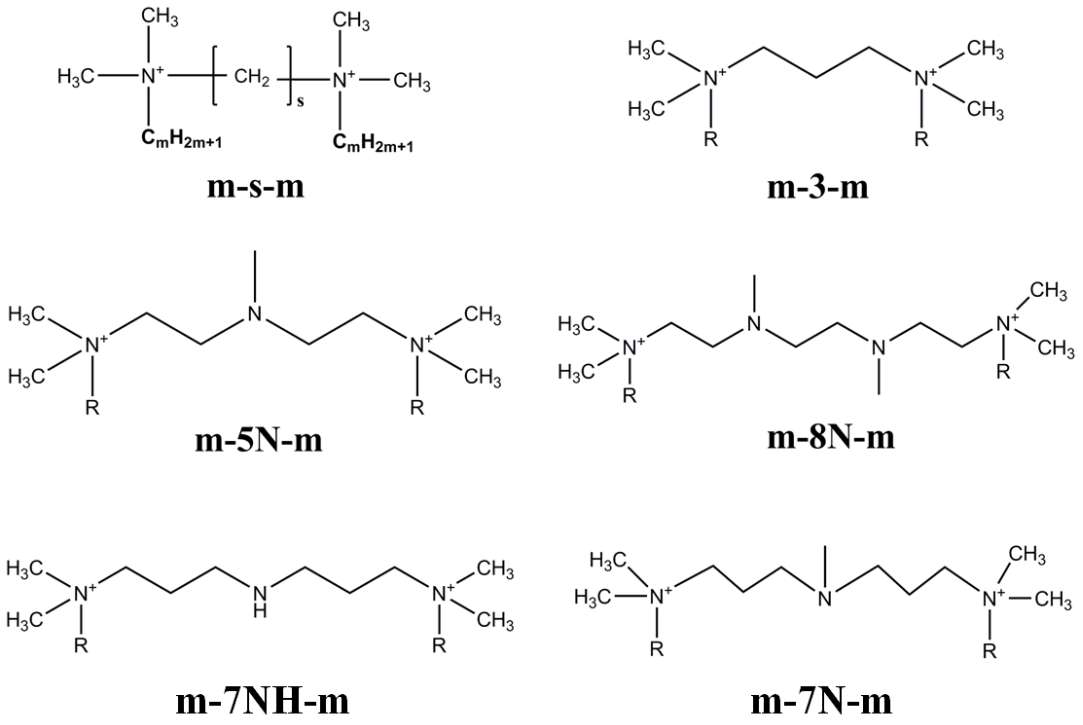

Figure 1.11 Chemical Structure of m-s-m gemini surfactants.

Despite the evident correlations between improved DNA complexation and transfection efficiencies, the ability of such gemini-based lipoplexes to adopt structural polymorphisms is considered to be the most important factor contributing to improved gene delivery [10, 15, 85, 91, 93, 97, 98]. Depending on the lipid to surfactant mol ratio and surfactant to DNA

(N^+/P^-) charge ratios, the incorporation of DOPE results in the formation of numerous phase structures including the previously mentioned lamellar, hexagonal, inverted hexagonal structures as well as cubic phase structures, characterized as spherical micelles arranged on a cubic lattice. In the absence of DOPE, 12-3-12/DNA, 16-3-16/DNA, and 18:1-3-18:1/DNA gemini based lipoplexes demonstrated insignificant gene delivery capacities due to their inability to adopt polymorphic structures [98]. However, the abovementioned lipoplexes, each possessing short trimethylene spacers (s = 3), demonstrated profound structural polymorphism upon the incorporation of DOPE [97]. The significance of DOPE may be attributed to the antagonistic mixing interactions between gemini surfactants and the neutral lipid [99], which may be responsible for structural polymorphisms that contribute to endosomal escape and successful gene delivery.

The application of imino substituted spacers, as in the m-7NH-m (m = 12, 16, 18, 18:1) series, demonstrated increased transfection rates, in the presence or absence of DOPE, when compared to unsubstituted gemini based lipoplexes. The transition from basic to acidic conditions, similar to that of early to late endosomes, conferred significant changes in aggregate size as result of the buffering capacity from the imino group and the corresponding pH-induced structural changes consistent with endosomal escape and increased transfection [93, 94]. Specifically, 12-7NH-12 gemini based lipoplexes exhibit a unique pattern with respect to changes in zeta potential upon changes in pH. The zeta potential curve for 12-7NH-12 revealed an initial rise in zeta potential at basic pH until reaching a plateau at pH of 7, before a sharp decrease around pH of 5.5; this corresponded to more prominent membrane fusion/collapse when compared to 12-3-12 gemini based lipoplexes [94]. As can be seen,

there are numerous factors at play in the rational design of gemini based synthetic vectors with optimal DNA complexation and high capacity for structural polymorphisms. However, highly efficacious gene therapeutics demand contributions from sound design of both the synthetic vector as well as the enclosed DNA cargo.

1.4 Recombinant Plasmid DNA (pDNA) Vectors

Recombinant plasmid DNA (pDNA) vectors for gene therapy typically consist of two essential components: i) an eukaryotic expression cassette containing genetic components pertinent to transgene expression in the eukaryotic host (gene of interest, promoter, intron, and transcription termination/polyadenylation signal), and ii) a prokaryotic backbone consisting of an origin of replication for plasmid amplification and an antibiotic resistance gene cassette for selection (Figure 1.12) [100].

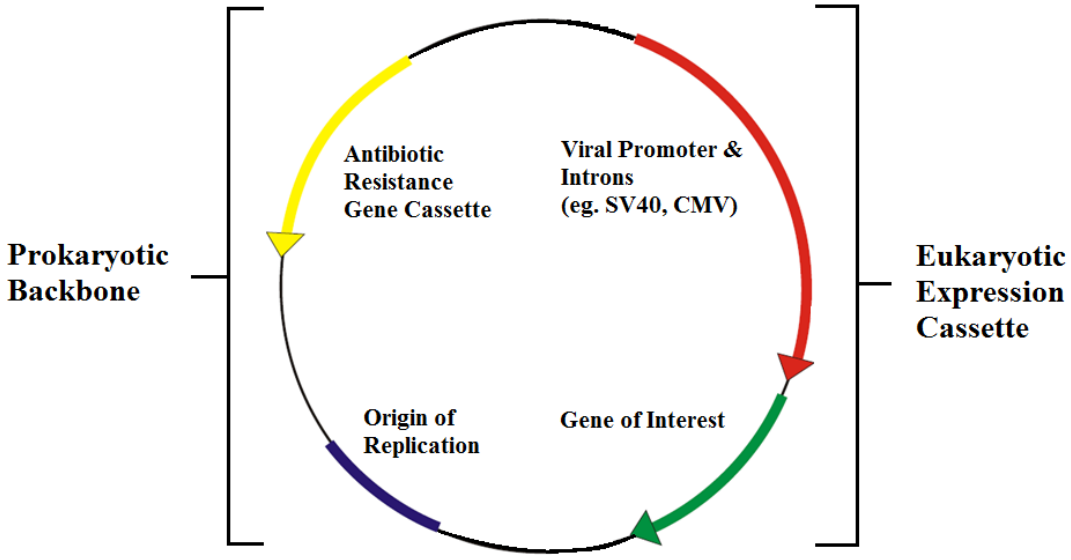

Figure 1.12 Recombinant plasmid DNA (pDNA) vectors.

While safer than their viral counterparts, non viral delivery of such circular covalently closed (CCC) pDNA vectors, alone or packaged within synthetic vectors, offers a limited safety profile as they often result in the transfer of antibiotic resistance genes as well as other unwanted prokaryotic sequences with CpG motifs. The unnecessary delivery of antibiotic resistance genes may enable horizontal gene transfers, giving rise to antibiotic resistant pathogens. Unmethylated CpG dinucleotides, or CpG motifs, have the potential for eliciting immunostimulatory responses which reduces the efficacy of the gene therapeutic and potentially impose detrimental effects onto the administered host. The bacterial genomic DNA has a higher frequency of CpG dinucleotides, and, unlike vertebrate animals, most of these dinucleotides remain unmethylated [101]. CpG motifs are capable of inducing immune responses as they are recognized as pathogen associated molecular patterns (PAMPs) primarily through interactions with toll-like receptor (TLR) 9 embedded in the endosomal membrane of immune cells including dendritic cells, B lymphocytes, monocytes, and macrophages [1, 102]. CpG binding to TLR9 results in the activation of eukaryotic transcription factors and upregulated pro-inflammatory cytokine production [103]. As TLR9 is situated within the endosome, the administration of synthetic vectors may heighten CpG mediated immunostimulatory responses. In particular, *in vitro* incubation of lipoplexes with macrophages/dendritic cells and *in vivo* intravenous administration of lipoplexes into mice both showed CpG mediated release of inflammatory cytokines at levels greater than naked pDNA [102]. The *in vivo* administration of modified pDNA vectors, with reduced CpG motifs, in to BALB/c mice demonstrated a 40-75% reduction in pro-inflammatory cytokine release [101]. The removal of additional CpG motifs, through modifications to

cytomegalovirus (CMV) enhancer and promoter regions, further diminished inflammatory responses while improving sustained transgene expression [104]. The effects of reduced immune responses and prolonged expression was also indicated upon the removal of CpG motifs in PEI/DNA polyplexes and DOTAP/DOPE/DNA lipoplexes [105]. Despite these improvements, Hyde et al. [106] revealed detectable inflammatory responses from the presence of even a single CpG motif upon intranasal delivery of lipoplexes into BALB/c mice. Aside from immune activation, CpG mediated TLR activation induces an antiviral state that inhibits gene expression and activates DNA degradation by nucleases [1]. Within the nucleus, the unmethylated CpG motifs may be subjected to DNA methylation which influences histone-DNA interactions and transgene expression. Recognition of methylated sites by methyl-CpG-binding domain proteins results in the repression of histone deacetylase which normally prevents histone hyperacetylation and the subsequent binding of transcriptional factors pertinent to transgene expression [102]. As such, transgene silencing severely hampers sustained expression upon successful delivery [107].

As pDNA vectors do not possess the inherent mechanisms for integration found in viral vectors, such vectors are significantly safer due to limited risks from insertional mutagenesis. However, conventional CCC pDNA vectors often possess elements or sequences, including viral promoters or cloned sequences, that could subject them to undesired recombination events [108]. Although rare, the potential risks of vector integration upon homologous recombination of CCC pDNA persist and this may lead to oncogenesis through the activation of proto-oncogenes or through the inactivation of tumor suppressor genes (see Section 1.1.2).

1.4.1 Novel DNA Vectors: DNA Minicircles and LCC DNA Minivectors

As previously explained, traditional recombinant pDNA vectors are flawed by the delivery of unnecessary prokaryotic sequences resulting in a risk of horizontal gene transfer of antibiotic resistance genes, CpG mediated immunostimulatory responses, and diminished transgene expression. Removal of the prokaryotic backbone for the generation of DNA minicircles and linear covalently closed (LCC) DNA minivectors serves a dual purpose of bypassing the abovementioned complications while improving the delivery process through the formation of smaller vectors that increase extracellular and intracellular bioavailability (Figure 1.13).

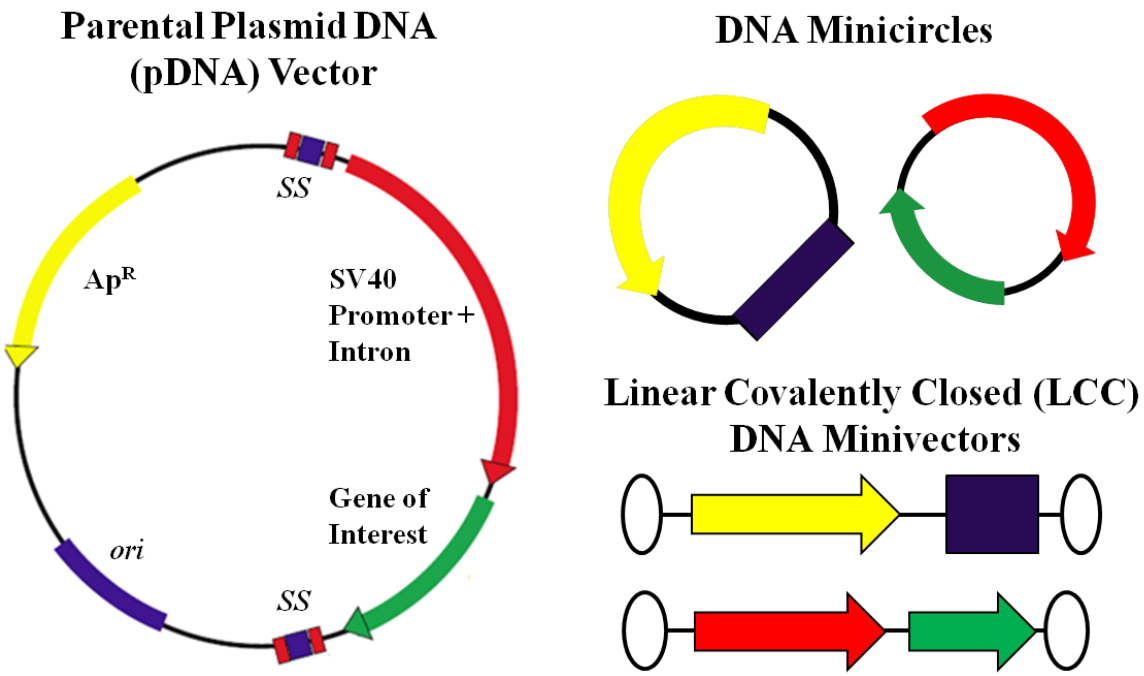

Figure 1.13 Schematic of plasmid DNA (pDNA) vectors, DNA minicircles, and Linear Covalently Closed (LCC) DNA minivectors.

1.4.1.1 DNA Minicircles

DNA minicircles are CCC supercoiled mini expression cassettes generated from *in vivo* site specific recombination mediated by phage derived recombinases [109]. These recombinases typically undergo "cut-and-paste" recombination processes by acting on specific recognition sites generally ranging from 30-40 base pairs or longer [110]. Such processes are employed for the production of DNA minicircles as site specific recombination offers excellent specificities while attaining high activity for efficient pDNA processing in the absence of any additional co-factors. The generation of DNA minicircles involves recombinases acting on target parental pDNA substrates, carrying a eukaryotic expression cassette flanked by two respective recognition sites, that results in the separation of the parental pDNA into two distinct parts: 1) a replicative miniplasmid carrying the prokaryotic backbone, and 2) a DNA minicircle with the expression cassette [103].

Depending on the catalytic amino acid residues involved in the recombination process, site specific recombinases are classified into: 1) the tyrosine or λ integrase family, and 2) the serine, or invertase/resolvase, family [110]. λ integrase, P1 Cre recombinase, and FLP recombinase from the tyrosine family along with ΦC31 integrase and ParA resolvase from the serine family have all been previously applied for the production of DNA minicircles (Table 1-1) [103, 109, 111-114].

Gene delivery using DNA minicircles have previously documented 10 to 1000 fold increases in long term transgene expression, *in vitro* and *in vivo*, over conventional CCC pDNA vectors [114]. Such improvements may be attributed to the elimination of transgene silencing, not simply through the elimination of CpG motifs, but specifically through the

removal of the prokaryotic backbone. Using DNA minicircles to examine backbone induced effects, Chen et al. [115] demonstrated transgene silencing from backbone sequences covalently linked to the eukaryotic expression cassette; however, such silencing was not observed from the co-delivery of backbone DNA and the expression cassette as separate entities. Despite improved transgene expression when compared to unaltered parental pDNA, transgene silencing persists upon the delivery of a modified parental pDNA absent of CpG motifs in the prokaryotic backbone [115]. Such findings were consistent with the hypothesis of transgene silencing from backbone sequence induced, heterochromatin-associated histone modifications spreading to the adjacent eukaryotic expression cassette [107, 115].

Table 1-1 Integrase involved in DNA minicircle production.

	Recognition Site	**Recombination Directionality**	**Notes**
Tyrosine Family			
λ Integrase	*attB/attP*	Unidirectional	Dimers observed
Cre Recombinase	34 bp *loxP*	Bidirectional	Intramolecular and Intermolecular recombination leading to dimeric or trimeric species. Mutation to *loxP* to favor unidirectional processing.
FLP recombinase	48 bp *FRT*	Bidirectional	Intramolecular and Intermolecular recombination leading to dimeric or trimeric species
Serine Family			
ΦC31 integrase	*attB/attP*	Unidirectional	Strictly unidirectional without concatemers
ParA resolvase	*Res*	Unidirectional	Strictly unidirectional without concatemers

1.4.1.2 LCC DNA Minivectors

LCC DNA minivectors are small, dumbbell shaped vectors possessing hairpin ends enclosing an eukaryotic expression cassette. The hairpin loops offer vast improvements in protection from exonucleases conferring greater stability, an issue that drastically hinders the successful delivery of linear DNA. Such vectors may be generated through three distinct *in vitro* enzymatic mechanisms: 1) pDNA digestion and ligation, 2) PCR amplification and ligation, and 3) protelomerase, or prokaryotic telomerase, mediated processing (Figure 1.14).

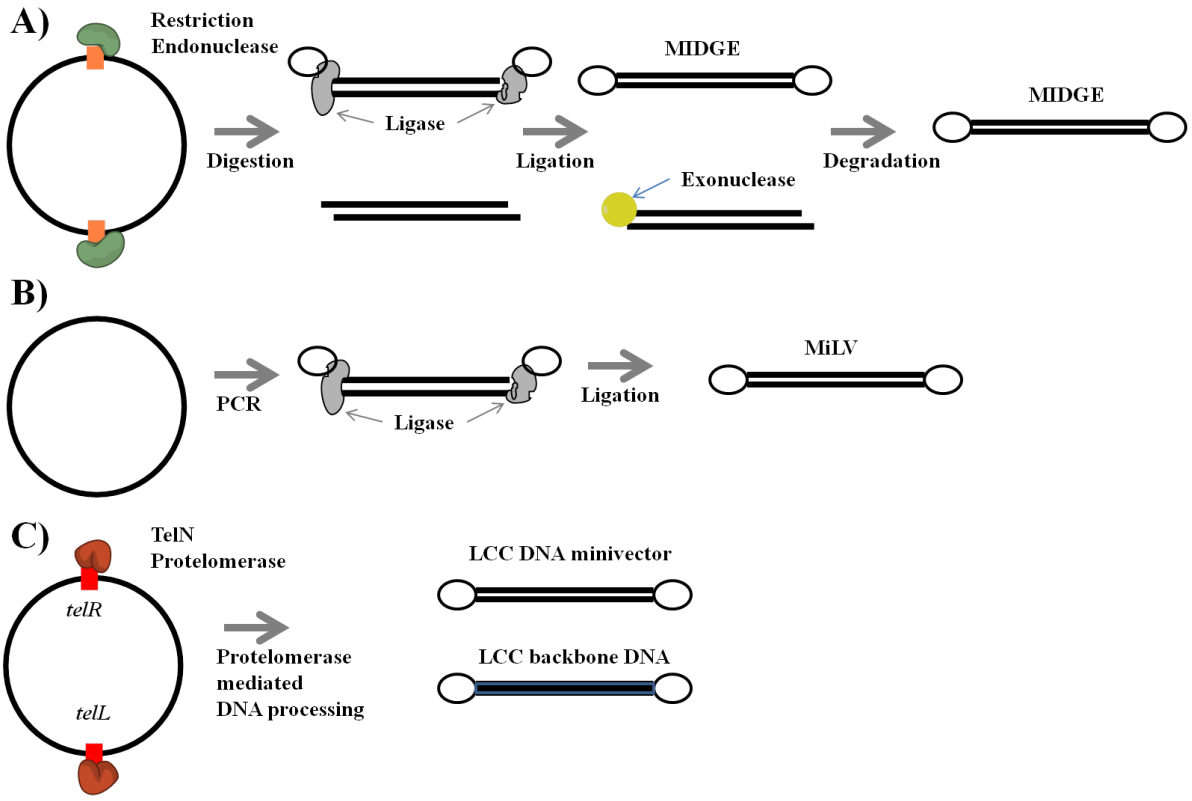

Figure 1.14 *In vitro* production of LCC DNA minivectors: A) Targeted pDNA digestion and ligation with hairpin oligonucleotides for the generation of minimalistic immunogenic defined gene expression vectors (MIDGE); **B)** PCR amplification and ligation with hairpin oligonucleotides for the generation of micro-linear vectors (MiLV); **C)** TelN protelomerase mediated pDNA processing for the generation of LCC DNA minivectors. Adapted from [116].

Minimalistic immunogenic defined gene expression vectors, or MIDGE, are the first generation of such vectors involving restriction endonuclease digestion of the parental pDNA vector, at sites flanking the eukaryotic expression cassette, followed by ligation with hairpin oligonucleotides for the formation of covalently closed ends [116]. The unprotected prokaryotic backbone sequences are subsequently removed by exonucleases, isolating the generated MIDGE vectors. Application of MIDGE vectors has previously shown improved transgene expression in colon carcinoma cells upon complexation with PEI and Lipofectamine [117] as well as improvements in transfection efficiencies to liver (2.5 fold), lungs (3.5 fold), kidneys (3.9 fold) and heart (17 fold) when compared to the parental pDNA vector upon *in vivo* hydrodynamic injection into BALB/c mice [118]. MIDGE vectors also have demonstrated potential to be effective DNA vaccines as the administration of such vectors, encoding the LACK antigen, offered protection from *Leishmania* infection in susceptible BALB/c mice at lower doses compared to conventional pDNA vectors [119].

As an alternative to MIDGE, micro-linear vectors (MiLV) are mini linear vectors generated from PCR amplification of the eukaryotic expression cassette followed by subsequent ligation with hairpin oligonucleotides. These vectors avoid additional steps involved in the removal of prokaryotic sequences and can be purified using PCR clean up kits. MiLV vectors were previously demonstrated to resist exonuclease degradation, improve transfection efficiency, prolong transgene expression, and reduce immunostimulatory effects when compared to conventional pDNA vectors [120].

With respect to protelomerase processing as a means of producing of LCC DNA vectors, certain strains of temperate bacteriophage replicate utilizing linear plasmids generated from a

protelomerase processing pathway. In contrast to most temperate bacteriophages, N15, PY54, and ϕKO2 are three prophages that do not undergo chromosomal integration and replicate extra-chromosomally as linear plasmids. N15 and PY54 are of particular interest as they share four distinct similarities: 1) both can infect *Escherichia coli*; 2) both exhibit structural features (hexagonal head and long contractile tail) that resemble lambda phages; 3) both are comprised of a 43.6 kb linear double stranded DNA genome that replicates as a low copy number plasmid; and 4) both use protelomerase, or prokaryotic telomerase, for the generation and replication of linear plasmids with covalently closed terminal ends [121].

Bacteriophage N15 derived protelomerase, TelN, has previously been applied for *in vitro* protelomerase mediated processing of parental pDNA vectors into LCC DNA minivectors. TelN protelomerase possesses catalytic tyrosine residues for unidirectional, cleave-joining activity in the absence of any additional co-factors. They recognize and associate with a 310 bp telomere occupancy site (*tos*) comprised of a series of inverted repeats centered on *telRL*, a 56 bp palindrome sequence [122, 123]. The 56 bp *telRL*, composed of a central 22 bp palindrome *telO* flanked by an inverted repeat (R3/L3), serves as the essential recognition sequence required for TelN binding and protelomerase mediated processing [124]. The two other inverted repeats (R1/L1 & R2/L2) within *tos* serve as additional association points offering better stability to the TelN-DNA complexes. TelN mediated processing begins with the binding of two TelN molecules, as a dimer, to *telRL* followed by the generation of a pair of staggered cuts within *telO* that results in 3’ phosphotyrosine DNA intermediates and subsequent rapid resolution into linear covalently closed (LCC) hairpin ends [123]. Heinrich et al. [100] generated bacterial sequence-depleted LCC DNA minivectors by inserting *telRL*

recognition sites, flanking the EGFP or IL-12 expression cassette, into the parental pDNA vector followed by *in vitro* processing using TelN protelomerase. The expression of EGFP or IL-12 was determined to be unaffected by the presence of hairpin ends and increased anti-metastatic capacity was observed, in an *in vivo* metastatic model, for IL-12 expressing minivectors when compared to parental CCC pDNA vector.

The bacteriophage PY54 derived protelomerase, Tel, shares an overall 60% similarity with TelN and possesses TelN-like unidirectional, cleave-joining activity in the absence of any additional co-factors [125]. Tel protelomerase recognizes and associates with a 140 bp *pal* site consisting of a 15 bp inverted repeat flanking a 42 bp perfect palindrome sequence that serves as the target site for protelomerase mediated processing. However, unlike TelN, the flanking inverted repeat is necessary for efficient processing under *in vivo* conditions [125]. Despite numerous similarities with TelN-*telRL* system, the Tel-*pal* system was not previously explored for *in vitro* production of LCC DNA minivectors.

1.4.1.3 Impact of Vector Size and Topology on Gene Delivery

DNA minicircles and LCC DNA minivectors are assumed to improve bioavailability due to their small sizes permitting efficient DNA packaging into synthetic vectors and rapid intracellular trafficking upon cytoplasmic release. Despite the fact that lipoplex size and structure do not vary with increasing pDNA length, the number of pDNA vectors incorporated into each lipoplex increases linearly with decreasing pDNA size [126]. Transfection activity of lipoplexes is proportional to the number of enclosed pDNA with the most active lipoplexes possessing the largest amounts of pDNA. The advantages of smaller pDNA were confirmed as smaller pDNA attained higher transfection efficiency over larger

pDNA when lipoplexes were restricted to possess a single coding cassette in each particle [126]. In a more systematic approach, Yin et al. [127] assessed the transfection efficiencies of varying pDNA sizes by incorporating "stuffer" DNA of different lengths. An inverse correlation between relative transgene expression and pDNA size was observed with most significant decreases occurring upon the addition of stuffer DNA ranging from 0 and 6.5 kb in size. Promoter activity and the effects of enhancer elements were both negatively affected by increasing stuffer DNA and such trends were consistent across all tested promoters and cell types [127].

With respect to DNA topology, no differences were observed in the complexation of linear and circular DNA with PEI, PLL, or Lipofectamine [128]. However, LCC DNA vectors exhibited enhanced transgene expression over CCC pDNA vectors as demonstrated by Kamiya et al. [129] through cytoplasmic and nuclear microinjections along with transfection using Lipofectamine. Microinjection of LCC vectors into the nucleus of Cos-7 cells elicited a 5-10 fold increased transgene expression over its CCC pDNA counterpart. Transgene expression of LCC DNA vectors was observed to be more efficient than CCC pDNA for up to 14 days post-microinjection; in contrast, linear open (LO) DNA vectors exhibited a more rapid decrease in transgene expression when compared to CCC pDNA. Subsequent studies involving cytoplasmic microinjection and transfection with Lipofectamine also demonstrated improved transgene expression from LCC DNA vectors over CCC pDNA. Size dependent effects on transgene expression were observed as higher transgene expression was correlated with decreasing LCC vector sizes upon cytoplasmic/nuclear microinjection and Lipofectamine mediated transfections. In all cases,

the smallest tested LCC DNA minivector (2.3kb) exhibited the highest expression [129]. Such improvements in transgene expression from LCC DNA vectors were postulated to be associated with drastic improvements in stability and easier transcriptional factor loading in absence of DNA supercoiling.

1.5 One-Step *in vivo* Linear Covalently Closed (LCC) DNA Minivector Production System

LCC DNA minivectors serve to be superior to conventional CCC pDNA vectors due to enhancements to transfection efficiency and safety. However, the abovementioned multi-step enzymatic approaches hinder downstream large-scale productions due to the high costs of enzymes as well as the labor intensive processes associated with minivector production and purification. To address such drawbacks, Nafissi & Slavcev [108] developed a one-step, *E. coli* based *in vivo* LCC DNA minivector production system for facile and efficient production of LCC DNA minivectors referred to as DNA ministrings (Figure 1.15). The production system was constructed through the genetic engineering of W3110 $RecA^+$ *E. coli* cells and the design of specific genetic constructs catered to *in vivo* processing of parental pDNA substrates by protelomerases. In brief, the construction of TelN and Tel recombinase expressing cells (R cells) involved the following steps: 1) PCR amplification of protelomerase encoding *telN* and *tel*; 2) genetic cloning of the PCR products into an inducible prokaryotic expression plasmid, pPL451, for CI[Ts]857 mediated thermoregulation of *telN/tel* gene expression; and 3) chromosomal integration of thermoregulated *telN/tel* expression cassette into the *lacZ* gene using a pBRINT-cat integrating plasmid followed by

subsequent confirmation of integrants through blue/white screening [108]. The successful construction of R cells serves as the basis of the LCC DNA minivector production system.

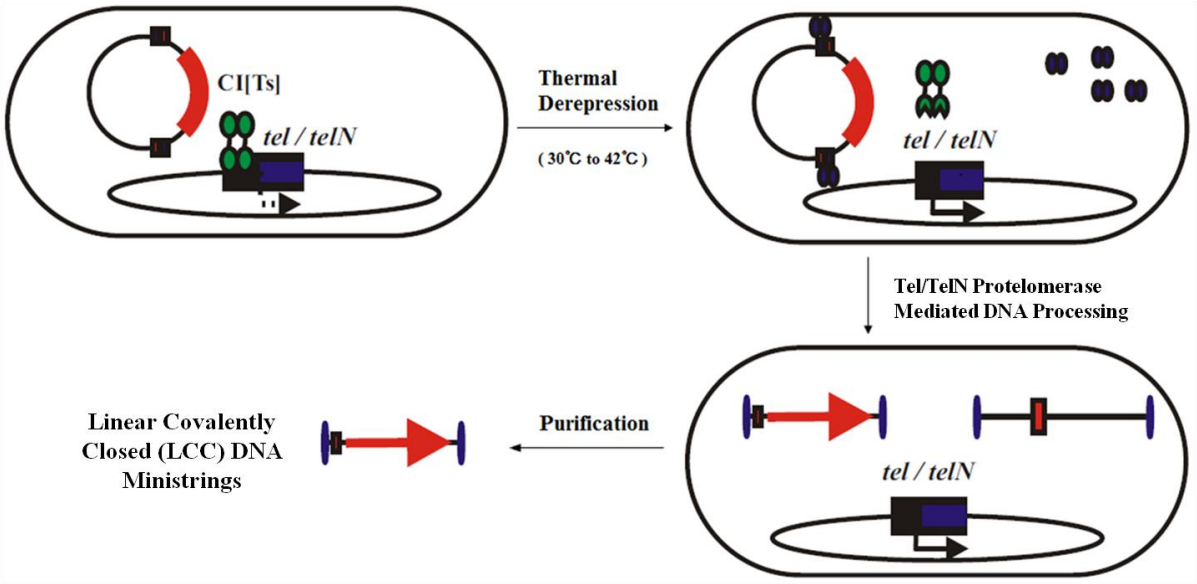

Figure 1.15 Schematic of the one-step *in vivo* LCC DNA minivector production system. The *in vivo* production system involves a recombinant *E. coli* for thermoregulated expression of TelN/Tel protelomerase. In the temperature inducible system, protelomerase expression is repressed by a CI[Ts]857 repressor at temperatures below 37° C. Temperature upshift to 42° C causes instability and dissociation of the thermolabile repressor which allows for controlled expression of protelomerase. Subsequent enzymatic activity of the expressed protelomerase on parental pDNA vector substrates results in DNA processing into LCC DNA ministrings.

In order for parental pDNA vectors to become substrates for protelomerase processing, the vector must inherit respective protelomerase recognition sequences of *telRL* and *pal*. This was accomplished by the insertion of specific genetic constructs, referred to as the "SuperSequence", flanking the eukaryotic expression cassette (Figure 1.16). The SuperSequence was comprised of the entire 142 bp *pal* sequence with the inclusion of Cre, FLP, and TelN minimal target sites (*loxP, FRT, telRL*) within the non-specific regions outside of the 42 bp perfect palindrome and the 15 bp inverted repeats [108]. In each

SuperSequence, the 142 bp *pal* was flanked by two 72 bp SV40 enhancer sequences acting as DNA-targeting sequences (DTS) for improved nuclear entry. The constructed vector was a 5.6 kb pDNA that possessed a 3.2 kb prokaryotic backbone and the resulting 2.4 kb DNA ministring, consisting of two SuperSequences flanking the EGFP eukaryotic expression cassette. This system offers high versatility as the eukaryotic expression cassette can be interchanged to suit the expression of the desired gene of interest.

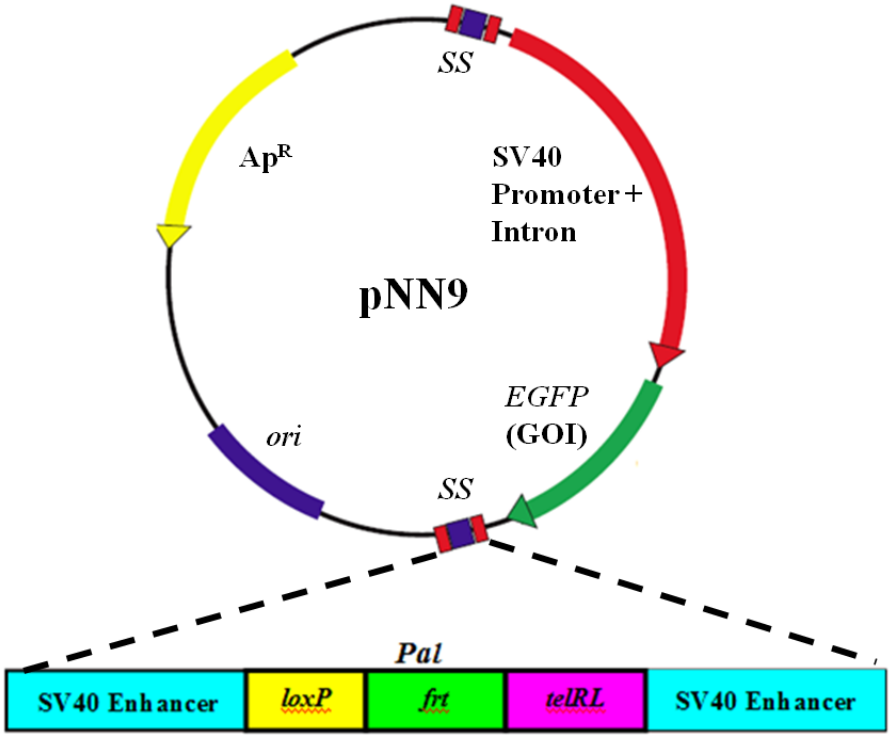

Figure 1.16 Parental pDNA vector substrate (pNN9) for the production of LCC DNA ministrings. The 5.6 kb pDNA vector (pNN9) possesses two SuperSequences flanking the eukaryotic expression cassette for the generation of LCC DNA ministrings. Within each SuperSequence, *pal* and *telRL* act as protelomerase recognition sequences for the production of LCC DNA ministrings upon processing by Tel and TelN protelomerases. In addition, *loxP* and *FRT* act as recognition sequences for Cre and FLP mediated production of DNA minicircles. SV40 enhancer sequences serve as DNA-targeting sequences (DTS) for improved nuclear entry during gene delivery.

1.5.1 Incorporation of Multiple DNA-targeting sequences (DTS) for Improved Nuclear Entry

The SV40 enhancers within each SuperSequence act as DTS for NFκB assisted nuclear transport of LCC DNA ministrings through the NPC. Previously, the SV40 enhancer was demonstrated to bind to over 10 distinct transcriptional factors. [21, 130]. In particular, the ubiquitously expressed NFκB possesses high binding affinity (K_D ~10^{-10} to 10^{-13}M) for DTS and, upon binding, NFκB undergoes conformational changes that exposes the buried NLS peptide for shuttling of the multiprotein/DNA complex through the NPC [1, 131, 132]. Previous studies indicated rapid gene expression at lower dosages with SV40 DTS containing pDNA upon cytoplasmic microinjection; however, differences in expression were lost after cell division, signifying the ability of SV40 enhancers to bypass the intact nuclear membrane [133]. The inclusion of six DTS was demonstrated to result in rapid nuclear accumulation and higher number of pDNA in the nucleus, but such improvements were abrogated in the presence of an NFκB inhibitor [132]. Due to the small sizes of LCC DNA ministrings and the close proximities of the SV40 DTS to the enclosed eukaryotic expression cassette, the binding of NFκB could act as transcriptional enhancers that improve transgene expression. Hence, the incorporation of multiple SV40 DTS into DNA ministrings may serve a dual purpose driving rapid nuclear entry and transgene expression.

1.5.2 DNA Ministrings: A DNA Vector with a Heightened Safety Profile

Aside from the removal of CpG motifs deterring immunostimulatory responses, DNA minicircles pose potential safety concerns with regards to undesired recombination events leading to insertional mutagenesis. In contrast to DNA minicircles, LCC DNA ministrings

have a heightened safety profile as insertional mutagenesis is inhibited by covalently closed terminal ends conferring double-strand breaks that cause chromosomal disruption and cell death in the low frequency event of chromosomal integration. Such notions of heightened safety were demonstrated by Nafissi & Slavcev [108] as forced chromosomal integration of LCC DNA followed by subsequent thermoregulated expression of TelN/Tel protelomerase led to dramatically reduced cell viability in Tel^+ R cells, exhibiting a 5-fold greater killing effect than in the $TelN^+$ counterpart. Upon visualization of the *E. coli* integrants, induced protelomerase expression conferred highly contracted and irregular cell morphology when compared to integrants without the SuperSequence or integrants with repressed protelomerase expression. The surviving colonies of protelomerase expressing integrants were drastically lower and retained such irregular cell morphologies when grown in the presence or absence of protelomerase [108].

1.6 Summary & Thesis Objectives

GT offers limitless potential for the treatment of numerous diseases with demonstrated applications in vaccine development. Despite continuing successes of viral based gene therapeutics achieving significant clinical outcomes, these highly efficacious vectors pose important safety concerns with respect to undesired immunostimulatory effects and/or insertional mutagenesis. Non-viral delivery systems are considered to be safer alternatives to viral vectors with tremendous upside in terms of versatility, scalability, and cost-effectiveness. However, they suffer from low transfection efficiencies as they lack inherent mechanisms to overcome the numerous extracellular and intracellular barriers to gene delivery. Among the different physical and chemical systems, lipid-based synthetic vectors have shown the capacity to bypass such barriers and extensive understanding into the intrinsic mechanisms involved allow the subsequent production of highly efficacious synthetic vectors. Gemini surfactants possess inherent properties that make them suitable candidates for the generation of synthetic vectors with improved transfection efficiencies. Investigations into the molecular properties of gemini surfactants, their interaction with DNA, and the structural activity of resulting lipoplexes contributed to the rational design of novel gemini surfactants as synthetic vectors catered to GT. Similarly, the rational and intelligent design of novel DNA vectors serves to further improve therapeutic outcomes, allowing the generation of vectors with heightened safety profile while achieving efficacies that parallel their viral counterparts. Specifically, linear covalently closed (LCC) DNA ministrings are genetically designed to improve intracellular delivery of the DNA cargo, leading to enhanced transgene expression. In addition, LCC DNA ministrings offer an

additional level of safety as they inhibit insertional mutagenesis through covalently closed ends conferring double-strand breaks that cause chromosomal disruption and cell death in the low frequency event of chromosomal integration. The development of a one step *in vivo* LCC DNA minivector production system allows facile and rapid production of LCC DNA ministrings, thus addressing the limitations of scalable production as seen previously with the *in vitro* production of such minivectors.

1.6.1 Objectives

The overall objective of this project aims to streamline the production and purification of LCC DNA ministrings for the generation of novel lipid-based synthetic vectors with numerous potential downstream applications. Although, the *in vivo* LCC DNA minivector production system permits rapid, cost-effective, and scalable production of LCC DNA ministrings, the current system suffers from imperfect yields due to incomplete plasmid processing. Hence, the system must be optimized to improve processing of CCC pDNA precursors for greater yields during large scale productions. In order for the resulting DNA ministrings to be suitable for use in clinical settings, the minivectors are required to be purified towards the generation of pharmaceutical grade vectors in the absence of residual CCC pDNA precursors. Synthetic vectors derived from LCC DNA ministrings were characterized and assessed, with comparison to CCC pDNA derived vectors for their potential as gene therapeutics. Lastly, as a proof of concept demonstrating the versatility of LCC DNA ministrings in different applications, the minivector production system was used to generate LCC DNA ministrings catered to the downstream development of a HIV DNA virus-like particle (VLP) vaccine.

Specific objectives are listed below (Figure 1.17):

1) Optimization of the one-step *in vivo* LCC DNA minivector system through the assessment of induction duration, cultivation strategy, and genetic/chemical modifications on LCC DNA ministring production efficiency.
2) Separation and purification of LCC DNA ministrings towards the generation of pharmaceutical grade DNA vectors using anion exchange membrane chromatography.
3) Characterization of DNA/16-3-16/DOPE gemini based lipoplexes for the delivery of LCC DNA ministrings. This includes physical characterization by particle size, zeta potential, and DNase sensitivity along with transfection efficiencies.
4) Design and production of LCC DNA ministrings conferring the expression of a chimeric gag-V3 virus-like particle (VLP) with aims of demonstrating targeted delivery of the synthetic vector into dendritic cells. This serves as a proof of concept highlighting the versatility of DNA ministrings and act as the initial steps in the downstream development of a HIV DNA-VLP vaccine.

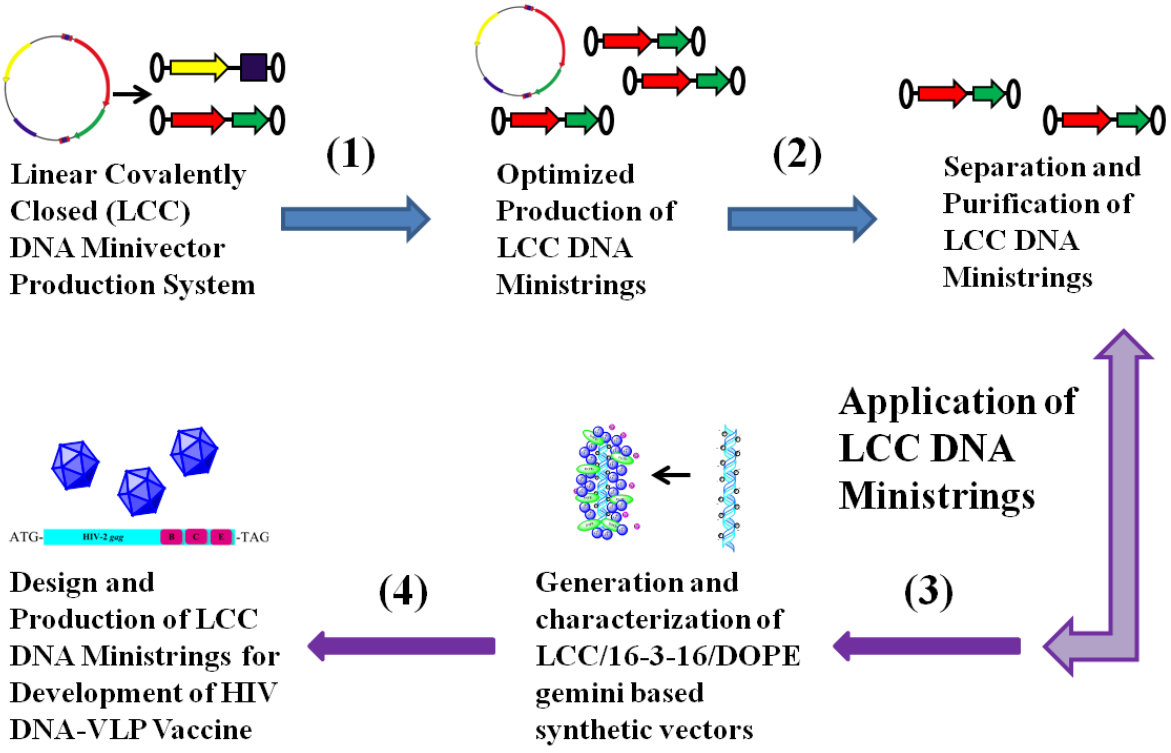

Figure 1.17 Flow chart of progression from production and purification to application of LCC DNA ministrings.

Chapter 2

Optimization of a One-Step Heat Inducible *in vivo* LCC DNA Minivector Production System

2.1 Introduction

The application of a one-step, *E. coli* based *in vivo* LCC DNA minivector production system generates minivectors through site-specific recombination on target parental pDNA substrate possessing an eukaryotic expression cassette flanked on each side by a multi-target site called SuperSequence [108]. The *in vivo* expression of TelN or Tel protelomerases results in the separation of the parental pDNA into two distinct parts: 1) a LCC mini-plasmid carrying the prokaryotic backbone, and 2) a LCC DNA minivector, referred to as DNA ministrings (Figure 2.1). LCC DNA ministrings are minimalistic expression vectors carrying the eukaryotic expression cassette necessary for the expression of the gene of interest. Within this *E. coli* based system, protelomerase expression, through a strong λ *pL* promoter, is regulated by temperature sensitive CI[Ts]857 repressor, whereby high level expression of the protelomerase occurs under temperature-induced conditions but not under repressed conditions. The current approach involving chromosomal integration of a single copy of the protelomerase gene, controlled by this temperature inducible system, corresponds to effective but imperfect plasmid processing efficiency that is comparable to the overall 50-90% recombination efficiency exhibited by DNA minicircle production employing an inducible system [103, 108].

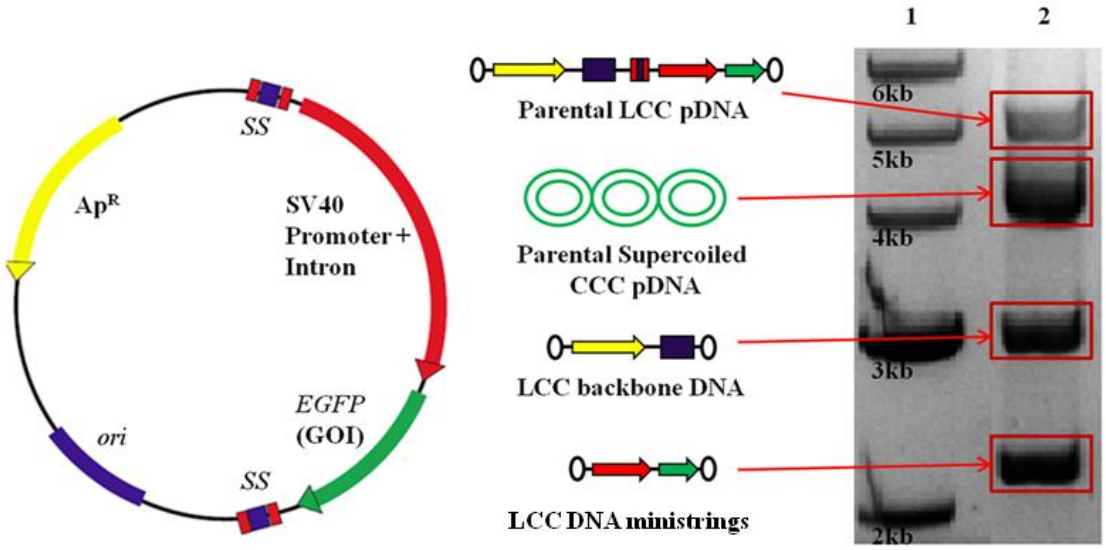

Figure 2.1 LCC DNA ministring production using the one-step *in vivo* LCC DNA minivector production system. Generation of LCC DNA ministrings involves TelN or Tel protelomerase acting on the SuperSequence multi-target site. A variety of DNA isoforms/species arises during LCC DNA ministring production: 1) parental LCC pDNA (5.6 kb); 2) parental supercoiled CCC pDNA (~4.0 kb); 3) LCC plasmid backbone DNA (3.2 kb); 4) LCC DNA ministring possessing *egfp* as the gene of interest (2.4 kb).

The *E. coli* K-12 host has often been exploited for recombinant protein expression due to rapid, scalable, high density growth contributing to high quantities at low production costs [134-136]. High recombinant protein yields are attributed to the highly characterized genetic profile of *E. coli* and the availability of numerous strong inducible promoters, vector designs, and mutant strains. [134, 137, 138]. Strong inducible promoters drive dedicated recombinant protein expression through induction of an inducer (eg. IPTG), an alteration to nutrient availability, or a manipulation of specific growth conditions (eg. temperature, pH) [134]. Temperature inducible systems enable fine control of recombinant protein expression through transcriptional regulation using the combination of strong major leftward (*pL*) /

rightward (*pR*) promoters and CI[Ts]857, a mutant thermolabile repressor derived from bacteriophage λ. At lower temperatures, typically around 30° C, the tight binding of CI[Ts]857 repressors to *pL/pR* operators outcompetes RNA polymerase from binding to overlapping *pL/pR* promoters which subsequently inhibit transcription.

However, at elevated temperatures above 37° C, the thermolabile repressor becomes increasingly unstable and dissociates from the operator [134, 139]. Release of the repressor thereby enables transcription of recombinant genes downstream of the *pL/pR* promoter. Depending on the protein, bacterial strain, and culture conditions, the application of the *pL/pR*-CI[Ts]857 temperature inducible system confers yields as high as 30% of total protein [134], and has been shown to attain 160% of total protein synthesis in non-induced cells [140]. Such high yields are attributed to several inherent advantages: 1) fine repressor control as a single copy of *cI857* gene on each multicopy plasmid is capable of eliciting transcriptional control over its *pL/pR* promoters; 2) cost effective and scalable production as recombinant protein is expressed in absence of any special media or expensive inducers; 3) high efficiency as contamination risks and additional downstream processing, including the removal of potentially toxic inducer by-products, are limited; and 4) high versatility as the expression system can be implemented into various *E. coli* strains [134].

Difficulties in achieving optimal recombinant protein expression stem from various issues relating to low expression levels, poor protein solubility, activation of stress responses, and protein degradation [135]. Despite the implementation of *pL/pR* strong promoters, mitigating low expression levels, there are several interrelated factors that must be taken into consideration when applying temperature inducible expression systems: 1) host strain

selection, 2) plasmid maintenance, 3) culturing strategies, and 4) heating strategies [134, 136, 139]. Different *E. coli* strains possess varying recombinant protein expression capacities and efficiencies. For efficient recombinant protein expression, the producer strain must attain: stable plasmid maintenance, protein solubility, high protein yields, and restricted proteolytic activity [136]. Stable maintenance of plasmids requires sufficient plasmid replication and partitioning for even distribution across dividing bacterial cells. However, excessive replication, in conjunction with recombinant protein expression, may introduce metabolic burden and cell exhaustion rendering growth arrest and low production [141]. Plasmid copy number, the average number of plasmids in host bacterial cells and an indicator of plasmid replication rate, must be maintained within range to allow plasmid propagation into daughter cells while preventing negative effects of host exhaustion. Temperature upshift and recombinant gene overexpression has been shown to inhibit plasmid replication while plasmid instability and degradation are observed upon extended incubation at high temperatures around 42° C [140, 142]. This demonstrates an intricate balance between recombinant protein expression, temperature upshift, and plasmid maintenance. Recombinant protein expression is favored during exponential growth phase as there is adequate cellular activity and metabolic resources for protein expression [141]. High levels of recombinant protein expression warrant high cell density cultures achieved by batch, fed-batch, and/or continuous cultivation [136, 143]. Fed-batch systems have often been utilized for fine control over growth phase and its separation from production phase, ensuring plasmid maintenance and low levels of metabolic stress during recombinant protein expression [134]. Similarly, two phase continuous systems have been implemented to achieve high cell density and

plasmid stability prior to the induction of recombinant protein expression, thereby ensuring higher productivity [144].

An optimal heating strategy is the most important factor in successful recombinant expression using temperature inducible systems, as numerous stress responses become activated upon expression. Induced overexpression of recombinant proteins contributes to metabolic aberrations and stresses triggering numerous cellular responses including: general stress response, heat shock like response, stringent (a.a. starvation) response, and SOS (DNA damage) response. Such responses may elicit altered physiological states including growth arrest and decrease in specific growth rates [139], ribosome degradation and diminished protein synthesis [145], and protein misfolding/degradation [141, 146]. As overexpressed recombinant proteins often require folding modulators, high level expression may overload translational machinery resulting in protein misfolding. Hence, the potential for misfolding increases with the utilization of strong promoters and high levels of induction [138]. The accumulation of unfolded/misfolded proteins favours protein aggregation, inclusion body formation, and the activation of the RpoH (σ^{32}) regulon triggering a heat shock-like response. The RpoH regulon consists of at least 120 genes conferring the expression of heat shock proteins (HSPs) including chaperones (ClpB, DnaK/J, GrpE GroEL/ES, ibpA, ibpB) and proteases (FtsH/HflB, Lon, ClpP, DegP, OmpT) that are associated with protein folding and degradation [134, 141, 147, 148]. Upon analysis of transcript profiles after induced recombinant protein expression, Gill et al. [147] linked overexpression with the upregulation of 11 stress related genes including most of the abovementioned chaperones and proteases. High level expression downregulates translational machinery and diverts resources away

from cell growth/division as demonstrated by a six fold increase in ATP demand upon the activation of recombinant overexpression and HSPs [134]. The formation of aggregates with varying size and complexity interferes with normal cellular metabolism [149]. These combined effects become significantly more prominent under the nutrient-depleted conditions found in high density cultures. High cell density and recombinant protein production constitute nutrient-limiting and slow growth conditions that introduce general stress response and subsequent entry into stationary phase upon activation of the RpoS regulon [139, 141, 150, 151].

Simultaneously, heat induction activates the heat shock response (HSR) affecting the quantity and overall quality of the recombinant protein. Heat induction negatively affects protein folding and increases inclusion body formation [139, 143]. The activation of heat shock proteases results in the degradation of recombinant protein, lowering yields. Recombinant proteins are more susceptible to proteolytic degradation mediated by five **A**TPase-**A**ssociated with diverse cellular **A**ctivities (AAA+) heat shock proteases: Lon, ClpYQ/Hs1UV, ClpAP, ClpXP, and FtsH [136-138, 151]. These AAA+ proteases are involved in various cellular processes including DNA replication, transcription, membrane fusion, and proteolysis. They perform processive proteolysis through several key steps: 1) substrate recognition/binding; 2) unfolding; 3) translocation; and 4) proteolytic cleavage [152].

The optimization of the one-step *in vivo* LCC DNA minivector production system warranted investigation into optimal induction schedules as temperature must be finely tuned in order to avoid detrimental effects of deceased growth rate, cellular damage, reduced

viability, plasmid instability, and diminished recombinant protein expression. In this study, various heating conditions were explored with the intention of effective recombinant protelomerase expression corresponding to high DNA ministring yields upon maximal protelomerase mediated pDNA processing. Induction duration was optimized to circumvent the negative effects arising from prolonged heat stress. As scalability is one of the key advantages associated with temperature inducible systems, induction duration was optimized to accurately reflect changes to culture volume. In addition, the two stage continuous culturing strategy was implemented for comparison with batch cultivation, a strategy commonly employed in laboratory settings. Concurrent with optimization through manipulations to heating and culturing strategies, genetic and chemical modifications were also applied in an attempt to improve DNA ministring production. Since heat shock proteases are known to play a critical role in the degradation of recombinant proteins upon activation by heat stress and induced expression, protease-specific and associated gene deletions were introduced to promote chaperone mediated protein re-folding such that protein degradation by heat shock proteases would be minimized. It was hypothesized that the introduction of these deletions would extend Tel protelomerase turnover, thereby enhancing Tel-mediated LCC DNA processing and DNA ministring production. The introduction of *dnaB* helicase mutations and the antibiotic ciprofloxacin, to transiently curb pDNA replication during induced protelomerase expression, were also investigated as alternative strategies to promote the complete processing of all substrates.

2.2 Materials and Methods

2.2.1 Strains and Plasmids

The pNN9 vector [108] was used as the parental pDNA substrate for the production of LCC DNA ministrings (see Figure 1.16). *E. coli* K-12 strains were use to generate all recombinant cell constructs and JM109 was employed as hosts for plasmid amplification. A list of bacterial strains used in this study is shown in Table 2-1.

2.2.2 Assessing Effects of Volume and Culturing Conditions on DNA Ministring Production

For batch cultivation, a single colony of $TelN^+$ W2NN [pNN9] or Tel^+ W3NN [pNN9] was grown overnight in 5 ml LB + Ap (100 µg/ml) under repressed conditions at 30° C with aeration. Fresh cells were grown from the overnight culture at 1:100 dilution of various culture volumes (10, 20, 50, 500 ml) in a 250 ml or 2 L Erlenmeyer flask at 30° C with aeration to late log phase A_{600} = 0.8. Protelomerase expression was induced upon temperature upshift and incubation at 42° C for various timed durations (15, 30, 60, 120 min). After induction, the cultures were subjected to post-induction temperatures 37° C for 30 min prior to overnight incubation at 30° C. Cells were harvested and plasmid extracted with *E.Z.N.A.* Plasmid Mini/Maxi-Prep Kit (Omega, VWR). DNA ministring production efficiency was assessed by AGE and densitometry (AlphaImager, Alpha Innotech). Production efficiencies were calculated as a percentage of the total amount of the two LCC DNA product species over the total amount of monomeric DNA comprising of LCC DNA and all isoforms of the parental pDNA.

For representative two-stage continuous cultivation, a single colony of Tel^+ W3NN [pNN9] was grown overnight in 5 ml LB + Ap (100 µg/ml) under repressed conditions at 30° C with aeration. Two batches of fresh cells were grown from the overnight culture at 1:100 dilution of 50 ml LB + Ap in 250 ml Erlenmeyer flasks at 30° C with aeration to late log phase A_{600} = 0.8. Cells were then collected, centrifuged at 4K RPM for 10 min, and re-suspended in 1 ml of LB + Ap. The re-suspensions were added into a preheated 2L Erlenmeyer flask containing 500 ml of LB + Ap (100 µg/ml) for incubation at 42° C until A_{600} = 1.0 (Two Stage Continuous A). An alternative heating condition was assessed where temperature upshift was extended for an additional 60 minutes after A_{600} = 1.0 (Two Stage Continuous B). Cultures were subjected to gradual temperature downshift and grown at 30° C overnight. Cells were harvested and plasmid extracted with *E.Z.N.A.* Plasmid Maxi-Prep Kit (Omega, VWR). DNA ministring production efficiency was assessed by AGE and densitometry (AlphaImager, Alpha Innotech). Calculations for the approximate amount of DNA ministring in each extraction was accomplished through densitometry comparisons between the 2.4 kb band and the 3 kb band of the DNA ladder, a known standard containing 125 ng of DNA for every 10 µl of DNA ladder, along with subsequent extrapolations accounting for the amount of sample loaded and the total eluted volume from each respective extraction. The estimated bacterial cell concentration in the extracted culture was calculated according to optical density readings from A_{600}.

2.2.3 Assessing the Introduction of Protease-specific and Associated Gene Deletions to Enhance LCC DNA Processing

Temperature inducible protelomerase expression cassettes (*lacZ::Cm-cI857-telN* and *lacZ::Cm-cI857-tel*) from the previously established LCC DNA minivector production systems (W2NN/W3NN) [108] were introduced into four different strains, conferring four protease and protease associated single gene knockouts (Δ*clpP*, Δ*lon*, Δ*hflx*, Δ*hflk*) [153], and their parental strain (BW25113) by P1 bacteriophage-mediated transduction. W2NN/W3NN cells were grown overnight in 5 ml LB + Cm (25 µg/ml) at 30° C. Phage generation from the donor strain was accomplished by the addition of 1:10 dilutions of P1rev6, prepared in 1 ml of TN buffer (0.01 M Tris-HCl and 0.1M NaCl, pH 7.8; Fisher Scientific, USA), into 300 µl of bacterial cells before adding 3 ml of top agar (Bacto Tryptone and Bacto Agar from Difco Laboratories, Sparks, MD). The solution was poured onto LB plates and incubated for 24 h at 37° C prior to lysate preparation. Approximately 5 ml of TN buffer was added to the surface of the plate and incubated for an additional 8 h at 4° C. TN buffer and the underlying top agar were collected into a sterile conical tube and centrifuged at 12K RPM (Avanti J-E Centrifuge, Beckman Coulter, Mississauga, Canada) at 4° C for 20 min. Lysate was poured into a new pre-chilled conical tube and briefly vortexed upon the addition of 50 µl of $CHCl_3$ (Fisher Scientific, USA). The five recipient strains were grown overnight in 5 ml LB or 5 ml LB + Kan (50 µg/ml) at 30° C prior to transduction. 1 ml of each of the overnight cultures was centrifuged at 6000 RPM for 5 min. The supernatant was discarded and the pellet was re-suspended with 1ml of 10 mM $MgSO_4$ + 10 mM $CaCl_2$ salt solution. 100 µl of the cell re-suspension was mixed with 100 µl LB and 100-1000 µl of

phage lysate depending on phage titre. The cell mixture was incubated at 37° C for 20 min to allow phage adsorption and infection. Subsequently, 200 µl of 1M sodium citrate and 1 ml of LB were added prior to 1.5-2 h incubation at 30° C. Cells were centrifuged at 6K RPM for 5 min and re-suspended in 10 µl of 1M sodium citrate and 90 µl of LB. The complete cell re-suspension was plated on LB + Cm (25 µg/ml) using the spread plate technique. Plates were incubated at 30° C for 24-48 h and colonies were re-plated on new LB + Cm (25 µg/ml) plates supplemented with sodium citrate. Transfer of the pNN9 vector was accomplished using standard transformation techniques described by [154]. Transformation of the pNN9 vector in the respective single gene knockouts, in absence of protelomerase expression, was confirmed to yield supercoiled CCC pDNA without LCC products (Figure 2.2). Heat induction using batch cultivation was performed as previously described.

2.2.4 Assessing Effects of Ciprofloxacin on Plasmid Replication and DNA Ministring Production

A single colony of W3NN [pNN9] and JW0429-Tel (Δ*lon*) [pNN9] was grown overnight in 5 ml LB + Ap (100 µg/ml) under repressed conditions at 30° C with aeration. Fresh cells were grown from the overnight culture at 1:100 dilution of 50 ml LB + Ap (100 µg/ml) in a 250 ml Erlenmeyer flask at 30° C with aeration until late log phase A_{600} = 0.8. Protelomerase expression was induced upon temperature upshift and incubation 42° C for 60 min. After induction, the 50 ml cultures were divided into four 10 ml batches followed by the addition of ciprofloxacin at different concentrations (0, 1, 10, 100 µg/ml). The different batches were then incubated at 37° and 30° C for 30 and 60 min respectively prior to plasmid extraction by

E.Z.N.A. Plasmid Mini-Prep Kit (Omega, VWR). DNA ministring production efficiency was assessed by AGE and densitometry (AlphaImager, Alpha Innotech).

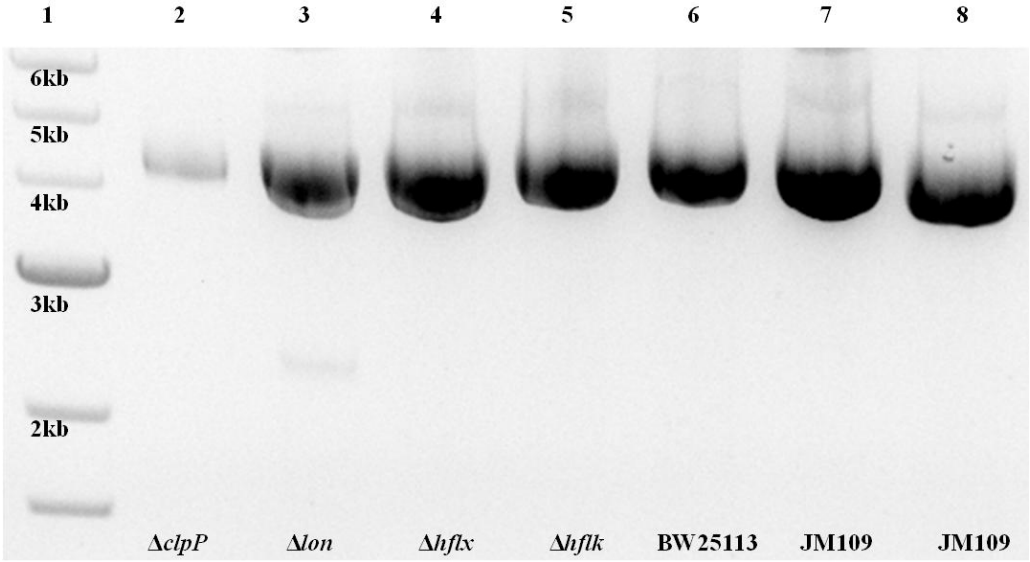

Figure 2.2 Protease mutants cannot generate DNA ministrings in absence of *tel/telN* expression. Representative gel image confirming the absence of LCC DNA products without protelomerase expression after transformation of the parental pDNA vector, pNN9, into each respective single gene knockout and parental strain: DNA ladder (lane 1); Δ*clpP* (lane 2); Δ*lon* (lane 3); Δ*hflX* (lane 4); Δ*hflK* (lane 5); BW25113 *wild type* (lane 6); JM109 (lane 7, 8).

2.2.5 Assessing the Introduction of DnaB Helicase Mutations on DNA Ministring Production

The temperature inducible protelomerase expression cassettes (*lacZ::cat-cI857-tel* and *lacZ::cat-cI857-telN* (Cm^R)) were introduced into two different mutant strains, conferring two respective DnaB helicase mutations (*dnaB8* (fast stop) & *dnaB252* (slow stop)) [155], and their parental strain (N99) by P1 bacteriophage-mediated transduction. Transfer of the pNN9 vector and subsequent heat induction, using batch cultivation, were performed as previously described.

2.2.6 Statistical Analysis

ANOVA and Welch's T-test was used as statistical analysis to compare production efficiencies of tested samples with controls. Production efficiencies for all tested samples and controls were repeated and averaged with a minimum of three trials ($N \geq 3$).

Table 2-1 Strains used in this study.

Strain	Genotype	Source
JM109	F', Δ*(gpt-lac)0*, *glnV44*(AS), λ⁻, *rfbC1*, *gyrA96*(NalR), *recA1*, *endA1*, *spoT1*?, *thi-1*, *hsdR17*, pWM5, F128-x	New England Biolabs
W3110-TelN (W2NN)	F-, λ⁻, *IN(rrnD-rrnE)1*, *rph-1 lacZ::Cm-cI857-telN*	[108]
W3110-Tel (W3NN)	F-, λ⁻, *IN(rrnD-rrnE)1*, *rph-1 lacZ::Cm-cI857-tel*	[108]
JW0427	F-, *Δ(araD-araB)567, ΔlacZ4787(::rrnB-3), ΔclpP723::kan, λ-, rph-1, Δ(rhaD-rhaB)568, hsdR514*	*E. coli* Genetic Stock Center (CGSC)#8590
JW0429	F-, *Δ(araD-araB)567, ΔlacZ4787(::rrnB-3), Δlon-725::kan, λ-, rph-1, Δ(rhaD-rhaB)568, hsdR514*	CGSC#8592
JW4131	F-, *Δ(araD-araB)567, ΔlacZ4787(::rrnB-3), λ-, rph-1, Δ(rhaD-rhaB)568, ΔhflX723::kan, hsdR514*	CGSC#10974
JW4132	F-, *Δ(araD-araB)567, ΔlacZ4787(::rrnB-3), λ-, rph-1, Δ(rhaD-rhaB)568, ΔhflK724::kan, hsdR514*	CGSC#10975
BW25113	F-, *Δ(araD-araB)567, ΔlacZ4787(::rrnB-3), λ-, rph-1, Δ(rhaD-rhaB)568, hsdR514*	CGSC #7636
JW0427-Tel (Δ*clpP*)	F-, *Δ(araD-araB)567, ΔlacZ4787(::rrnB-3), ΔclpP723::kan, λ-, rph-1, Δ(rhaD-rhaB)568, hsdR514*, Δ*clpP*, *lacZ::Cm-cI857-tel*	This Study
JW0427-TeN (Δ*clpP*)	F-, *Δ(araD-araB)567, ΔlacZ4787(::rrnB-3), ΔclpP723::kan, λ-, rph-1, Δ(rhaD-rhaB)568, hsdR514*, Δ*clpP*, *lacZ::Cm-cI857-telN*	This Study
JW0429-Tel (Δ*lon*)	F-, *Δ(araD-araB)567, ΔlacZ4787(::rrnB-3), ΔclpP723::kan, λ-, rph-1, Δ(rhaD-rhaB)568, hsdR514*, Δ*lon*, *lacZ::Cm-cI857-tel*	This Study
JW0429-TelN (Δ*lon*)	F-, *Δ(araD-araB)567, ΔlacZ4787(::rrnB-3), ΔclpP723::kan, λ-, rph-1, Δ(rhaD-rhaB)568, hsdR514*, Δ*lon*, *lacZ::Cm-cI857-telN*	This Study
JW4131-Tel (Δ*hflX*)	F-, *Δ(araD-araB)567, ΔlacZ4787(::rrnB-3), ΔclpP723::kan, λ-, rph-1, Δ(rhaD-rhaB)568, hsdR514*, Δ*hflX*, *lacZ::Cm-cI857-tel*	This Study
JW4131-TelN (Δ*hflX*)	F-, *Δ(araD-araB)567, ΔlacZ4787(::rrnB-3), ΔclpP723::kan, λ-, rph-1, Δ(rhaD-rhaB)568, hsdR514*, Δ*hflX*, *lacZ::Cm-cI857-telN*	This Study
JW4132-Tel (Δ*hflK*)	F-, *Δ(araD-araB)567, ΔlacZ4787(::rrnB-3), ΔclpP723::kan, λ-, rph-1, Δ(rhaD-rhaB)568, hsdR514*, Δ*hflK*, *lacZ::Cm-cI857-tel*	This Study
JW4132-TelN (Δ*hflK*)	F-, *Δ(araD-araB)567, ΔlacZ4787(::rrnB-3), ΔclpP723::kan, λ-, rph-1, Δ(rhaD-rhaB)568, hsdR514*, Δ*hflK*, *lacZ::Cm-cI857-telN*	This Study
BW25113-Tel	F-, *Δ(araD-araB)567, ΔlacZ4787(::rrnB-3), λ-, rph-1, Δ(rhaD-rhaB)568, hsdR514, lacZ::Cm-cI857-tel*	This Study
BW25113-TelN	F-, *Δ(araD-araB)567, ΔlacZ4787(::rrnB-3), λ-, rph-1, Δ(rhaD-rhaB)568, hsdR514, lacZ::Cm-cI857-telN*	This Study
N99	*galK*	[155]
BF843	*galK lacI*::*tet dnaB8* miniTn*10kan*	[155]
BF865	*galK dnaB252 zjb504*::Tn*10*	[155]
N99-Tel	*galK, lacZ::Cm-cI857-tel*	This Study
N99-TelN	*galK, lacZ::Cm-cI857-telN*	This Study
BF843-Tel	*galK lacI*::*tet dnaB8* miniTn*10kan, lacZ::Cm-cI857-tel*	This Study
BF843-TelN	*galK lacI*::*tet dnaB8* miniTn*10kan, lacZ::Cm-cI857-telN*	This Study
BF865-Tel	*galK dnaB252 zjb504*::Tn*10, lacZ::Cm-cI857-tel*	This Study
BF85-TelN	*galK dnaB252 zjb504*::Tn*10, lacZ::Cm-cI857-telN*	This Study

2.3 Results

2.3.1 Comparative Analysis of DNA Ministring Production between Tel and TelN

Tel protelomerase-mediated processing was previously demonstrated to achieve improved efficiencies over TelN protelomerase [108], however, the significance of such improvements was not quantitatively determined. In an attempt to quantify differences in pDNA processing by each respective protelomerase, LCC DNA ministring production efficiency was estimated by densitometry. Through direct comparisons using two different culture volumes and heating conditions, Tel mediated processing was confirmed to yield higher, but not statistically significant, ministring production efficiencies (Figure 2.3). Tel mediated processing attained production efficiencies of 53.6% and 65.5% for culture volumes of 20 ml and 50 ml respectively. This was higher than the 52.5% and 60.7% production efficiencies attained from TelN mediated processing. Although both protelomerases achieved similar ministring production efficiencies, Tel mediated processing was more consistent as evidenced by smaller standard deviations. Hence, Tel mediated processing was applied for subsequent investigations into optimal heating/culturing conditions for scalable DNA ministring production.

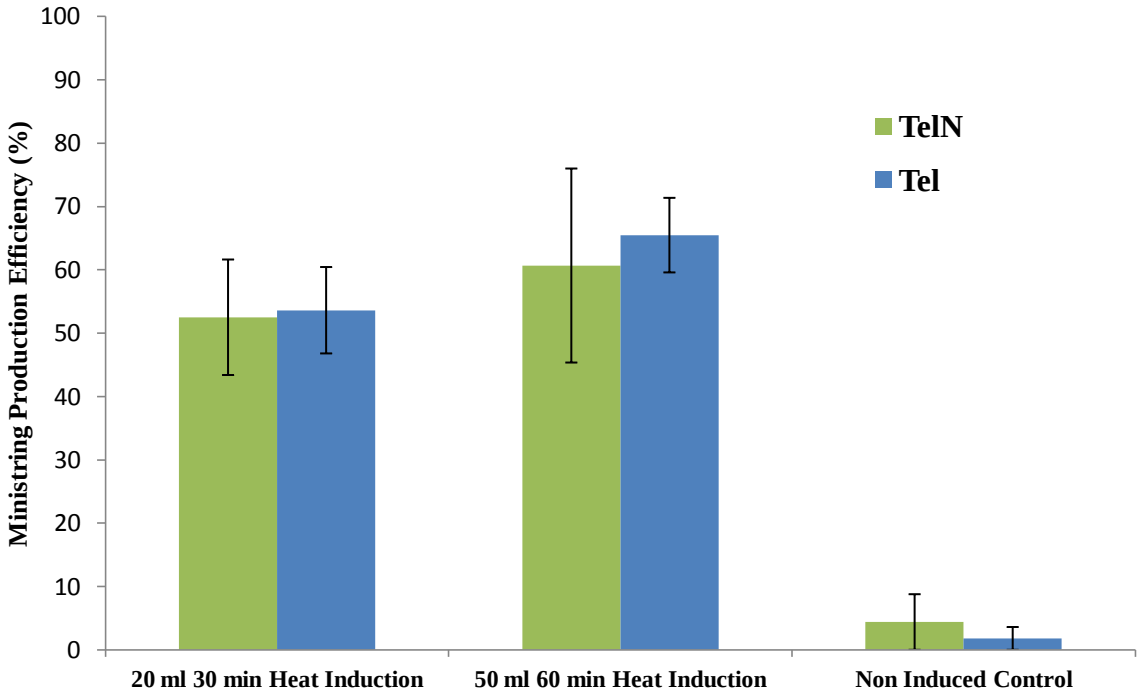

Figure 2.3 Comparative analysis of TelN and Tel protelomerase-mediated processing. LCC DNA ministring production efficiencies for $TelN^+$ (W2NN) and Tel^+ (W3NN) cells for heat induced batch cultivations across different culture volumes (20 & 50 ml) and heating conditions (30 & 60 min). Production efficiencies between TelN and Tel mediated processing were not statistically different but greater standard deviations were observed for TelN. All heat induced cultures had production efficiencies significantly greater than non-induced samples ($P << 0.01$).

2.3.2 A Two Stage Continuous Cultivation Improved LCC DNA Ministring Production Efficiency and Scalability

Various *tel*-induction schedules were explored with the intention of maximizing protelomerase expression for high DNA ministring production upon protelomerase processing of parental pDNA. Induction duration was optimized in order to avoid the detrimental effects associated with prolonged heat shock. LCC DNA ministring production from 10, 20, 50, and 500 ml batch cultivations required a corresponding increase in induction duration (15, 30, 60, 120 min) to sustain high production efficiencies (Figure 2.4). Such

trends were made obvious by the significant differences in production efficiency between 30 min (38.0%) and 60 min (65.5%) heat induction in 50 ml cultures (P << 0.01).

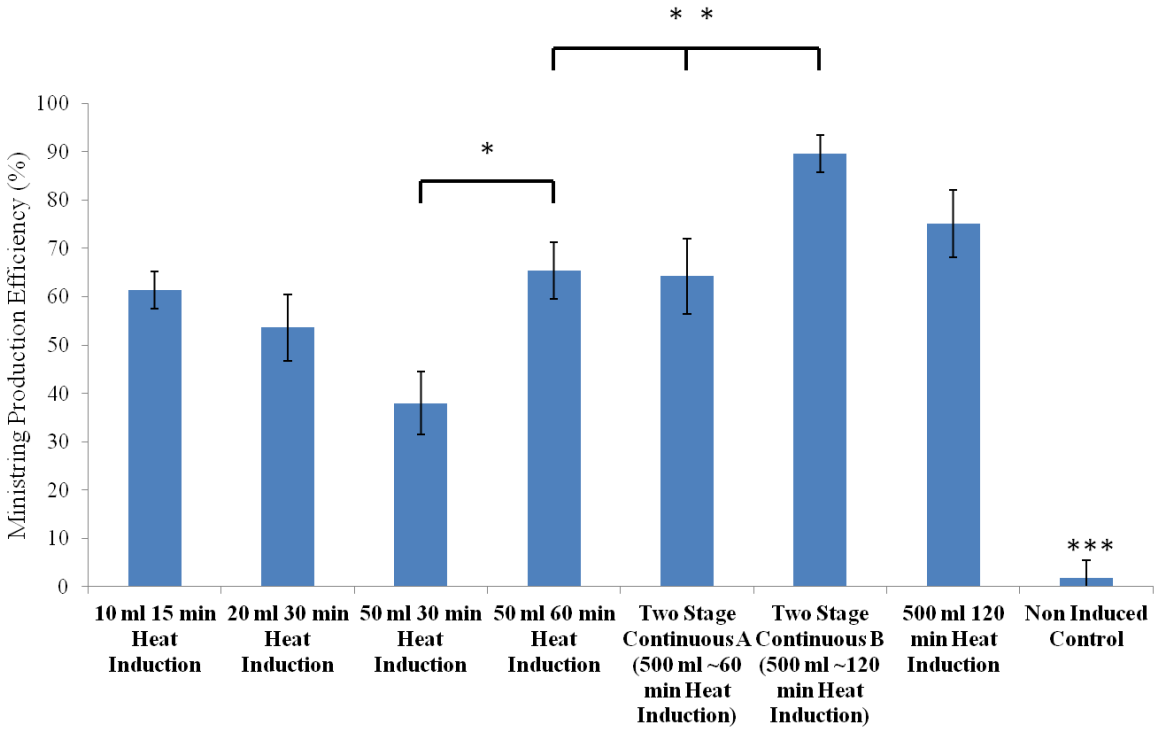

Figure 2.4 Effects of culturing technique and volume on DNA ministring production. LCC DNA ministring production efficiencies of Tel+ (W3NN) cells for: **1)** heat induced batch cultivations across different culture volumes (10, 20, 50 ml) and heat induction duration (15, 30, 60 min); **2)** heat induced two stage continuous cultivations (A & B); **3)** 500 ml batch cultivation; and **4)** non-induced controls. For 50 ml cultures, heat induction for 60 min led to production efficiencies significantly greater than heat induction for 30 min * (P << 0.01). Production efficiencies for two stage continuous (B) was significantly greater than two step continuous (A) ** (P << 0.01) and 500 ml batch cultivation ** (P < 0.05). All heat induced cultures had production efficiencies significantly greater than non-induced samples *** (P << 0.01).

Batch cultivations of 500 ml demanded increases in induction duration, where the 120 minute duration resulted in DNA ministring production (75.1%) while the 60 minute induction did not (Figure 2.4 & 2.5). In both cases, the lower production efficiencies were

denoted by greater residual parental pDNA substrate, signifying insufficient protelomerase expression and pDNA processing.

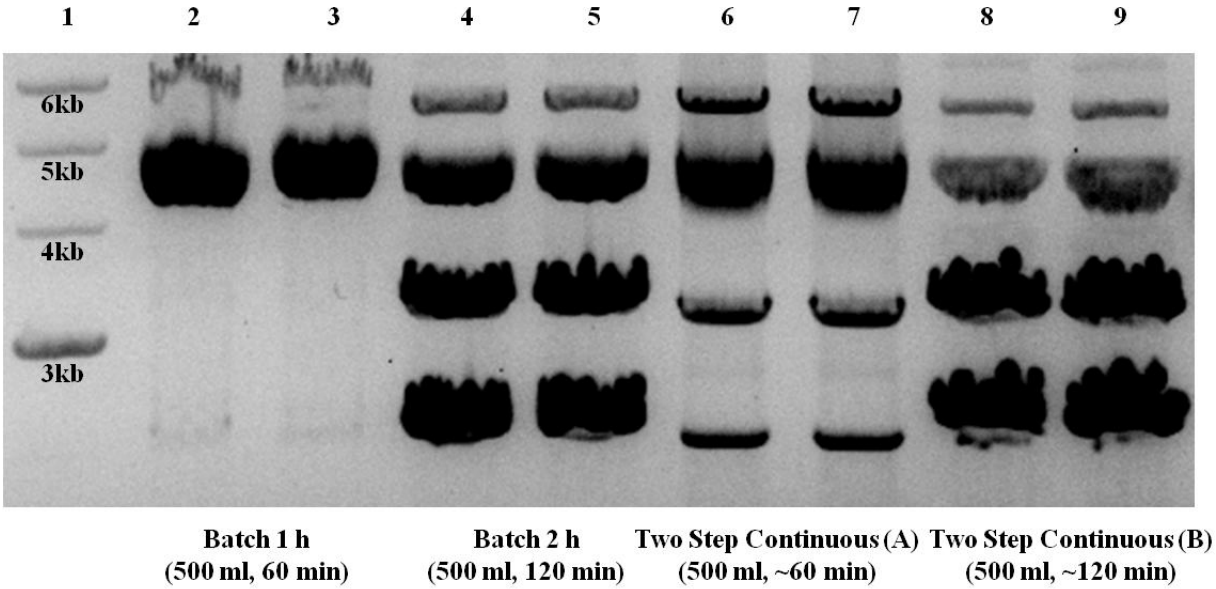

Figure 2.5 Gel analysis of LCC DNA ministring production between batch and two stage continuous cultivations. Representative gel image of LCC DNA ministring production in 500 ml batch and two step continuous cultivations: ladder (lane 1); W3NN Batch 1 h (500 ml, 60 min) (lanes 2-3); W3NN Batch 2 h (500ml, 120 min) (lanes 4-5); W3NN Two Step Continuous (A) (lanes 6-7); and W3NN Two Step Continuous (B) (lanes 8-9). The four DNA bands corresponded to the different species attained from Tel mediated processing: LCC DNA ministrings (2.4 kb), LCC backbone DNA (3.2 kb), parental CCC supercoiled pDNA (~4 kb), and parental LCC pDNA (5.6 kb). Under similar culture volumes and induction durations, two step continuous cultivations demonstrated greater ministring yields over batch cultivation. Specifically, two step continuous (A) demonstrated observable ministring production whereas batch cultivation 1 h (500 ml, 60 min) did not. Two step continuous (B) exhibited greater reduction in parental pDNA substrate over batch cultivation 2 h (500 ml, 120 min).

Between batch and two stage continuous cultivation, ministring production with two stage continuous culture (A) resulted in efficiency of 64.2% while batch cultivation, using equivalent 500 ml culture volumes and similar induction duration of ~60 minutes, did not

yield any observable LCC DNA ministrings (Figure 2.5). Two stage continuous cultures with additional 60 minutes of heat induction (B) resulted in a significant increase in ministring production efficiency (89.7%) when compared to two stage continuous (A) ($P << 0.01$) and batch cultivation with 120 min of heat induction ($P < 0.05$). Once again, the differences in efficiency was attributed to protelomerase processing as the amount of parental pDNA substrate was observably less for two stage continuous cultivation (B). In absolute terms per extraction, DNA ministring yields were approximated to be 27.5 µg, 87 µg, and 150 µg for two stage continuous (A), 500 ml batch cultivation, and two stage continuous (B) respectively. This corresponded to an estimated 3.2 pg, 12.1 pg, and 20.5 pg of DNA ministrings produced per bacterial cell for each of the three above listed variations.

2.3.3 LCC DNA Ministring Production was Enhanced in a Δ*hflX* Host Mutation Background

Induced overproduction of recombinant proteins contributes to metabolic aberrations and stresses and may result in numerous cellular responses including general stress, heat shock, stringent, and SOS responses. Such responses may elicit altered physiological states including growth arrest and decrease in specific growth rates. Hence, it was hypothesized that protelomerase turnover time may be compromised at elevated temperatures due to protease-mediated degradation, thereby reducing the processing of parental pDNA. To test the effects of proteases and associated gene products on DNA ministring production efficiency, pDNA processing outcomes were assessed in a variety of protease and protease-associated isogenic mutants for Tel (Figure 2.6) and TelN (Figure 2.7).

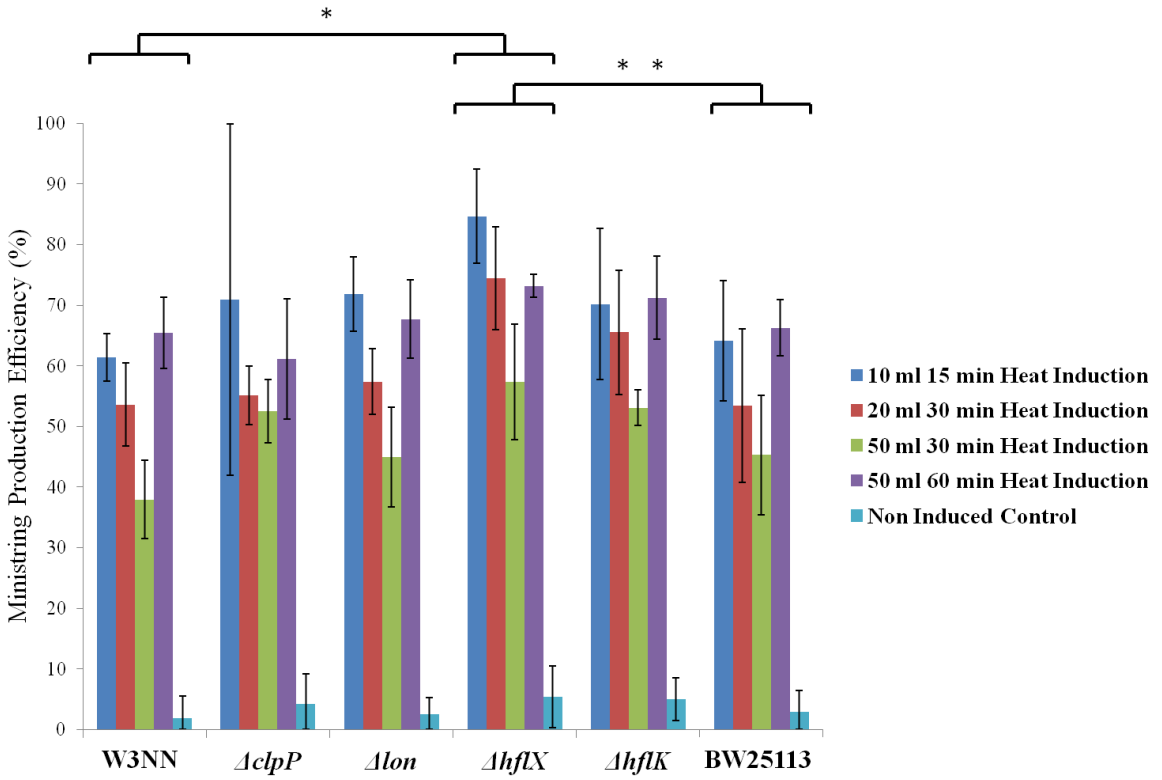

Figure 2.6 Effects of protease-specific and associated deletions on Tel-mediated DNA ministring production. LCC DNA ministring production efficiencies were assessed at various culture volumes and heat induction durations for strains possessing various protease and associated gene deletions (Δ*clpP*, Δ*lon*, Δ*hflx*, Δ*hflk*) and isogenic Tel$^+$ strain (BW25113, *wild type*). Across all conditions, the introduction of *hflX* gene deletion conferred significant increases in ministring production efficiencies over the original Tel$^+$ wild type cells (W3NN) * ($P \leq 0.01$) and isogenic Tel$^+$ cells (BW25113) ** ($P < 0.05$).

Similar trends across all strains were observed as DNA ministring production efficiencies were significantly lower ($P < 0.05$) in non induced samples when compared to induced samples at all culture volumes. In correlation with results from Tel+ wild type W3NN [pNN9], DNA ministring production from 10, 20, and 50 ml batch cultivations required similar increases in induction duration (15, 30, and 60 min) for high production efficiency by Tel and TelN protelomerases.

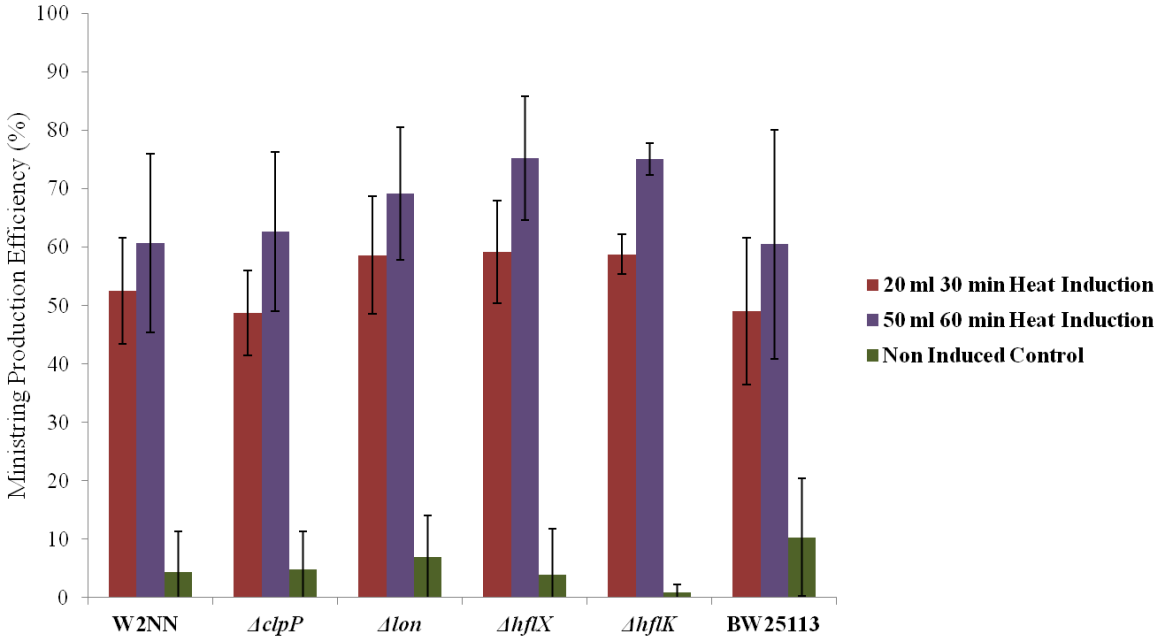

Figure 2.7 Effects of protease-specific and associated deletions on TelN-mediated DNA ministring production. LCC DNA ministring production efficiencies were assessed at various culture volumes and heat induction durations for strains possessing various protease and associated gene deletions (Δ*clpP*, Δ*lon*, Δ*hflx*, Δ*hflk*) and isogenic TelN$^+$ strain (BW25113, *wild type*). The introduction of *hflX* gene deletion conferred significant increases in ministring production efficiencies over the original TelN$^+$ wild type at culture volumes of 20 ml ($P < 0.05$), however, such increase was lost at larger volumes of 50 ml due to inconsistent TelN mediated processing.

Across all conditions, the introduction of an *hflX* gene deletion conferred a significant increase in Tel mediated production efficiencies compared to the wild type W3NN ($P \leq 0.01$) and isogenic wild type BW25113 ($P < 0.05$) counterparts, with ideal production seen in 10 ml cultures after 15 min *tel* heat induction (84.7%) (Figure 2.6). The introduction of an *hflX* gene deletion conferred a significant increase in TelN mediated production efficiencies compared to wild type W2NN ($P < 0.05$) for culture volumes of 20 ml (Figure 2.7), however, such significant increase was lost at larger volumes of 50 ml due to inconsistent production

with TelN, as evidenced by an approximate 5 fold increase in standard deviation from the Tel$^+$ (Δ*hflX*) counterpart. For both culture volumes of 20 ml and 50 ml, TelN mediated processing was most efficient in the Δ*hflX* derivative, resulting in 59.2% and 75.2% production efficiencies respectively.

2.3.4 Ciprofloxacin Enhanced DNA Ministring Production

Ciprofloxacin was administered in an attempt to synchronize plasmid replication rates with protelomerase expression to enhance LCC DNA ministring production efficiency in the *in vivo* system. It was hypothesized that transient inhibition by the fluoroquinolone antibiotic would elicit diminished plasmid replication, thereby enhancing plasmid processing. The Δ*lon* derivative was of particular interest as it was expected to curb the metabolic burden associated with SOS response triggered by ciprofloxacin. The application of ciprofloxacin to Tel$^+$ cells led to a gradual increase in pDNA processing, conferring improvements to production efficiency from about half to 76.6% (Figure 2.8).

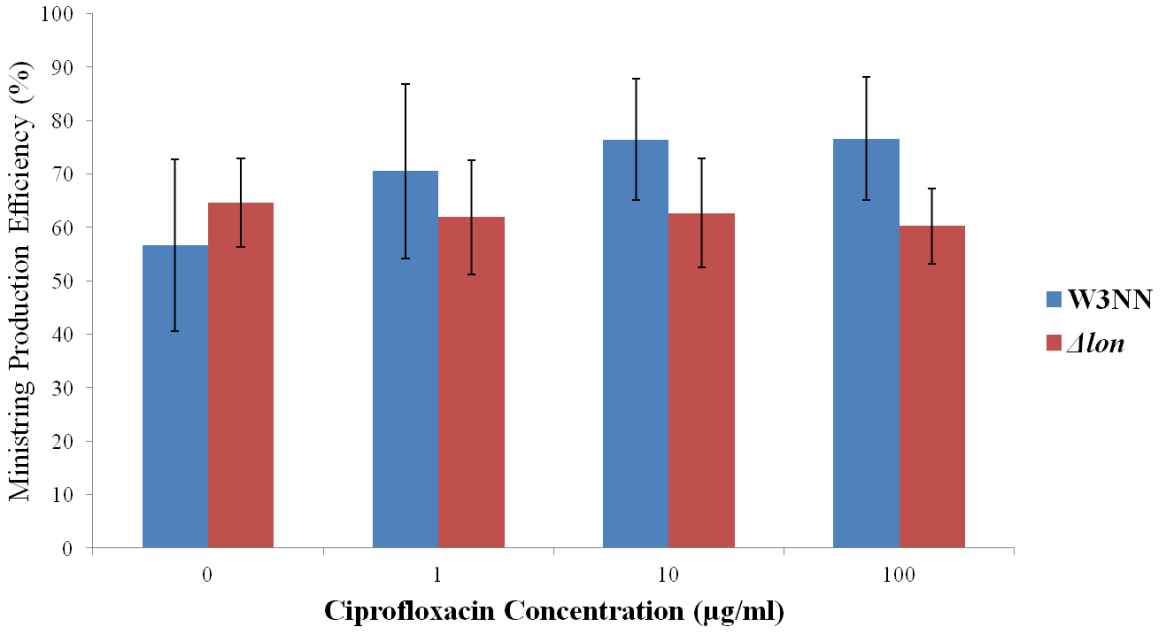

Figure 2.8 LCC DNA ministring production efficiency upon the introduction of ciprofloxacin at various concentrations. Application of 0, 1, 10, and 100 µg/ml of ciprofloxacin to wild type Tel^+ cells (W3NN) and Δ*lon* derivative harboring the parental pNN9 plasmid. Addition of 10 and 100 µg/ml of ciprofloxacin to Tel^+ cells conferred a 19.8% and 20.0% increase in DNA ministring production efficiency compared to the untreated induced control. Improvements to DNA ministring production efficiency was not observed for the Δ*lon* derivative.

Ciprofloxacin marginally increased production efficiency (~20%) at 10 µg/ml ($P < 0.1$), and little impact on efficiency was observed when ciprofloxacin concentration was increased 10-fold to 100 µg/ml. In contrast, the application of ciprofloxacin to the Δ*lon* derivative did not confer any improvement in processing efficiency. Differences in the influence of ciprofloxacin on wild type and the Δ*lon* derivative were attributed to hypersensitivity of the Δ*lon* derivative to ciprofloxacin as indicated by the progressive decrease in total pDNA with increasing concentrations of the antibiotic (Figure 2.9). In addition, the introduction of ciprofloxacin to the Δ*lon* derivative contributed to incomplete Tel processing as sustained production of parental LCC pDNA (5.6 kb) and decreases in LCC DNA ministring (2.4 kb),

were observed. Thus, there was a greater preference for Tel processing at a single recognition site in contrast to both respective sites required for DNA ministring production.

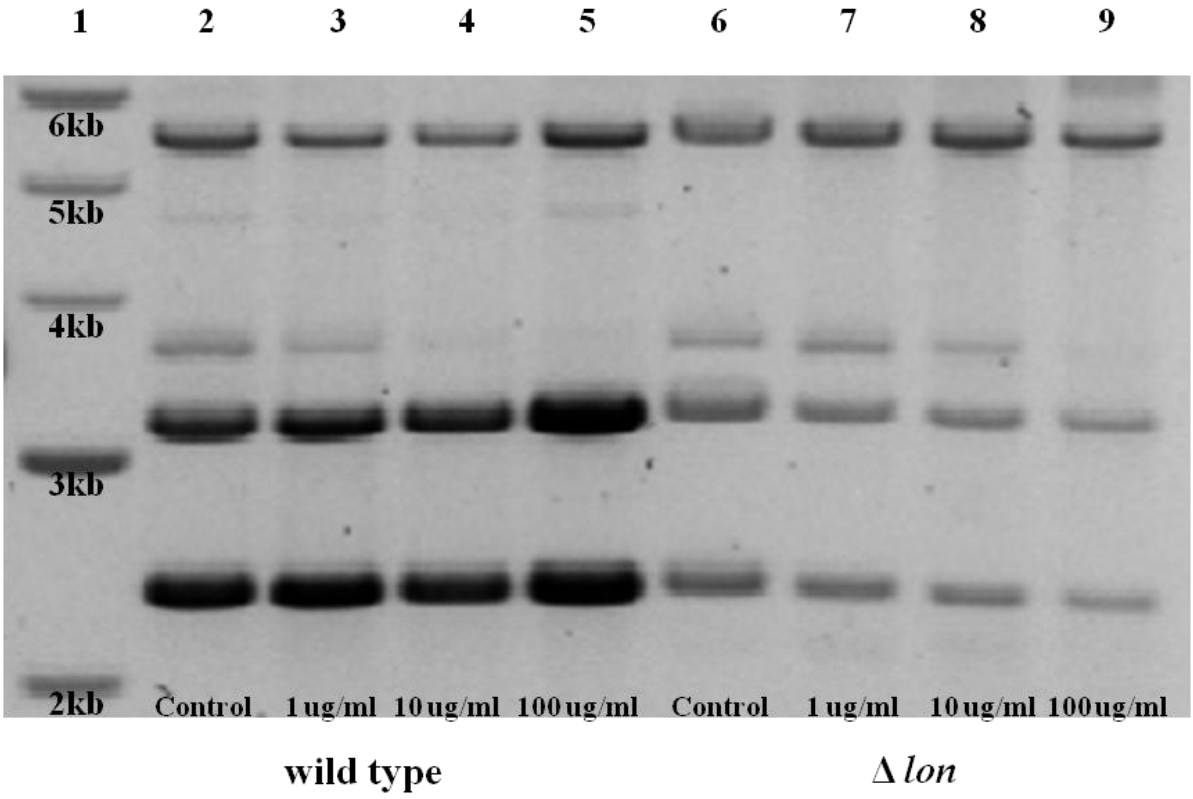

Figure 2.9 LCC DNA ministring production after the introduction of ciprofloxacin: DNA ladder (lane 1); W3NN wild type R-cell with 0, 1, 10, and 100 µg/ml of ciprofloxacin (lanes 2-5); JW0429-Tel (Δ*lon*) with 0, 1, 10, 100 µg/ml (lanes 6-9). A progressive disappearance of parental supercoiled pDNA (3.5-4 kb) was observed at increasing concentrations of ciprofloxacin. Gradual decrease in LCC DNA ministrings (2.4 kb) and LCC backbone DNA (3.2 kb) along with sustained production of the parental LCC pDNA (5.6 kb) were observed for the Δ*lon* derivative at increasing concentrations of ciprofloxacin.

2.3.5 Effects of DnaB Helicase Mutations on DNA Ministring Production

Similar to ciprofloxacin, temperature sensitive *dnaB*[Ts] helicase mutants serve to induce transient interruptions in plasmid replication for improved protelomerase processing and

production efficiencies. The *dnaB* gene encodes a 470 a.a. polypeptide that assembles into a homohexamer [155] and is a major replicative DNA helicase critical to chromosomal replication of *E. coli* and plasmids containing the *ColE1* origin of replication (*OriC*) [156, 157]. DnaB is a multifunctional essential enzyme with ATP and single-stranded DNA binding activity, DNA dependent ATPase activity, DNA helicase activity, and priming activity with primase [158]. Temperature sensitive *dnaB* helicase mutants exhibit greatest phenotypic effects at non-permissive temperatures (42° C) and such effects may vary depending on the mutation. The *dnaB8* mutation, referred to as a fast stop mutant, exhibits negligible primer RNA synthesis, ATPase activity, and helicase activity at non-permissive temperatures, resulting in immediate cessation of DNA synthesis. In contrast, the *dnaB252* mutation, referred to as a slow stop mutation, attains the abovementioned functions lacking in *dnaB8*, but exhibits interferences to interactions with DnaC, a helicase loading factor. As such, the mutation confers a delayed cessation of DNA synthesis and rather prevents re-initiation of replication events [155, 158]. Hence, induced protelomerase expression and inhibition of plasmid replication simultaneously occurs upon temperature upshift to 42° C, potentially improving precursor plasmid processing efficiency.

DNA ministring production efficiency in slow stop mutants (*dnaB252*) was significantly higher than that observed in wild type W3NN Tel^+ cells, for culture volumes of 20 ml ($P < 0.01$) and 50 ml ($P < 0.05$) respectively, but not compared to the isogenic wild type N99 Tel^+ cells (Figure 2.10 A). The application of the *in vivo* system into *dnaB* fast stop mutants (*dnaB8*) resulted in lower production efficiencies. Similar trends were observed with respect to TelN-mediated processing in the two respective *dnaB*[Ts] mutants. However, no

significant increase in production efficiencies, over wild type Tel^{+} W2NN wild type cells, was observed for slow stop mutants due to inconsistent production (Figure 2.10 B).

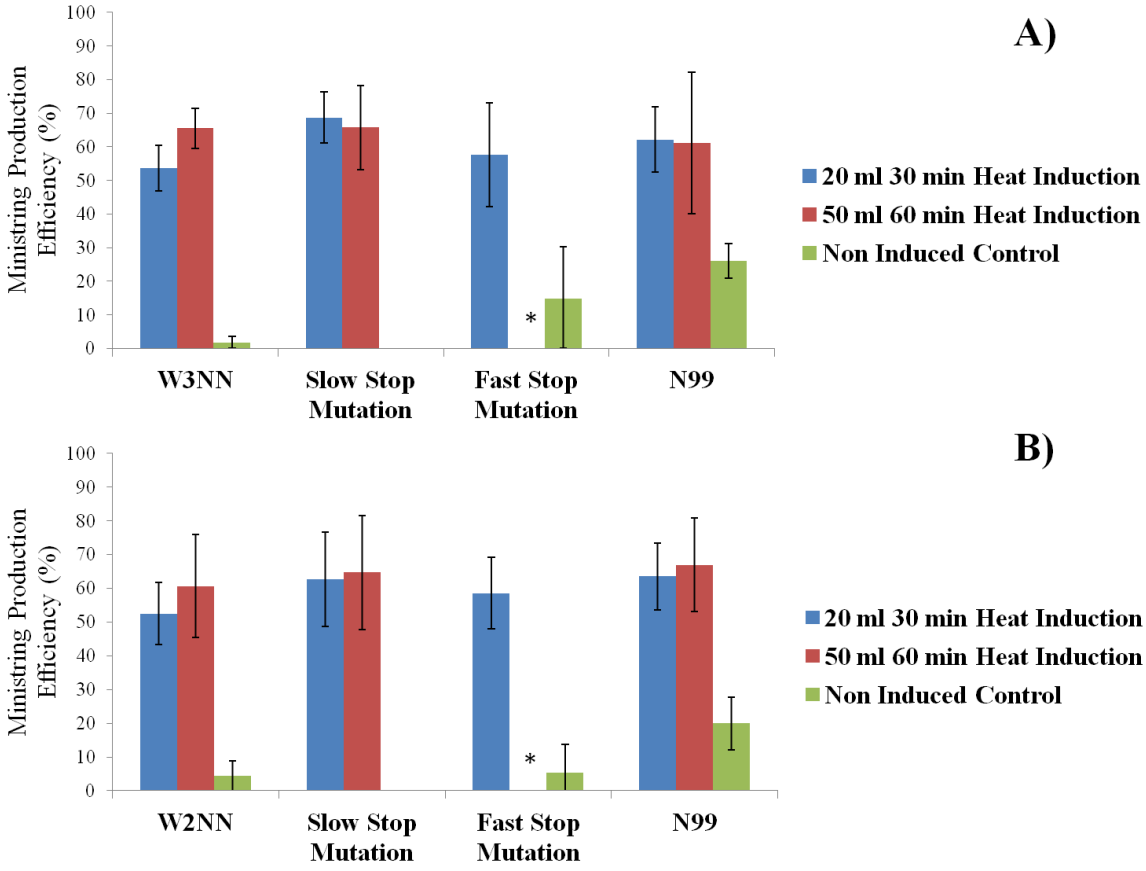

Figure 2.10 Tel and TelN-mediated DNA ministring production efficiency in *dnaB*[Ts] mutants. For Tel processing **(A)**, slow stop mutants exhibited significantly higher production efficiencies over wild type W3NN at culture volumes of 20 ml (68.7%; $P < 0.01$) and 50 ml (65.7%; $P < 0.05$). However, such increases were not evident with respect to TelN processing **(B)** as the isogenic wild type N99 was shown to elicit the highest production efficiencies at culture volumes of 20 ml (63.5%) and 50 ml (66.9%); both of which were comparable to production efficiencies attained in DnaB slow stop mutants (62.7%, 20ml & 64.7%, 50 ml). * *Data not available.*

The isogenic N99 wild type strain demonstrated slight increases in production efficiency over other wild type (W2NN/W3NN) cells and this may partially account for the significant increases observed in *dnaB* slow stop mutants. Interestingly, gel analysis of ministring production in slow stop mutants denoted reduced amounts of LCC backbone DNA, the component comprising the prokaryotic backbone sequences with *OriC*; this was in conjunction to greater amounts of resulting LCC DNA ministring (Figure 2.11). However, the amount of residual parental supercoiled CCC pDNA was observably higher in slow stop mutants over the fast stop mutants and the two tested wild type strains.

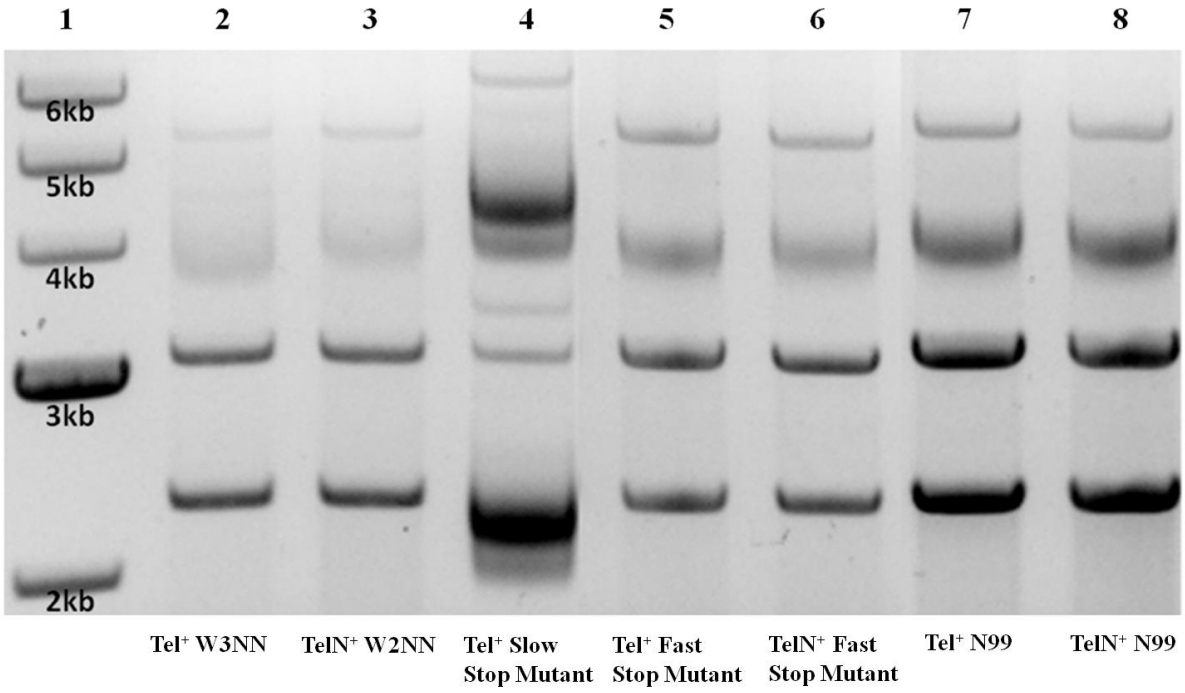

Figure 2.11 LCC DNA ministring production in *dnaB*[Ts] mutants: DNA ladder (lane 1); Tel^+ W3NN (lane 2); $TelN^+$ W2NN (lane 3); Tel^+ slow stop mutant (lane 4); Tel^+ fast stop mutant (lane 5); $TelN^+$ fast stop mutant (lane 6); Tel^+ isogenic wild type N99 (lane 7); $TelN^+$ isogenic wild type N99 (lane 8). Tel^+ slow stop mutant exhibited a different gel profile with reduced amounts of LCC backbone DNA (~3.2 kb) and greater amounts of LCC DNA ministring (2.4 kb).

2.4 Discussion

The one-step heat inducible *in vivo* LCC DNA minivector production system was specifically designed with the chromosomal integration of a single copy of protelomerase gene (*telN* or *tel*) in an attempt to overcome certain drawbacks associated with the overproduction and episomal expression of protelomerase that contribute to metabolic imbalances, activation of stress responses, improper protein folding, and inclusion body formation [159]. Chromosomal integration of the protelomerase expression cassette, in combination with thermoregulated control *via* λ CI[Ts]857 repressor, permitted greater constraints on protelomerase expression that is unattainable in an episomal pDNA expression system. Complications associated with sustained plasmid partitioning and stable plasmid inheritance during temperature upshift can also be resolved. Simultaneously, issues relating to plasmid maintenance of protelomerase expression and substrate pDNA, prior to induction, can be avoided. Despite such improvements, maintenance and replication of the pDNA substrate consumes additional cellular resources and such metabolic burden was exacerbated by subsequent induced expression of the protelomerase. The interplay of these numerous factors constituted imperfect plasmid processing and reduced DNA ministring production from the current system. As such, careful considerations were made to culture conditions and induction scheduling in order to improve the overall production of DNA ministring in the *in vivo* system.

In all instances of induction, a gradual temperature increase from 30° to 42° C was applied as previous findings indicated an observed improvement in recombinant protein expression

with slowest heating rates when compared to more rapid rates. Rapid heating rates resulted in decreased recombinant protein expression, likely due to the high ATP demand associated with rapid recombinant protein production and expression of heat shock proteins. Transcriptional analysis by Caspeta et al. [160] indicated a dramatic increase in mRNA levels for heat shock genes and such increases were most significant at rapid heating rates that contributed to high ATP demands from cellular responses mediating heat stress. The high ATP demand caused an imbalance between glycolytic and TCA cycles, shifting ATP production *via* cellular respiration to glycolysis, and led to increases in substrate level phosphorylation along with the generation of acetate byproduct [160]. Correlations between rapid heating rates and rapid onset of heat stress are likely supported due to the corresponding increase in *rpoH* mRNA levels imparted by more rapid heating rates [160]. In contrast, slower heating rates allow cells to better accommodate for heat induction and dampen the negative effects associated with rapid heat shock. These findings bode well for large scale production of DNA ministrings since slow heating rates are generally attained in large scale fermenters. In addition, Caspeta et al. [161] demonstrated higher maximum recombinant protein concentrations with 2.3-4.0 fold increases in biomass concentration and 48-62% decrease in organic acid by-products after the implementation of temperature oscillations in conjunction with post-induction nutrient feeding strategies [161]. Such oscillations allowed the cells to better accommodate heat stress leading to improved cell growth, higher recombinant protein yields, and reduced by-product accumulation. Future studies involving temperature oscillations may prove to further improve DNA ministring production.

Comparisons between DNA ministring production upon TelN and Tel protelomerase mediated processing indicated greater inconsistencies in TelN processing across wild type (W2NN), genetically modified strains, and isogenic background controls despite comparable production efficiencies. Inconsistencies arising from TelN mediated processing were attributed to the influences of the recognition site, in the SuperSequence, on DNA binding and the overall stability of the protelomerase/DNA complex. Previously, Deneke et al. [124] noted a near 5-fold decrease in stability for TelN-*telRL* complexes compared to TelN-*tos* complexes. The TelN recognition site, *telRL*, was the minimal recognition site required for TelN processing and the absence of the accessory inverted repeats, found in *tos*, may have caused reduced binding or instability in the resulting target site. More consistent results were observed using Tel, likely because the SuperSequence encodes the complete 142 bp *pal* target sequence.

For small volume batch cultivations of 10, 20, and 50 ml, there was an approximately linear increase in induction duration with progressive increases to culture volume. However, deviations from this linear trend were observed for 500 ml batch and two step continuous cultivations as optimal production efficiencies and overall DNA ministring yields were observed with shorter induction durations. Since the expressed Tel protelomerase was capable of acting on multiple copies of the target plasmid, high DNA ministring production efficiencies can be attained with relatively moderate protelomerase expression. This attribute contributed to reducing the duration of heat induction required for protelomerase expression and optimal DNA ministring production. Previous studies have shown diminished cell growth upon 1-2 hours of heat induction, at 42° C, due to metabolic burden associated with

recombinant protein production, the expression of heat shock proteins and reduced translation activities. This treatment also resulted in slight decrease in biomass concentration and reduced accumulation of recombinant proteins beyond two hours following heat induction [160]. It was interesting to note that the high production efficiencies achieved by batch and two stage continuous (B) were accomplished approximately two hours following initial shift to 42^{o} C. In relation to the experimental findings, optimal DNA ministring production was speculated to be achieved through heat induction at durations with high recombinant protelomerase expression, prior to cessation of cell growth and other negative effects associated with prolonged heat shock. With respect to batch and two step continuous cultivations, more effective expression and DNA processing was observed for two step continuous cultivations as evidenced by DNA ministring yields 60 min after heat induction. Such improvements were attributed to high cell density in co-ordination with continuous nutritional supplementation for ample Tel expression during the production phase. This contributed to the greater DNA ministring yields in two step continuous cultivations when subjected to similar induction durations.

In this study, the introduction of protease-specific and associated gene deletions was hypothesized to prevent protease-mediated protelomerase degradation, thereby extending protein turnover of functional protelomerases. Contrary to the initial hypothesis, gene deletions of *clpP*, *lon*, and *hflK* did not result in any significant improvements to Tel or TelN protelomerase-mediated processing and DNA ministring production. Lack of observed differences in production efficiency may be attributed to the fine control of protelomerase expression and the minimal heat induction necessary for optimal protelomerase mediated

DNA ministring production. Short induction durations applied in this study did not result in high levels of recombinant protein that would overburden the activity of folding chaperones, a common observation seen in traditional recombinant protein production systems. As such, the activities and impact of heat shock proteases became less prominent in affecting DNA ministring production since folding chaperones likely re-folded the majority of misfolded proteins effectively and prevented the formation of non-functional proteins or inclusion bodies. Nevertheless, slight improvements in production efficiencies were observed upon the deletion of *lon* and *hflK* gene across all culturing and heating conditions for both Tel and TelN. Improvements to ministring production for Δ*lon* derivatives were speculated to be attributed to diminished degradation of small heat shock proteins, IbpA and IbpB, by Lon protease [162]. IbpA and IbpB are holding chaperones that intercalate into protein aggregates and stabilize folding intermediates for folding chaperones [138, 143, 148]. The Δ*lon* derivative should impart reduced IbpA and IbpB degradation and improved protein re-folding. HflKC, a heterodimer consisting of HflK and HflC, has been shown to modulate the proteolytic activity of FtsH (HflB) protease. It was previously demonstrated that the deletion of *hflKC* genes resulted in reduced degradation of cytosolic λ CII (lysogeny decision) protein and enhanced the degradation of membrane bound SecY (membrane secretion) protein [163-166]. Hence, the deletion of *hflK* gene was expected to confer decreased degradation of cytosolic recombinant protelomerase leading to the slight improvement in LCC DNA processing efficiency.

There was an observably greater variability in DNA ministring production efficiencies for Δ*clpP* derivatives, particularly with Tel-mediated processing in culture volumes of 10 ml and

50 ml that were subjected to 15 min and 60 min of heat induction, respectively. This may be explained by previous work of Schweder *et al*. [167] who reported a suppression of general stress response, mediated by RpoS (σ^{38}), during strong overexpression of recombinant proteins. Deletion of the *clpP* gene, expressing the ClpP protease that specifically cleaves RpoS, was shown to negatively impact recombinant protein production due to greater sigma factor competition as a result of higher RpoS stability [167]. For temperature inducible systems, higher stability of RpoS may outcompete RpoH for RNA polymerase and negatively affect the accumulation of heat shock proteins necessary to effectively respond against heat stress [160]. Influences of higher RpoS stability in Δ*clpP* cells under dual stress of heat shock and high levels of recombinant protelomerase expression may contribute to highly variable efficiencies in LCC DNA processing.

A statistically significant improvement in LCC DNA processing was observed in the Δ*hflX* derivative, potentially due to the interactions between HflX and ribosomal subunits. HflX is one of eight universally conserved GTPases found in prokaryotes and eukaryotes [168, 169]. HflX is a monomeric GTPase and ATPase previously shown to interact with 16S and 23S rRNA, the 30S and 50S ribosomal subunit, and the 70S ribosome; their expression becomes upregulated under heat stress similar to HSPs [168-171]. Activities of HflX likely serve to regulate and control protein translation rates in co-ordination with the down-regulation of translation related genes and reduced concentrations of ribosomal components upon heat stress and recombinant protein production [160, 167, 172]. As such, deletion of the *hflX* gene may prompt higher rates of protein translation and protelomerase expression, improving ministring production efficiency.

The addition of ciprofloxacin after induced protelomerase expression served to inhibit plasmid replication and bacterial cell division in order to enhance DNA ministring production by maximizing processing from parental pDNA. Ciprofloxacin is a broad spectrum fluoroquinolone antibiotic that inhibits the activity of DNA gyrase and topoisomerase IV, both of which are essential in the regulation of DNA topological states during replication and transcription in *E. coli* [173, 174]. The inhibitory effects of ciprofloxacin results in DNA damage and activation of the SOS response, causing cell cycle arrest and DNA repair mediated by the upregulation of RecA along with corresponding inactivation or degradation of LexA repressor. The upregulation of RecA following SOS activation can contribute to the formation of aggregates with various denatured and misfolded proteins. Such events result in the activation of heat shock regulon as genes associated with both SOS and HSR would be up-regulated following treatment with ciprofloxacin [173, 174]. In particular, the Lon protease is a critical component in both SOS and HSR. LexA and SulA, SOS response proteins that inhibit cell division through its binding to FtsZ, are direct targets of Lon-mediated proteolysis. Hence, the inactivation of Lon leads to diminished SOS response and DNA repair contributing to hypersensitivity to ciprofloxacin [173, 174].

It was hypothesized that transient inhibition by ciprofloxacin on Δ*lon* derivatives may elicit additional improvements to protelomerase expression by temporarily limiting the metabolic burden associated with SOS response, while averting cell death associated with prolonged exposure to ciprofloxacin. While ciprofloxacin did impact and improve LCC DNA processing efficiency in wild type W3NN cells, no impact was observed in the Δ*lon*

derivative, thereby disproving our hypothesis. This finding may potentially be due to ciprofloxacin-mediated hypersensitivity, despite limited exposures to the antibiotic. Significant cell death and cellular aberrations would lead to down-regulation of protelomerase expression and could induce expression of non-functional protelomerase. Effects of hypersensitivity were confirmed as DNA ministring yields, upon qualitative observations from AGE, were far greater for wild type W3NN than the Δ*lon* derivative. A lower concentration of ciprofloxacin in conjunction with shorter exposure time may effectively promote improved DNA ministring production in Δ*lon* derivatives.

With respect to DNA ministring production in *dnaB*[Ts] helicase mutants, significant increases to production efficiencies observed in *dnaB252* slow stop mutants was partially attributed to strain variations as the isogenic control yielded an overall minor increase over wild type W3NN cells. However, interestingly, gel analysis denoted a disparity between LCC backbone DNA and DNA ministring with greater amounts of DNA ministrings being observed. This was in conjunction to the appearance of structural intermediates and topoisomers of parental supercoiled CCC pDNA with varying degrees of supercoiling. This is likely due to inefficient helicase loading, due to inhibited interactions with DnaC that may result in DnaA-*oriC* intermediates leading to the degradation of the DnaA-*oriC* bearing backbone DNA upon interference with replication initiation. The extent of DNA degradation was exacerbated in *dnaB8* fast stop mutants that possess a mutation in the helicase enzymatic domain. The *dnaB8* mutation yielded significant overall reductions in pDNA yields and negligible DNA ministring upon 60 minutes of heat induction. These cells are sick even at the permissive 30^{o} C temperature and would experience significant cell death after 60 min

possessing trapped replication intermediates. As such, the observed findings were attributed to cell death and SOS-independent filamentation upon temperature upshift to the non-permissive temperature. Previously, replication arrest upon *dnaB8* inactivation was shown to result in cessation of growth and degradation of over half of nascent DNA upon a temperature upshift of 60 minutes [175]. Diminished plasmid propagation and reduced viabilities, upon DnaB[Ts] inactivation and the introduction of multiple stressors, may have severely compromised DNA ministring production.

With considerations to the production efficiencies attained in all of the abovementioned modifications, two step continuous cultivation in a genetically modified *ΔhflX* strain possessing *dnaB*[Ts] slow stop mutation may potentially serve to attain complete pDNA processing with dramatically high yields of LCC DNA ministrings. Future studies assessing ministring production efficiencies from the proposed genetically modified LCC DNA minivector production system will be warranted.

2.5 Conclusion

The results of this study served as an optimal protocol to significantly improve LCC DNA ministring production using the novel *in vivo* system. In particular, two step continuous cultivation with 120 minutes of heat induction constituted a ~90% DNA ministring production efficiency resulting in approximately 150 µg of DNA ministring per extraction. The versatility of this novel technology invites numerous potential applications in gene transfer-mediated therapeutics. As such, downstream purification of LCC DNA ministring will be warranted for future clinical applications using these new generation DNA vectors.

Chapter 3

Separation and Purification of Linear Covalently Closed (LCC) DNA by Q-Anion Exchange Membrane Chromatography

3.1 Introduction

The development of any successful gene therapeutic demands effective and efficient gene delivery with careful considerations to the safety profile of the therapeutic. Although viral vectors enable effective delivery of the DNA cargo with high efficiency, such vectors prompt significant safety concerns with regards to potential undesired immune responses to viral capsid proteins, regeneration of virulent viruses, and insertional mutagenesis [108]. As such, non-viral gene delivery strategies are generally safer. However, while safer, the use of conventional circular covalently closed (CCC) plasmid DNA (pDNA) vectors may still potentiate DNA vector integration into the host chromosome. The application of linear covalently closed (LCC) DNA vectors addresses the above limitations by promoting a heightened safety profile [108]. Previously, the one-step heat inducible *in vivo* DNA minivector production system was optimized for rapid and scalable processing of precursor CCC pDNA into LCC DNA vectors. This production system involves temperature inducible expression of the PY54 bacteriophage-derived recombinant Tel protelomerase followed by subsequent protelomerase mediated enzymatic reactions. The protelomerase acts on genetically engineered multi-target sites called "SuperSequences", converting conventional CCC pDNA into LCC DNA derivatives [108].

In most plasmid extractions, the plasmid DNA (pDNA) population consists of various monomeric topological isoforms: supercoiled CCC, open circular (OC), and linear open (LO). Generally, supercoiled CCC pDNA exists as the predominant form with varying levels of OC and LO pDNA derivatives that arise from single and double strand breaks. Application of our processing system, based on the exploitation of TelN and Tel protelomerase, toward the production of LCC DNA vectors added an additional level of complexity with respect to the many different isoforms arising from the extracted plasmid population (see Figure 2.1). As such, additional purification was necessary to ensure that LCC DNA vectors could be recovered at purities suitable for clinical testing. High resolution achieved by column chromatography constituted high pDNA purity, making it an essential component in downstream purification processes [176-178]. Various chromatography techniques have been applied for plasmid purification including: 1) size exclusion chromatography (SEC), 2) reversed-phase chromatography, 3) hydrophobic interaction chromatography (HIC), and 4) anion exchange chromatography (AEC) [176, 178-181].

AEC is commonly employed for pDNA capture and purification, offering several advantages: rapid separation; lack of required solvents; and sanitation of chromatography columns by sodium hydroxide [182, 183]. AEC functions through the interactions between negatively charged pDNA and non-specific positively charged ligands on the stationary phase, where the strength of this interaction is dependent on both net charge and local charge density. The introduction of a salt gradient displaces such interactions and pDNA elutes in order of increasing charge density, influenced by chain length, conformation, and topology [182, 184-187]. Although the different DNA isoforms possess the same chain length, charge

and molecular weight, separation can be achieved through differences in charge density and physicochemical properties between the isoforms. A high degree of compaction in supercoiled pDNA confers greater local charge density in comparison to OC pDNA; contributing to stronger interactions that cause supercoiled pDNA to elute at a later point than OC pDNA [186, 187]. Linear pDNA, characterized as superhelical rods with random coils, inherently possess greater degrees of elasticity and may be subject to stretching by shear forces; such a distinct property thereby contributes to the separation of linear pDNA from the other two isoforms [187, 188]. Using a TSK_{gel} DNA-NPR weak anion exchange column, Smith et al. [187] found size and gradient change-rate dependent variations in the elution order between supercoiled and LO pDNA. Although separation between the different isoforms was observed, complete separation was unattainable under experimental conditions. In a subsequent study using a quinine-carbamate based weak anion exchanger, Mahut et al. [185] reported that the elution order of isoforms was indifferent to changes in mobile phase, gradient change-rate, or plasmid size, but varied depending on changes in temperature. At temperatures above 35° C, they noted a higher retention of supercoiled pDNA, as it eluted after LO pDNA. However, at temperatures below 25° C, supercoiled pDNA eluted at points between that of OC and LO pDNA, and co-elution of supercoiled and LO pDNA was observed at 30° C. [185].

The generally large size of pDNAs poses significant limitations on commercial purification processes by column chromatography, primarily due to the inability of large biomolecules to pass through the porous beads (<0.2 μm) of the stationary phase, resulting in pDNA to be adsorbed predominantly on the surface, thereby limiting capacity [177, 181-183,

186, 189]. Previous studies reported that substantive amounts of resin beads were required for pDNA purification as fractional amounts of pDNA (~ 0.2–2 g) were loaded per liter of resin, in contrast to the 10-100 g achieved for protein purification [181]. Time consuming and labour-intensive processes involved in column packing, cleaning, and regeneration, along with reported low recovery and irreversible pDNA binding, pose further limitations on conventional column chromatography [177]. Anion exchange membrane chromatography may overcome such limitations as anion exchange membranes possess large convective pores (2 μm), enabling rapid transport of pDNA to membrane surface while attaining binding capacities an order of magnitude higher than their resin counterparts [176-178, 184, 189]. High throughput is attainable as pDNA purification efficiencies are achieved even at elevated flow rates [176, 178]. Commercial pDNA purification can be achieved as purification is scaled up linearly using the disposable, ready-to-use membranes [177, 189].

Zhong et al. [177] previously showed that using a hydrogel-based strong anion exchange (Q) membrane yielded high binding capacity (12.4 mg/ml) and ~90% plasmid recovery upon pDNA purification. This membrane was composed of a polypropylene membrane support completely encased by a functionalized hydrophilic hydrogel upon swelling. The inherent property of high adsorption and desorption associated with hydrogel-based membranes prompts further exploration of their potential in separating different pDNA sizes and isoforms for purification of LCC DNA.

In this study, anion exchange membrane chromatography was applied toward the separation and purification of LCC DNA isogenic derivatives from CCC pDNA parent precursor after passage through the one step *in vivo* LCC DNA vector production system. As

such, anion exchange membrane chromatography was assessed for its utility as a scalable system for the purification of human grade therapeutic LCC DNA minivectors.

3.2 Material and Methods

3.2.1 Production of LCC DNA products

A single colony of Tel^+ W3NN cells [108] was grown overnight in 5 ml LB + Ap (100 µg/ml) under repressed conditions at 30° C. Overnight cultures were grown at 1:100 dilution with 100 ml LB + Ap (100 µg/ml) at 30° C until late log phase A_{600} = 0.8. Cells were collected, centrifuged and re-suspended in 500 ml of LB + Ap (100 µg/ml) for induced protelomerase expression at 42° C until A_{600} = 1.0. This was followed by a gradual temperature downshift and overnight incubation at 30° C. Cells were harvested and plasmid extracted with *E.Z.N.A.* Plasmid Maxi-Prep Kit (Omega, VWR).

3.2.2 DNA Separation by Anion Exchange Membrane Chromatography

3.2.2.1 Buffers

The loading and washing buffers were 50 mM Tris-HCl (pH = 8.1) and the elution buffers were composed of loading and washing buffers with the addition of various concentrations of NaCl (0.1, 0.2, 0.3, 0.4, 0.5, 0.6, 0.7, 0.8, and 2.0 M). All buffers were prepared in 18MΩ sterile MilliQ water.

3.2.2.2 Membrane material, pre-treatment, loading and elution

The hydrogel-based strong anion exchange (Q) membrane syringe columns were provided by Natrix Separations Inc. (Burlington, Canada). The membrane column was connected to MPT-2 Autotitrator (Malvern, UK) for membrane soaking, pDNA loading and elution. The

membrane was pre-treated by soaking in loading buffer for 16 h at room temperature prior to pDNA loading. Plasmid DNA feeds for membrane chromatography experiments were prepared by diluting the extracted pDNA to ~50 µg/ml with loading buffer. For each experiment, 10 ml of the diluted pDNA sample was fed into the membrane column. After loading pDNA, the membrane column was incubated at room temperature for 10-15 min prior to flushing with 40 ml of washing buffer at 4 ml/min. Different experiments were conducted with elution buffer of varying salt gradient, by changing salt concentration, buffer volumes, and flow rates (2.5-4 ml/min). Individual fractions of 0.5-2 ml were collected from the start of elution until complete elution as confirmed by elution with 2 M NaCl elution buffer.

3.2.3 DNA Analysis

A NanoDrop spectrophotometer (Thermo Scientific, USA) was used to measure DNA concentration at 260 nm. Eluted pDNA concentrations (ng/µl) in each fraction were calculated from absorbance values using the Beer-Lambert equation, $A = E \times b \times c$; A is the absorbance; E is the extinction coefficient (50 ng-cm/µl); b is the path length; and c is the concentration. Eluted fractions with detected DNA concentrations were analyzed by AGE. Plasmid isoform compositions were assessed by AGE and densitometry (AlphaImager, Alpha Innotech).

3.3 Results and Discussion

Following the generation of LCC DNA products through our *in vivo* processing system, anion exchange membrane chromatography was applied to effectively separate successfully converted LCC DNA products from residual supercoiled CCC precursor parent plasmid. The experimental conditions for LCC DNA product purification were examined according to manufacturer recommendations and findings from Zhong et al. [177] to purify our DNA species of varying isoforms and sizes (2.7-5.6 kb). DNA was initially detected in eluted fractions at 0.7 M NaCl. Prolonged elution at this threshold salt concentration resulted in effective DNA recovery as DNA was not detected after elutions with 0.8 M and 2 M NaCl. From the total 357 fractions collected, those with detectable DNA fell between 189 and 329, all of which were collected and fractions 189-300 were further analyzed, using densitometry, by dividing individual fractions into 11 distinct sets of fractions (Figure 3.1). Visual inspection of selected fractions from each of the 11 sets indicated the initial elution of parental supercoiled CCC pDNA (~4.0 kb) in absence of LCC DNA. Subsequent fractions denoted increasing elution of supercoiled CCC pDNA accompanied by the initial elution of three LCC DNA species: parental LCC pDNA (5.6 kb), LCC backbone DNA (3.2 kb), and LCC DNA ministrings (2.4 kb) (Figure 3.1 A). The elution of LCC DNA corresponded with a decrease in the elution of CCC pDNA and the eventual separation of nearly all LCC DNA from CCC pDNA (Figure 3.1 B). Investigation of the yielded LCC DNA products showed a trend of increasing contribution of parental LCC pDNA at later elutions from 11.2% (set 6) to 52.8% (set 11) (Figure 3.1 C). Further analysis of the late elutions by AGE indicated a pattern of increasing elution of parental LCC pDNA over the two smaller LCC DNA

products, although with limited resolution (Figure 3.2). This suggested a partial separation between LCC DNA species according to size. However, complete separation of the different species by charge density, as a function of chain length, was unattainable as the different species were relatively similar in size. Subsequent studies were conducted to assess the effect of flow rate and salt gradient on the observed elution pattern. Manipulations to the flow rate (2.5-4 ml/min) were confirmed to have negligible effect on the observed elution pattern. However, the observed separation between LCC DNA and CCC pDNA was lost upon the application of a rapidly changing salt gradient.

Zhong et al. [177], found that plasmid size does not affect the adsorption rate but influences the degree of irreversible adsorption and the recovery fraction at pH of 8.0. They observed recovery rates of 75%, 89%, and 65% for plasmids of 6.4, 3.7, and 2.7 kb, respectively. The noted differences in elution efficiency were attributed to irreversible adsorption for the 6.4 (22.5%), 3.7 (2.5%), and 2.7 (32.6%) kb plasmids, respectively. As the size of the different CCC plasmids roughly matched the sizes of the LCC DNA species, it was suspected that similar trends for DNA recovery amongst the three species would be observed. Based on the composition of LCC DNA species recovered, greater yields of LCC backbone DNA (3.2 kb) were observed compared to LCC minivector DNA (2.4 kb) despite the expected 1:1 ratio in the feed (Figure 3.1 C). This finding can likely be attributed to the differences in irreversible adsorption rates since the adsorption fraction was nearly constant for all plasmid sizes at pH of 8.0. To improve LCC DNA ministring recovery, a pH of 9.0 may prove ideal as it promotes recovery of smaller sized DNA in conjunction with a minimal level of irreversible adsorption [177].

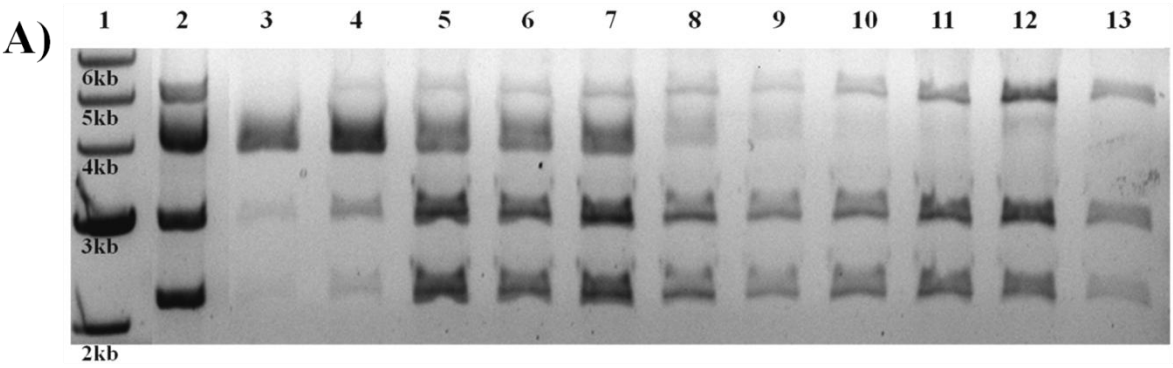
A)
1
2
3
4
5
6
7
8
9
10
11
12
13
6kb
5kb
4kb
3kb
2kb

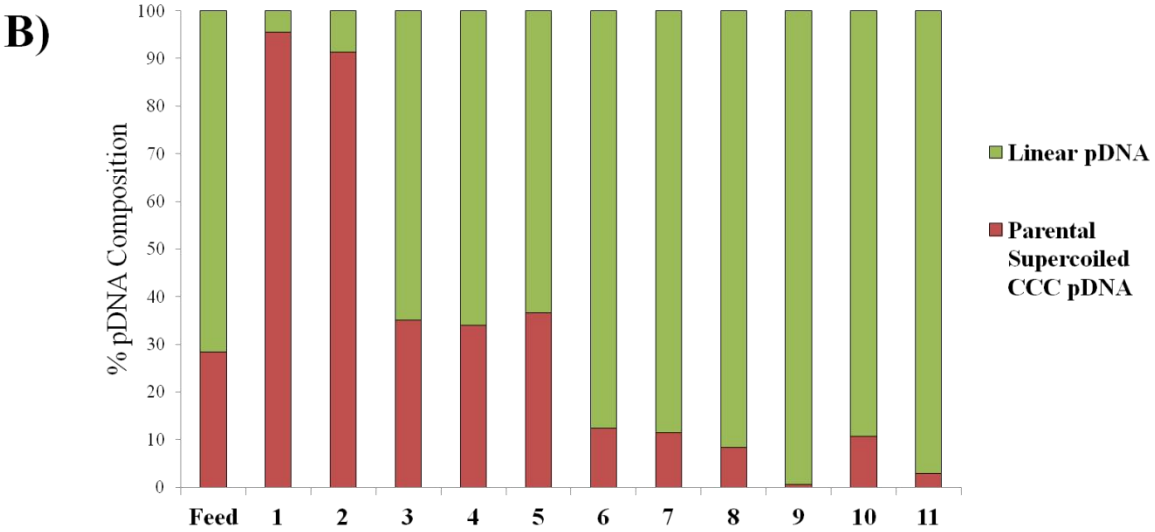
B)
% pDNA Composition
100
90
80
70
60
50
40
30
20
10
0
Feed
1
2
3
4
5
6
7
8
9
10
11
Linear pDNA
Parental Supercoiled CCC pDNA

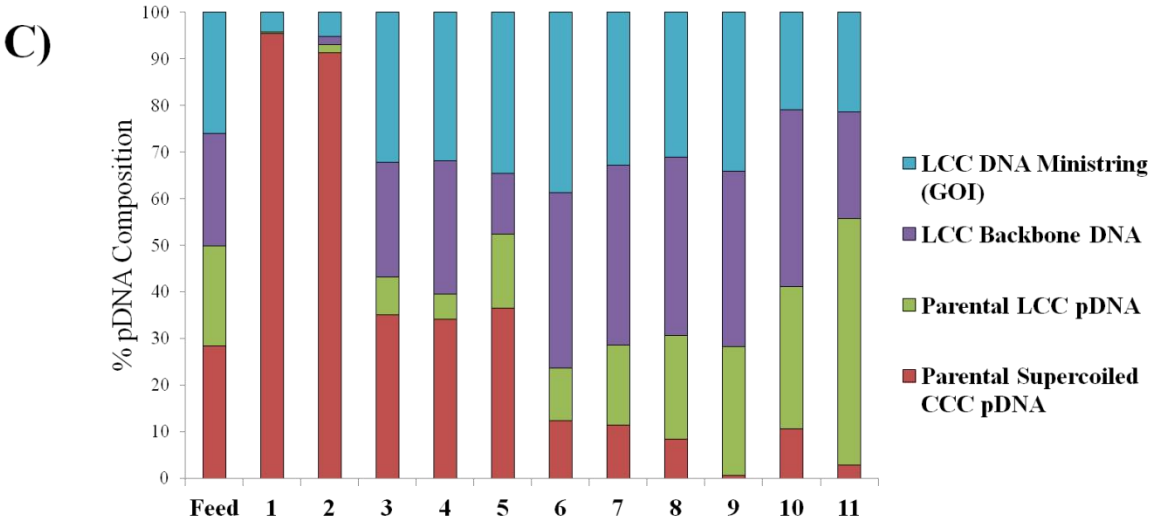
C)
% pDNA Composition
100
90
80
70
60
50
40
30
20
10
0
Feed
1
2
3
4
5
6
7
8
9
10
11
LCC DNA Ministring (GOI)
LCC Backbone DNA
Parental LCC pDNA
Parental Supercoiled CCC pDNA

Figure 3.1 Separation of DNA isoforms by anion exchange membrane chromatography. Agarose gel electrophoresis and densitometry analysis of DNA isoforms attained from sequential sets of eluted fractions using anion exchange membrane chromatography. Eluted fractions (fractions 189-300) were categorized into 11 distinct sets according to their elution order. **A)** Analysis of DNA isoforms of eluted fractions by 0.8% gel electrophoresis: DNA Ladder (lane 1); pDNA feed solution (lane 2); a selected fraction from each of the 11 distinct sets - fraction 191 (lane 3); fraction 199 (lane 4); fraction 205 (lane 5); fraction 211 (lane 6); fraction 216 (lane 7); fraction 226 (lane 8); fraction 238 (lane 9); fraction 254 (lane 10); fraction 266 (lane 11); fraction 276 (lane 12); fraction 292 (lane 13). Visual inspection confirmed early elution of parental supercoiled CCC pDNA (~4.0 kb) followed by increasing elution of the LCC DNA: parental LCC pDNA (5.6 kb), LCC backbone DNA (3.2 kb), and LCC DNA ministring (2.4 kb) (see Figure 2.1). Separation of DNA isoforms was denoted by the disappearance of the ~4.0 kb band, conferring the absence of parental supercoiled pDNA in later fractions. **B)** Analysis of the average composition of LCC DNA and parental supercoiled CCC pDNA within the 11 distinct sets highlighting the separation of LCC DNA from parental supercoiled CCC pDNA. **C)** Complete breakdown of all three LCC DNA species within each of the 11 sets of fractions.

In agreement with Haber et al. [184], the application of strong, positively charged membranes was successful in resolving different DNA isoforms and our findings, denoting early elution of parental supercoiled CCC pDNA followed by LCC DNA, matched well with the previous findings. According to Haber et al. [184], the elution order was due to convective flow-induced structural behavior of the different DNA isoforms. Compact supercoiled CCC DNA was able to reach the membrane first and gain early access to binding sites. The structural nature of OC DNA constituted a lower overall surface charge density resulting in loose binding interactions and earlier elution [177]. On the other hand, linear DNA was capable of undergoing strong cooperative interactions due to high elasticity and their ability to form loops and trains, thereby promoting strong binding and retention, contributing to later elution of linear DNA after supercoiled CCC DNA.

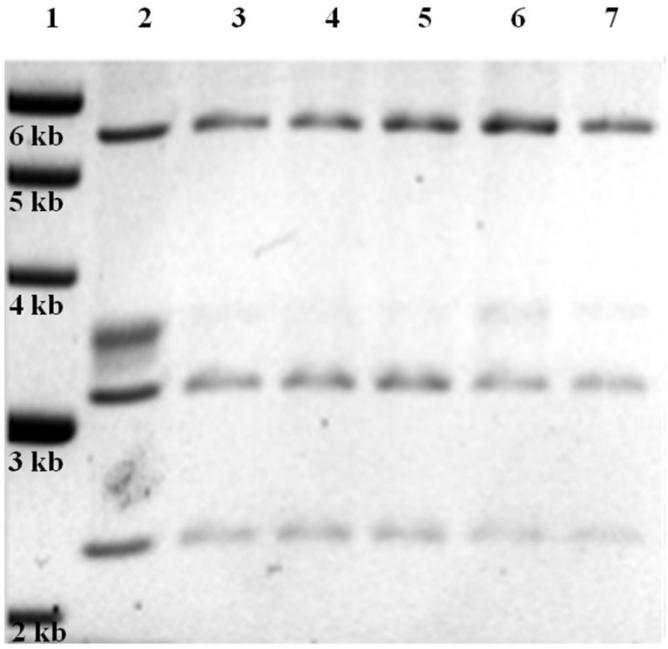

Figure 3.2 Analysis of LCC pDNA species in late elutions from anion exchange membrane chromatography. Gel analysis of LCC DNA species attained in late elutions using 0.8% gel electrophoresis: molecular mass markers (lane 1); pDNA feed solution (lane 2); sequential fractions attained at late elutions - fraction 284 (lane 3); fraction 288 (lane 4); fraction 292 (lane 5); fraction 296 (lane 6); fraction 300 (lane 7). A relatively greater recovery of parental LCC pDNA was observed in comparison to the other two LCC DNA species.

Purification of LCC DNA ministrings by affinity chromatography, a form of separation based on molecular recognition and sequence specific interactions, effectively enhances selectivity suitable for one step purification [190, 191]. Plasmid purification using triple-helix [192], amino acid-DNA [193], and protein-DNA [112] affinity chromatography had been previously demonstrated. Triple-helix affinity chromatography involved interactions between pyrimidine oligonucleotides, covalently linked to the chromatographic matrix, and corresponding polypurine sequences at the major groove of DNA via Hoogsteen hydrogen bonds. Such interactions resulted in the formation of TA-T and CG-C^+ triplexes that were

stable under acidic conditions [190-192]. Subsequent elution at alkaline pH prompted the dissociation of the triple-helix for DNA recovery. Such purification required genetic modifications for the inclusion of the polypurine sequences into the pDNA construct and were limited by low DNA recovery and slow kinetics of triple helix formation [190]. Similarly, protein-DNA affinity chromatography employed a protein for the recognition of specific sequences within the pDNA construct. Mayrhofer et al. [112] previously demonstrated recombination based plasmid separation (RBPS) for purification of minicircle-DNA at purities greater than 98.5%. Such separation involved highly efficient ParA resolvase recombination for production of minicircle-DNA followed by affinity chromatography, using immobilized LacI repressors, for minicircle-DNA purification. A tandem repeat of modified lactose operator sites (*lacOs* sites) was included into the pDNA construct and served as the recognition sequence for LacI repressors. Elution of the LacI-bound minicircle-DNA was achieved through the addition of isopropyl β-D-1-thiogalactopyranoside (IPTG) and NaCl. Further investigation into purification of LCC DNA ministrings by affinity chromatography will be warranted upon addressing limitations of low binding capacity and durability of natural ligands, production costs of chromatographic matrix for large scale purifications, and potentially reduced capacities upon repeat administrations.

Large scale production of pharmaceutical grade pDNA requires a rapid and economical means of generating purified pDNA free of animal-derived enzymes and toxic reagents [180]. Laboratory scale pDNA vector production generally involves extraction kits employing solvents, toxic chemicals (cesium chloride & ethidium bromide), or animal-derived enzymes (RNase A), which poses significant issues relating to cost, scalability, and

safety [176, 178, 180]. Previously, several groups had attempted large-scale pDNA purification using a combination of tangential flow filtration and various chromatography techniques including HIC, SEC, and AEC [176, 178-180]. Anion exchange membrane chromatography had been applied for such purification processes resulting in high concentration of pDNA and RNA removal [176, 178]. Reductions to endotoxin levels as high as four orders of magnitude had been previously demonstrated in large scale purifications using anion exchange membrane chromatography [189]. Subsequent application of HIC may further enhance pDNA purity as HIC was demonstrated to successfully remove proteins, endotoxins, chromosomal DNA, and residual RNA [178-180, 194]. In particular, application of HIC was reported to eliminate over 99% of impurities while increasing pDNA purity by 30.5 fold [178]. Improved transfection efficiency was also observed after purification by HIC [194]. Large scale production previously demonstrated an overall yield of 48% as 800 mg of pharmaceutical grade pDNA (protein <2 μg/mg plasmid; endotoxin <10 EU/mg plasmid; chromosomal DNA <1 μg/mg plasmid) was generated from 2 kg of bacterial cell paste [180]. As AEC had been utilized for large scale pDNA purification, its application for separating DNA isoforms should not impose additional costs or significant production delays in the generation of pharmaceutical grade DNA vectors. Hence, further exploration into optimal conditions for effective separation by anion exchange membrane chromatography will be warranted for downstream large scale production of LCC DNA ministrings.

3.4 Conclusions

Results from this study served as a proof-of-concept highlighting the advantages of anion exchange membrane chromatography in pDNA purification as well as demonstrating its potential in the separation of different DNA isoforms. Application of a hydrogel-based strong Q-anion exchange membrane and manipulations of the salt gradient constituted effective separation of parental supercoiled CCC pDNA from LCC DNA. Further exploration of the optimal conditions and additional modifications will be warranted as AEC serves to be an integral component in downstream purification processes for the large-scale production of clinical grade DNA ministrings.

Chapter 4

Transfection and Physical Characterization of DNA/16-3-16/DOPE Gemini Surfactant Based Vectors for the Delivery of LCC DNA Ministrings

4.1 Introduction

Gemini surfactants are amphiphilic molecules composed of two surfactant monomers chemically linked by a spacer. Gemini surfactants confer advantages of reduced cytotoxicity and cost effectiveness as they possess a critical micelle concentration (CMC) that is one to two orders of magnitude lower than their monomer counterparts [15, 85]. Gemini surfactant derived synthetic vectors offer numerous advantages including: 1) high positive charge for effective DNA complexation at low concentrations; 2) efficient DNA compaction generating smaller complexes than their monomeric counterparts; 3) effective endosomal escape alone or in combination with DOPE; and 4) suitability for long term storage, over two months at ambient temperatures, in lyophilized formulations without losing functionality [88, 89].

Among the different m-s-m or N,N-bis(dimethylalkyl)-α,ω-alkanediammonium surfactants (where m and s represent the number of carbon atoms in the alkyl tails and in the polymethylene spacer group), the 16-3-16 derivative has been extensively studied due to their structural nature, promoting effective DNA complexation, and their capacity to adopt structural polymorphisms critical to endosomal escape and successful gene delivery. 16-3-16 gemini surfactants possess a trimethylene spacer (s = 3) that constitutes compatible head group distances (~0.49 nm) with the spacing of phosphate groups (0.34 nm) in DNA [91]. Their high positive charge (relative to monomeric surfactants and lipids) promotes efficient

DNA binding and compaction, generating particles suitable for gene delivery. Numerous reports have previously indicated the ability of 16-3-16 gemini-based lipoplexes, in combination with DOPE, to form higher ordered phase structures including inverted hexagonal and cubic phase structures [15, 97, 98, 195]. Such structures are highly dependent on the lipoplex composition with hexagonal structures predominantly present at high mol ratios of DOPE and cubic phase structures at high mol ratios of gemini surfactant [98].

Owing to the inherent properties of 16-3-16 gemini-based lipoplexes, such synthetic vectors had been successfully applied for *in vivo* cutaneous interferon-γ gene delivery as part of a topical treatment for localized scleroderma [91, 196, 197]. Scleroderma is a chronic autoimmune disorder characterized by the excessive collagen synthesis and deposition in skin/connective tissue, contributing to fibrosis. Induced expression of interferon-γ (IFN-γ) acts to suppress collagen synthesis and this serves as the basis for treatment of localized scleroderma using a topical formulation comprised of IFN-γ encoding, 16-3-16 gemini-based synthetic vectors [91, 196, 197]. The pDNA/16-3-16/DOPE synthetic vector was shown to successfully transfect PAM212 keratinocytes *in vitro* as well as normal (CD1) and IFN-γ-deficient knockout mice *in vivo*. Topical application of gemini-liposomal formulation significantly improved IFN-γ expression in the skin of CD1 mice in conjunction with a 12 fold increase of IFN-γ in lymph nodes [91]. With respect to IFN-γ-deficient mice, higher IFN-γ expression was observed over pDNA only and untreated controls in absence of skin damage and irritation [197]. Using a Tsk/+ scleroderma mouse model, a 20-day treatment regimen with the topical formulation constituted uniform IFN-γ expression that resulted in

70-72% collagen reduction [196], thus demonstrating efficacy in treating localized scleroderma.

As seen in the abovementioned studies, synthetic vectors for gene delivery typically consists of CCC pDNA. However, the linear topology of LCC DNA ministrings may present differences to DNA interaction and physicochemical properties of the resulting vector. In this study, 16-3-16 gemini-based synthetic vectors, derived from CCC pDNA (CCC/16-3-16/DOPE) and LCC DNA ministrings (LCC/16-3-16/DOPE), were characterized and assessed for gene delivery into ovarian cancer cells (OVCAR-3). Comparative analysis of the physical properties for CCC/16-3-16/DOPE and LCC/16-3-16/DOPE lipoplexes, with respect to particle size, zeta potential, DNA encapsulation, and DNase sensitivity, was completed. Preliminary assessment of transfection efficiencies was conducted between the two vectors.

4.2 Materials and Methods

4.2.1 Production of CCC pDNA, LCC DNA products and LCC DNA ministrings

The pNN9 vector [108] was used as the parental pDNA substrate for the production of LCC DNA ministrings and for the generation of CCC/16-3-16/DOPE lipoplexes. Tel^{+} W3NN [pNN9] was used for the production of *egfp* LCC DNA ministrings and JM109 was employed as hosts for plasmid amplification. LCC DNA ministrings were generated according to procedures outline in section 2.2.2, with the 2.4 kb DNA ministring being subsequently purified using AGE and gel extraction with *E.Z.N.A.* Gel Extraction Kit (Omega, VWR). The purified DNA ministrings were used for the generation of LCC/16-3-16 and LCC/16-3-16/DOPE lipoplexes.

4.2.2 Generation of CCC/16-3-16/DOPE and LCC/16-3-16/DOPE Transfection Lipoplexes.

16-3-16 gemini surfactants were previously synthesized according to procedures outlined by Wettig and Verrall [92]. 1.5 mM 16-3-16 gemini surfactant stock solutions were prepared in molecular water (HyClone, Thermo Scientific) with sonication (50° C) and purification through a 0.2 μm sterile filter (Fisher Scientific, Canada). Different aliquots of the 16-3-16 stock solution (1.2 μl, 3 μl and 6 μl per 0.4 μg DNA) were used to generate gemini/DNA lipoplexes at 2:1, 5:1, and 10:1 N^+/P^- charge ratios. 1 mM DOPE vesicles were prepared in phosphate buffer saline (PBS) according to procedures outlined by Wettig et al. [93]. The vesicles were filtered through a 0.45 μm sterile filter and different aliquots (3 μl, 7.4 μl and 15 μl) were used to generate lipoplexes, of varying charge ratios, with a constant gemini to DOPE ratio of 1:2.5.

The two respective lipoplexes were prepared as follows: 0.4 μg of DNA, pNN9 or *egfp* LCC DNA ministring, was mixed with different aliquots of 1.5 mM 16-3-16 gemini surfactant solution to yield $N^{+/}P^-$ charge ratios of 2:1, 5:1, and 10:1. After 15 minute incubation at room temperature, different aliquots of 1 mM DOPE were added and the subsequent mixture was further incubated for 30 minutes at room temperature. All other DNA/16-3-16/DOPE lipoplexes of different N^+/P^- charge ratios were generated in the same manner using different aliquots/dilutions of 16-3-16 gemini and DOPE.

4.2.3 Characterization of 16-3-16 Gemini Based Lipoplexes

4.2.3.1 Particle Size and Zeta Potential

Particle sizes for DNA, 16-3-16, DOPE, and resulting DNA/16-3-16 & DNA/16-3-16/DOPE lipoplexes were measured by dynamic light scattering using Malvern Zetasizer Nano ZS instrument (Malvern instruments, UK). Particle size distributions were obtained from light scattering ($\theta = 173°$) in water at 25° C and the measured sizes were reported using a % volume distribution. Samples were measured in triplicates of triplicate and the resulting averages were reported.

Zeta potential (ζ) for the abovementioned samples was measured by Laser Doppler Electrophoresis using zeta potential capillary cells and Malvern Zetasizer Nano ZS instrument (Malvern instruments, UK). All measurements were made at 25° C and samples were measured in triplicates of quintuplicate with averages being reported.

4.2.3.2 DNase Sensitivity Assay

The DNase sensitivity assay involved the incubation of lipoplexes with DNase I (1 unit per 1 μg DNA) (Promega) and the DNase reaction buffer (Tris-HCl, M_gSO_4, $CaCl_2$) for 30 minutes at 37° C. Subsequently, DNase I was inactivated by the addition of DNase stop solution (ethylene glycol tetraacetic acid (EGTA)) and denatured upon 10 minute incubation at 60° C. Lipoplexes were disrupted with the addition of phenol:chloroform:isoamyl alcohol (25:24:1, v/v) (Invitrogen) for the recovery of non-degraded DNA upon centrifugation. The extent of DNaseI induced degradation was assessed by AGE upon equal loading across all samples.

4.2.3.3 Transfection of OVCAR-3 Cells

OVCAR-3 (ATCC HTB161) ovarian cancer cells were cultured in RPMI-1640 (HyClone, Thermo Scientific) supplemented with 20% fetal bovine serum (FBS) (HyClone, Thermo Scientific) and 1% penicillin-streptomycin (Fisher Scientific). OVCAR-3 cells were grown at 37° C with 5% CO_2 and maintained at 70-80% confluency prior to transfection. OVCAR-3 cells were seeded, 50,000 cells/well, into a 24-well plate and incubated at 37° C for ~24 hours. Cells were washed with PBS and fresh RPMI-1640, without FBS or antibiotics, was added. Transfection lipoplexes were prepared in Opti-Mem (Gibco, Invitrogen) and the resulting lipoplexes were added drop-wise at amounts corresponding to 0.4 μg of DNA per well. Transfection with 1.2 μl Lipofectamine™ 2000 (1 mg/ml) (Invitrogen), per 0.4 μg of DNA, were completed according to manufacturer's protocol and served as a positive control in the study. Cells were subsequently incubated at 37° C for 5 hours before the transfection medium was replaced by fresh RPMI-1640 with 20% FBS. Cells were further incubated at 37° C until 24 hours post-transfection at which point the cells were collected, washed, and re-suspended in PBS. Samples were stained with propidium iodide and analyzed by fluorescence activated cell sorting (FACS) (BD FACSVantage SE) for the assessment of transfection efficiency, as determined by EGFP expression, and cell viability post-transfection.

4.3 Results

4.3.1 Particle Size and Zeta Potential (ζ)

With regards to 5.6 kb pNN9 (CCC) and 2.4 kb DNA ministring (LCC), particle sizes of the two DNA vectors were surprisingly similar despite their inherent differences in DNA composition (Table 4-1). The differences were accounted by the supercoiled nature of CCC pDNA contributing to more compact conformations than their linear counterparts. Such notions were supported by the differences in observed zeta potentials (ζ) as DNA supercoiling in pNN9 (CCC) masked a fraction of the negative charges attained from the phosphate groups of DNA. In contrast, the structural nature of the linear isoforms contributed to more prominent surface charges as indicated by a greater (-) zeta potential. By itself, 16-3-16 gemini surfactants were able to rapidly self assemble into micelles due to high concentrations of the stock solution and due to conditions at which lipoplexes were generated. The 1.5 mM 16-3-16 stock solution was generated at concentrations well above the CMC of the gemini surfactant (0.0255 mM) and as lipoplexes were generated below the Krafft temperature (T_k = 42° C), referred to as the minimum temperature at which surfactant forms micelles, 16-3-16 micelles were rapidly self-assembled [91, 198]. The propensity for 16-3-16 gemini surfactant to form micelles/vesicles of varying sizes resulted in the observed high polydispersities as indicated by a PDI value of 0.752.

Table 4-1 Particle size & zeta potential of CCC pNN9, LCC DNA ministring, 16-3-16, and DOPE.

	Size (d.nm)	Polydispersity Index (PDI)	ζ-Potential (mV)
pNN9 (CCC)	371 ± 90	0.466	-25 ± 9
DNA ministring (LCC)	363 ± 74	0.494	-35 ± 2
16-3-16	50 ± 17	0.752	55 ± 5
DOPE	131 ± 18	0.257	-19 ± 5
16-3-16/DOPE	204 ± 67	0.657	

With respect to DNA/16-3-16 and DNA/16-3-16/DOPE lipoplexes, the two vectors generated lipoplexes of comparable particle sizes and zeta potentials across the three tested charge ratios (Table 4-2). For DNA/16-3-16 lipoplexes, both CCC/16-3-16 and LCC/16-3-16 lipoplexes exhibited the progressive formation of uniformly sized particles, as indicated by decreasing PDI values, at increasing charge ratios. With respect to DNA/16-3-16/DOPE lipoplexes, substantially larger particle sizes were observed for lipoplexes at charge ratios of 2:1. The large particles exhibited at lower charge ratios were likely the result of aggregation upon charge neutralization and subsequent addition of more gemini surfactants, at 5:1 and 10:1 charge ratios, resulted in a dramatic decrease in particle sizes with lower polydispersities. In closer inspection of particle size fluctuations across the spectrum of progressively increasing charge ratios (Figure 4.1), charge neutralization and aggregation for LCC/16-3-16/DOPE lipoplexes was observed to occur at the lower charge ratio of 1:1 whereas significant aggregation of CCC/16-3-16/DOPE lipoplexes occurred at a charge ratio of 2:1. Aggregation of the resulting lipoplexes and interference with light scattering

measurements, upon charge neutralization, contributed to large standard deviations and populations of highly variable particle sizes [199, 200].

Table 4-2 Particle size and zeta potential of DNA/16-3-16 and DNA/16-3-16/DOPE lipoplexes.

	pNN9 (CCC)			DNA ministring (LCC)		
	Size (d.nm)	PDI	ζ-Potential (mV)	Size (d.nm)	PDI	ζ-Potential (mV)
DNA/16-3-16						
2:1	141 ± 24	0.402	38 ± 1	143 ± 40	0.351	41 ± 9
5:1	127 ± 31	0.359	39 ± 3	114 ± 37	0.241	48 ± 7
10:1	100 ± 38	0.267	48 ± 9	132 ± 43	0.185	43 ± 3
DNA/16-3-16/DOPE						
2:1	2343 ± 1390	0.592	10 ± 18	1634 ± 655	0.561	22 ± 3
5:1	195 ± 95	0.346	24 ± 7	168 ± 65	0.243	29 ± 7
10:1	218 ± 119	0.372	36 ± 6	247 ± 144	0.409	29 ± 6

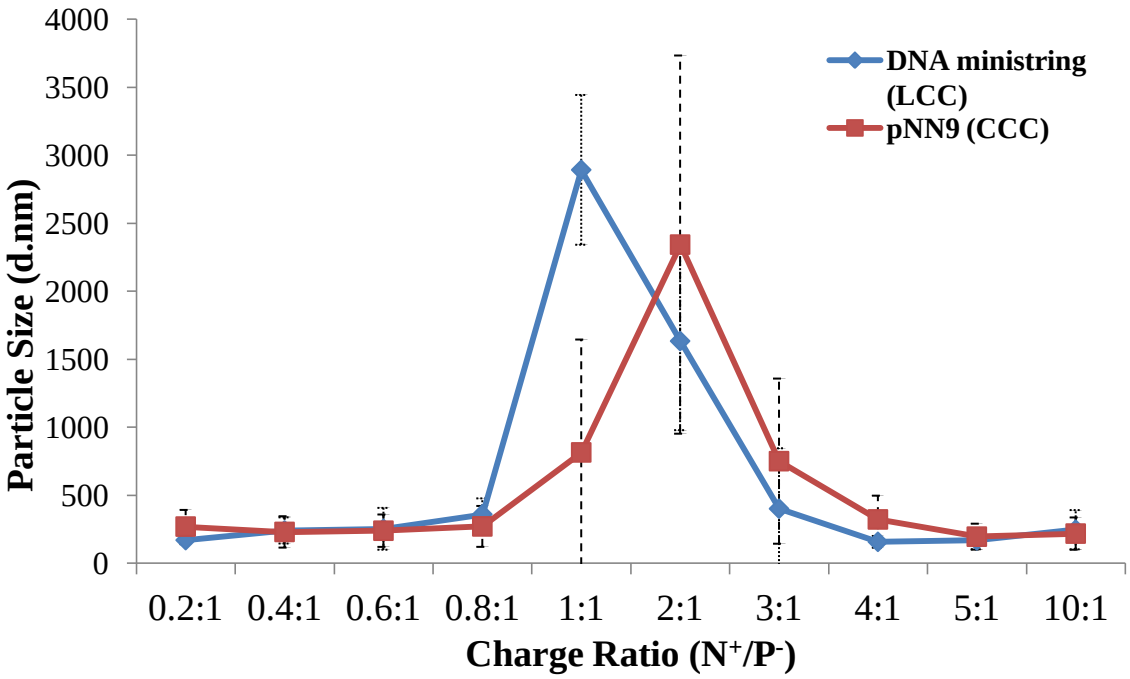

Figure 4.1 Particle size variations for DNA/16-3-16/DOPE lipoplexes with increasing N^+/P^- charge ratios. As lipoplexes approach charge neutralization, a significant increase in particle size led to highly variable particles conferring large aggregate formation. Large aggregates for LCC/16-3-16/DOPE and CCC/16-3-16/DOPE lipoplexes appeared most prominent at charge ratios of 1:1 and 2:1 respectively. Progressive decreases to particle sizes at higher charge ratios led to stable and uniform particle formation.

4.3.2 DNase Sensitivity

Results from the DNase sensitivity assay suggested better DNA protection in DNA ministring (LCC) derived lipoplexes (Figure 4.2). Lipoplexes formed in absence of DOPE offered better protection as indicated by improved DNA recovery. Across all three tested N^+/P^- charge ratios, DNA ministring (LCC) derived lipoplexes (lanes 15-17) exhibited improved stabilities over pNN9 (CCC) derived lipoplexes (lanes 5-7) as evidenced by greater DNA recovery upon DNase exposure. With respect to LCC/16-3-16 and LCC/16-3-16/DOPE lipoplexes, the incorporation of DOPE resulted in less stable complexes as limited amounts

of DNA were recovered for LCC/16-3-16/DOPE lipoplexes at 2:1 charge ratio (lane 18); however, greater stabilities and improved DNA recovery were observed at higher charge ratios for DOPE containing lipoplexes (lanes 19 & 20). Comparative analysis between CCC and LCC derived transfection complexes, at 2:1, 5:1, and 10:1 charge ratios, confirmed improved DNA protection for LCC/16-3-16/DOPE lipoplexes (Figure 4.3). As a majority of the complexed DNA was protected from DNaseI degradation, LCC/16-3-16/DOPE lipoplexes at 5:1 and 10:1 charge ratios may serve to be suitable candidates as synthetic vectors.

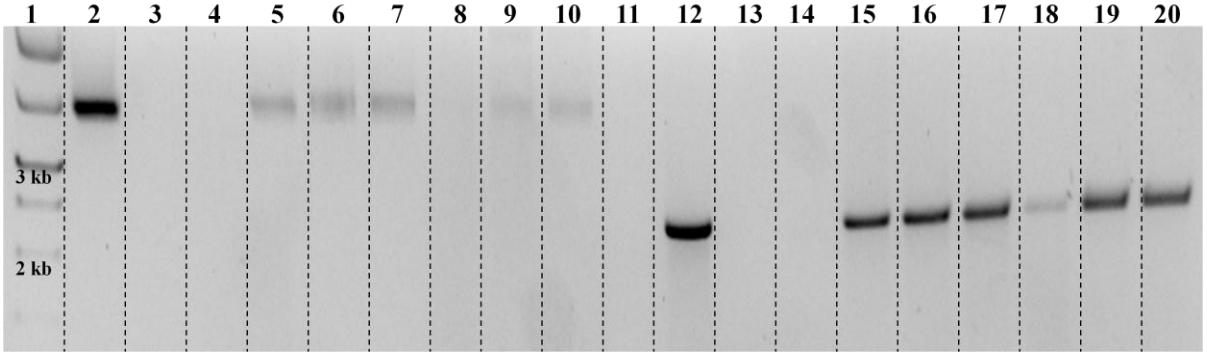

Figure 4.2 DNase sensitivity assay for DNA/16-3-16 and DNA/16-3-16/DOPE lipoplexes. DNA ladder (lane 1); pNN9 (CCC) (lane 2); DNaseI exposed pNN9 (CCC) (lanes 3 & 4); CCC/16-3-16 lipoplexes at 2:1, 5:1 and 10:1 charge ratios (lanes 5-7); CCC/16-3-16/DOPE lipoplexes at 2:1, 5:1, and 10:1 charge ratios (lanes 8-10); 16-3-16/DOPE (lane 11); DNA ministring (LCC) (lane 12); DNaseI exposed DNA ministring (LCC) (lanes 13 & 14); LCC/16-3-16 lipoplexes at 2:1, 5:1, and 10:1 charge ratios (lanes 15-17); LCC/16-3-16/DOPE lipoplexes at 2:1, 5:1, and 10:1 charge ratios (lanes 18-20). Equal loading of the recovered DNA solution after DNaseI exposure indicated improved DNA recovery for ministring (LCC) derived lipoplexes. DNA/16-3-16 lipoplexes conferred better DNA recovery after DNaseI degradation over DNA/16-3-16/DOPE lipoplexes across all of the tested charge ratios.

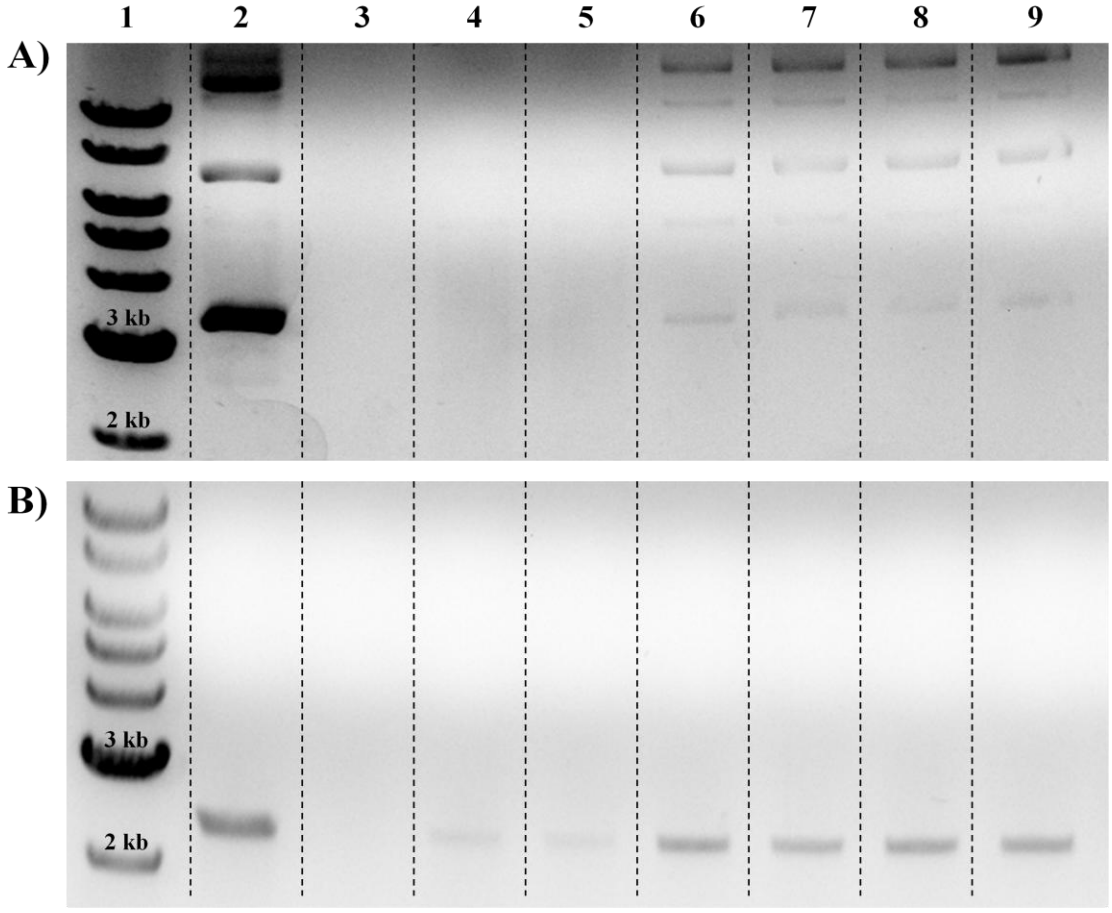

Figure 4.3 DNase sensitivity assay for A) CCC/16-3-16/DOPE lipoplexes and B) LCC/16-3-16/DOPE lipoplexes. DNA ladder (lane 1); DNA (lane 2); DNaseI exposed DNA (lane 3); DNA/16-3-16/DOPE lipoplexes at 2:1 charge ratio (lanes 4 & 5); DNA/16-3-16/DOPE lipoplexes at 5:1 charge ratio (lanes 6 & 7); DNA/16-3-/16/DOPE lipoplexes at 10:1 charge ratio (lanes 8 & 9). Equal loading confirmed improved DNA recovery after DNaseI exposure at higher charge ratios. A majority of the complexed DNA ministrings (LCC) was recovered in lipoplexes at 5:1 and 10:1 charge ratios.

4.3.3 Preliminary Investigation of the Transfection Efficiency of pNN9 (CCC) and DNA ministring (LCC) Derived Lipoplexes.

EGFP expression was assessed and quantified through FACS for the determination of transfection efficiencies across the different transfection lipoplexes (Figure 4.4). Lipofectamine served as the positive control and demonstrated a transfection efficiency of

12%. In contrast, untreated control and cells treated with uncomplexed DNA did not elicit any EGFP expression. For CCC/16-3-16/DOPE lipoplexes, increasing transfection efficiencies were observed with increasing charge ratios, however, such increases were not statistically significant. In conjunction with slight improvements to transfection efficiency, higher charge ratios constituted greater cytotoxicity with cell viabilities of 60% attained with CCC/16-3-16/DOPE lipoplexes. Of the three LCC/16-3-16/DOPE lipoplexes, lipoplexes with a 5:1 charge ratio demonstrated the highest transfection efficiency (8.2%).

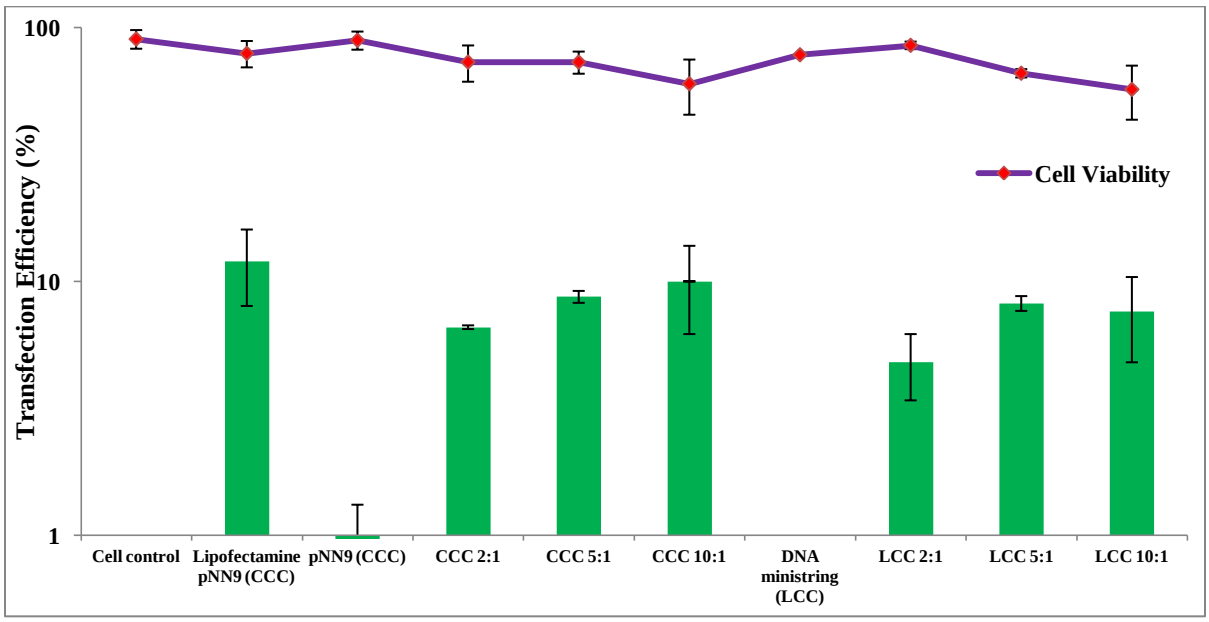

Figure 4.4 Preliminary analysis of transfection efficiencies for CCC/16-3-16/DOPE and LCC/16-3-16/DOPE lipoplexes in OVCAR-3 cells (N=2). Both pNN9 (CCC) and DNA ministring (LCC) derived lipoplexes exhibited comparable transfection efficiencies at 2:1, 5:1, and 10:1 charge ratios. Increasing charge ratios constituted increases to both transfection efficiencies and cytotoxicity. LCC/16-3-16/DOPE lipoplexes at 5:1 charge ratio demonstrated higher transfection efficiency with comparatively lower cytotoxicity than lipoplexes at 10:1 charge ratio.

4.4 Discussion

With regards to the influences of DNA topology, direct comparisons between pNN9 (CCC) and DNA ministrings (LCC) cannot be made due to the inherent differences in the size of the two respective vectors. More apparent differences may have arise had the parental supercoiled CCC pNN9 been compared with its parental LCC counterpart, however, results from this study denoted certain differences arising from the influences of DNA topological conformations. The supercoiling effect contributed to a lower effective negative charge for CCC pNN9 [201, 202] which led to lower surface charges (ζ = -25 $\pm$ 9 mV) when compared to LCC DNA ministrings (ζ = -35 $\pm$ 2 mV). In addition, DNA supercoiling reduced the overall size of the circular plasmid, which contributed to comparable particle sizes between pNN9 and DNA ministrings despite the fact that pNN9 was the larger sized plasmid. Such differences had significant effects on the interactions between DNA and 16-3-16 gemini surfactant in terms of counterion release during lipoplex formation. Previously, DNA/16-3-16/DOPE lipoplexes, comprised of linear calf thymus DNA (ctDNA), demonstrated complete release of Na^+ counterions during lipoplex formation; in contrast, a significant fraction of counterions remained bound during complex formation of CCC pDNA-derived lipoplexes [201, 202]. Counterion displacement was suggested to be inhibited due to the compact conformation of supercoiled CCC pDNA inducing geometric constraints on gemini/DNA interactions.

Resulting particle sizes and zeta potentials for DNA/16-3-16 and DNA/16-3-16/DOPE lipoplexes were in agreement with literature [97, 197] as all lipoplexes possessed positive zeta potentials critical to *in vitro* transfection. Upon inspection of particle size variations for

lipoplexes across different charge ratios, both CCC/16-3-16/DOPE and LCC/16-3-16/DOPE exhibited significant increases in particle sizes at charge ratios corresponding to charge neutralization and large aggregate formation. For CCC/16-3-16/DOPE lipoplexes, substantial large aggregation formation was observed at a higher charge ratio of 2:1 in contrast to 1:1 for LCC/16-3-16/DOPE lipoplexes. Differences may be attributed to the antagonistic interactions between 16-3-16 gemini and DOPE [99] in combination with incomplete counterion release for CCC/16-3-16 lipoplexes, prompting more prominent DOPE induced instabilities that prevented the generation of stable, discrete lipoplex particles. Lipoplex instabilities were exemplified by the lower and highly variable (+) zeta potentials ($\zeta = 10 \pm 18$ mV) for CCC/16-3-16/DOPE lipoplexes at a charge ratio of 2:1. Such zeta potentials were indicative of charge neutrality that contributed to aggregation and the observed large particle sizes.

DNA ministring (LCC) derived lipoplexes exhibited improved DNA encapsulation and protection properties as evidenced by improved DNA recovery upon DNaseI exposure. For both CCC/16-3-16/DOPE and LCC/16-3-16/DOPE lipoplexes, the higher charge ratios of 5:1 and 10:1 elicited better DNA encapsulation, protecting the DNA cargo from degradation. However, such protection was more prominent in LCC/16-3-16/DOPE lipoplexes and this was attributed to the higher (-) zeta potential of DNA ministrings and the complete release of counterions during complexation. The highly negative zeta potentials exhibited in DNA ministrings denoted significant surface charges for extensive electrostatic interaction with the positively charged 16-3-16 gemini surfactant, leading to complete counterion release and reduced head group repulsions. Reduced head group repulsion between individual gemini

surfactants conferred better encapsulation, effectively protecting the residing DNA from exposure to DNaseI. With regards to LCC/16-3-16 and LCC/16-3-16/DOPE lipoplexes, improved DNA encapsulation and protection for LCC/16-3-16 lipoplexes were attributed to tight associations between DNA ministring and gemini surfactant as supported by high (+) zeta potentials. Despite offering smaller particle sizes and better protection from degradation, LCC/16-3-16 lipoplexes were shown to consistently exhibit low transfection efficiencies most likely due to their inability to undergo structural polymorphisms, for endosomal escape and DNA release, in absence of DOPE [98].

Across the three charge ratios, CCC/16-3-16/DOPE lipoplexes exhibited similar transfection efficiencies with increasing transfection efficiency and cytotoxicity being observed at increasing charge ratios. This was in contrast to previous reports by Wang at el. [96] where transfection efficiency decreased with increasing charge ratios. Nevertheless, transfection efficiencies attained in this study were comparable to those reported by Wang et al. [96] across the three tested charge ratios. With respect to LCC/16-3-16/DOPE lipoplexes, a charge ratio of 5:1 corresponded to the highest transfection efficiency. However, preliminary results did not suggest substantial improvements in transfection efficiency for DNA ministring derived lipoplexes. Transfection efficiency of the Lipofectamine positive control was drastically lower than previous reports (12% vs 32.2%) [85, 96]. The lower transfection efficiencies may be attributed to high passage number (18-20), contributing to cellular senescence, during which transfections took place. Further studies, using OVCAR-3 as well as other cell lines, will be required for complete analysis of the differences in transfection efficiency attained from lipoplexes derived from CCC and LCC DNA vectors.

4.5 Conclusion

Despite the size disparities between pNN9 (CCC) and DNA ministrings (LCC), differences in DNA topology led to the generation of lipoplexes of comparable particle sizes between the two DNA vectors. The capacity for DNA ministring (LCC) derived lipoplexes to undergo complete counterion release during lipoplex formation contributed to improved DNA encapsulation and protection from DNase degradation. Preliminary analysis indicated comparable transfection efficiencies attained from both pNN9 and DNA ministring derived lipoplexes. Further investigation will be required to fully ascertain the influence of DNA topology on transfection capacities, in gemini-based synthetic vectors, across various cell types.

Chapter 5

Application of DNA Ministrings to the Development of an HIV DNA VLP Vaccine

5.1 Introduction

The one-step *in vivo* LCC DNA minivector production system confers versatility as the eukaryotic expression cassette can be interchanged to suit numerous downstream applications. As shown previously, the optimized production and delivery of DNA ministrings, with lipid-based synthetic vectors, imparted transgene expression in ovarian cancer (OVCAR-3) cells. Thus, expression of the gene of interest was not deterred upon vector manipulations from protelomerase-mediated processing. To demonstrate the numerous potential applications of LCC DNA ministrings, the aforementioned system was implemented for downstream development of an HIV (Human Immunodeficiency Virus) DNA-VLP vaccine. This vaccine strategy endeavours to target delivery of DNA ministrings to dendritic cells and confer the generation of HIV virus-like particles (VLP) for potent antigen presentation and subsequent activation of humoral and cellular immunity.

***HIV and AIDS*:** Acquired immunodeficiency syndrome (AIDS) stems from HIV infections through sexual contact, infected blood products, and mother-to-child transmissions. The disease is characterized by a progressive depletion of $CD4^+$ helper T-cells through different stages of infection: 1) rapid acute infection resulting in high viral loads and viremia; 2) asymptomatic viral latency upon viral integration; and 3) symptomatic AIDS rendering the host immunocompromised and susceptible to opportunistic infections. The HIV lentivirus

(retrovirus) is divided into two major types, HIV-1 and HIV-2. HIV-1 is the highly virulent form responsible for the AIDS pandemic while HIV-2 is the less virulent variation geographically confined to persist within West Africa [203]. HIV-1 is further divided into different groups (M, N, O, P) with the pandemic group M being subdivided into different subtypes or clades designated by letters A to K [203]. The HIV genome consists of two copies of a 9.5 kb ssRNA encoding polyproteins Gag (matrix, capsid, and nucleocapsid proteins), Pol (protease, reverse transcriptase, and integrase), and Env (surface envelope gp120 and transmembrane gp41); in addition, the genome also encodes regulatory proteins Tat and Rev and virulence accessory proteins Nef, Vif, Vpr, Vpu [203].

Despite our extensive understanding of the biological nature of HIV and HIV pathogenesis, a therapeutic cure against HIV/AIDS has yet to be discovered. Currently, the administration of highly active antiretroviral therapy (HAART) consisting of a cocktail of antiretroviral agents including reverse transcriptase-, protease-, integrase-, and fusion/entry-inhibitors can effectively suppress viral replication and disease progression. While HAART can significantly reduce morbidity and mortality of infected individuals, the treatment regimen cannot eradicate HIV infections due to latent HIV infections that persist as an integrated provirus, and due to low level viral replication permitting cell to cell infection [204]. The associated high costs of HAART, approximately $15000-20000 USD per individual annually, also limits the availability of this treatment regimen in developing countries [205]. Lifelong adherence to treatment and potential risks of HIV-resistance to anti-retrovirals pose additional roadblocks indicating the need for alternative solutions to combating HIV/AIDS.

HIV infections pose serious immune complications due to the absence of natural mammalian protective immunity against the virus; contributed by infection of $CD4^+$ immune cells, viral integration, and high genetic diversity of the virus [203, 206]. The capacity for genome integration into infected $CD4^+$ T-cells offers a limited time frame prior to the establishment of latently infected T-cells and lifelong persistent infection. This is compounded by the lack of natural immune responses against HIV, as the virus actively targets immune cells while possessing mechanisms to highjack and subvert immune responses. In early HIV pathogenesis, HIV infects or becomes internalized by $CD4^+$ monocytes/macrophages and immature dendritic cells. Dendritic cells are elite antigen presenting cells (APCs) with the capacity to present antigens two orders of magnitude more effectively than other APCs [207]. They serve as the primary cross-presenting cells *in vivo*, promoting effective (major histocompatibility complex) MHC class I antigen presentation critical to $CD8^+$ cytotoxic T lymphocyte (CTL) response and cellular immunity [208, 209]. HIV entry into immature dendritic cells is mediated by the CD4 receptor, CCR5 and CXCR4 co-receptors, and various C- type lectin receptors including mannose receptor/CD206, DEC-205/CD205, Langerin/CD207, DC immunoreceptor, and dendritic cell specific intercellular adhesion molecule-3-grabbing non-integrin or DC-SIGN/CD209 [210-212]. In particular, DC-SIGN serves to efficiently transmit intact virus to $CD4^+$ T-cells [211, 212]. Activation of these dendritic cells, via Toll-like receptors (TLRs) and proinflammatory cytokines, triggers their maturation and migration to lymph nodes where subsequent interactions with $CD4^+$ T-cells contribute to rapid viral transfer and infection [213, 214]. Although the abovementioned processes parallel those typically seen in innate and adaptive immune activation, the rapid

onset of HIV infection supersedes appropriate antiviral responses against the virus. HIV infection subsequently contributes to the dysregulation of dendritic cells that leads to increased apoptosis and diminished CTL responses through disruptions of cross-talk with natural killer cells [215]. The expression of regulatory Tat and Nef proteins induces additional effects that subvert immune responses and promote viral propagation. Tat possesses multiple functions of: 1) increasing viral mRNA production; 2) inducing proinflammatory cytokine and chemokine release for recruitment and infection of macrophages/T-cells; and 3) triggering apoptosis of uninfected $CD4^+$ T-cells [203, 214, 216]. Nef, a major virulence factor, also induces proinflammatory cytokine and chemokine release and triggers FasL-mediated apoptosis of uninfected $CD4^+$ and $CD8^+$ T-cells. In addition, Nef downregulates MHC I antigen presentation, thereby severely hampering the activation of CTL responses [203]. The absence of natural immunity and the inability of the host to intervene during early stages of infection contribute to successful viral integration and the generation of latently infected T-cells resulting in lifelong persistence of infection.

In addition to CTL responses and cellular immunity, the activation of humoral immunity, through the production of neutralizing and non-neutralizing antibodies, promotes an effective response against HIV infection. Neutralizing antibodies recognize and bind to HIV surface antigens (gp120 and gp41) thereby neutralizing the infectivity of the virus. In contrast, non-neutralizing antibodies bind to surface HIV antigens, stimulating the recruitment of immune cells to activate antibody-dependent cell-mediated cytotoxicity (ADCC) and virus inhibition (ADCVI). A neutralizing antibody response typically arises several weeks following HIV infection where the generated antibodies are strain specific, targeting idiotypic hypervariable

regions that are highly susceptible to mutations and sequence variations—such mutability corresponds to as high as 35% sequence variation in Env glycoproteins between viruses of different subtypes [217]. Broadly neutralizing antibodies capable of acting on cross-clade variants may be generated but often require chronic antigen exposure to impart affinity maturation [203]. Selective pressures from host immune responses and the error prone nature of reverse transcriptase, in combination with high viral loads, both contribute to significant genetic diversity that prompts viral escape and sustained viral replication [204, 206, 218]. Rapid viral escape and the gradual decline in humoral responses renders the acquired neutralizing antibodies ineffective in halting disease progression. As such, the activation of $CD8^+$ CTL responses and the generation of broadly neutralizing antibodies play critical roles during HIV infections; however, the inherent properties of HIV and the limited window prior to persistent infection greatly complicates the search of a therapeutic cure for HIV/AIDS. Hence, the development of a prophylactic/therapeutic vaccine, alone or in combination with antiretroviral therapy, may be a viable solution in curbing viral spread.

Various types of vaccines including whole inactivated, subunit, live recombinant viral, virus-like particles (VLP), DNA, and dendritic cell-based strategies have been previously explored as potential HIV therapeutics. Clinical trials for Remune, a whole inactivated vaccine free of envelope proteins, did not elicit immunological control over viral replication and offered no significant effect to CD4 counts or HIV progression [204]. Numerous clinical trials involving native and recombinant Env (gp160, gp120, gp41) subunit vaccines (eg. AIDSVAX) have been previously explored, but none have yet to demonstrate substantial clinical benefit [206]. Live recombinant vaccines are viral vectors genetically engineered to

carry genes encoding HIV antigens and serve to induce MHC I antigen presentation for activation of CTL responses. Clinical assessment of ALVAC-HIV-1, a canary pox vector expressing *env*, *gag*, *nef*, and *pol* gene products, enhanced HIV-1-specific cellular immunity for subjects receiving antiretroviral therapy during acute HIV infection but did not reduce viral loads upon discontinuation of antiretroviral therapy [204, 219, 220]. Detriments of using live recombinant vaccines are exemplified in the adenovirus serotype 5 (Ad5)-HIV vaccine where subjects with pre-existing immunity against Ad5 were found to be at greater risk of HIV infection [203, 206, 218, 221]. Results from the RV144/Thai trial, involving a ALVAC-HIV-1/AIDSVAX B/E prime-boost vaccine, showed very promising results as the Phase III vaccine study indicated a statistically significant (31.2%) reduction in HIV-1 acquisition over placebo, amongst heterosexual volunteers; however, the vaccine failed to impact early post-infection viral loads and CD4 counts [218, 222]. Findings from the RV144/Thai trial are promising and further investigations are underway investigating the mechanistic nature of the prime-boost vaccine.

Virus-like particles (VLP) are self-assembling, non-replicating, non-infectious, DNA-free particles of similar size to their wild type counterparts and display conformational epitopes that closely mimic the native virion [223-226]. Although HIV VLPs only require Gag polyprotein for efficient particle assembly, budding, and release, chimeric enveloped VLPs may be generated using Gag polyprotein in combination with recombinant Env glycoproteins. VLP-based vaccines possesses numerous advantages as VLPs possess multiple viral epitopes for the stimulation of both cellular and humoral immunity without the deleterious effects of live attenuated viruses. VLPs are able to induce dendritic cell

maturation and migration while possessing the capacity for promoting antigen presentation and cross-presentation in absence of infection. *In vitro* and *in vivo* studies previously confirmed MDDC-mediated natural killer cell activation in the presence of HIV-VLPs, suggesting the capacity for VLP-activated cross-talk [226] in combination with generating neutralizing antibodies as antigens are expressed in their native form.

Extensive efforts by Kang et al. [227-229] have culminated into the successful development of chimeric gene constructs corresponding to the generation of different VLPs with neutralizing (*gag*-V3 and *gag*-C3) and T cell (*gag*-TCE) epitopes. The *gag*-V3 construct confers the expression of a HIV-2 Gag polyprotein fused with neutralizing epitopes found within the variable 3 (V3) region of gp120. The HIV-2 Gag precursor protein was selected to carry the different HIV-1 V3 domains because: 1) HIV-2 Gag precursors secrete highly immunogenic VLPs, 2) HIV-2 Gag contains cross reactive CTL epitopes that confer protection from HIV-1, and 3) HIV-2 Gag forms chimeric VLPs with up to 198 additional amino acids [227].

Neutralizing epitopes within V3 are vital to the generation of neutralizing antibodies and the incorporation of V3 domains from different HIV clades (B, C, & E) corresponds to the induction of broadly neutralizing antibodies. The *in vivo* immunization of BALB/c mice with Gag-V3 chimeric VLPs induced CTL activity against V3-stimulated cells [229], denoting the capacity for activating both humoral and cellular immunity. And, as expected, the Gag-V3 VLPs conferred neutralizing antibodies and CTL responses against a broad spectrum of HIV-1 isolates [227]. Currently, the chimeric gene constructs are employed as part of a HIV-1 prime-boost prophylactic vaccine (SAV001-H) comprised of: 1) whole inactivated HIV virus

modified with a targeted deletion of *nef* gene and the replacement of the Env protein natural signal sequence (EnvNSS) with that of honeybee melittin; and 2) replication deficient adenoviral vectors, carrying the chimeric constructs, for VLP formation and release [228]. The success of this vaccine was highlighted by its recent completion of phase I clinical trials and future plans of phase II clinical trials in 2014.

Building on the advantages of VLP-based vaccines, the application of DNA-VLP vaccines targeting dendritic cells offers additional benefits. Dendritic cells are the most potent APCs offering the unique ability to undergo cross-presentation, for MHC I antigen presentation, and to induce primary/secondary responses from $CD4^+$ and $CD8^+$ T-cells [204, 221]. Direct delivery of DNA vectors encoding antigen to dendritic cells provides an internal source of immunogenic peptides for MHC I loading and presentation, while avoiding the inherent risks associated with the use of viral vectors [230]. In addition, simultaneous presentation of multiple epitopes derived from the same antigen can be achieved. Subsequent VLP formation and release serves to promote activation of nearby dendritic cells, prompting MHC II antigen presentation and the generation of neutralizing antibodies. In this study, DNA ministrings were generated towards the expression and production of Gag-V3 VLPs to be utilized in the downstream development of a HIV DNA-VLP prophylactic/therapeutic vaccine. Culturing and transfection conditions were optimized for gene delivery, via lipid-based synthetic vectors, into K562-$\alpha_v\beta_3$ cells for later assessment of targeted delivery using RGD peptides.

5.2 Materials and Methods

5.2.1 Construction of pGagV3(BCE) Vector

The 6.56 kb pGagV3(BCE) vector was designed using the pNN9 vector [108] as the template. The *egfp* gene, residing as the gene of interest in pNN9, was replaced with the chimeric gene construct *gagV3*(BCE) (gift from Dr. Chil-Yong Kang, UWO) to generate the pGagV3(BCE) vector. The chimeric gene construct *gagV3*(BCE*)* expresses a HIV-2 Gag polyprotein with three V3 neutralizing epitopes (from HIV-1 clades B, C, and E) near the C-terminus [227-229].

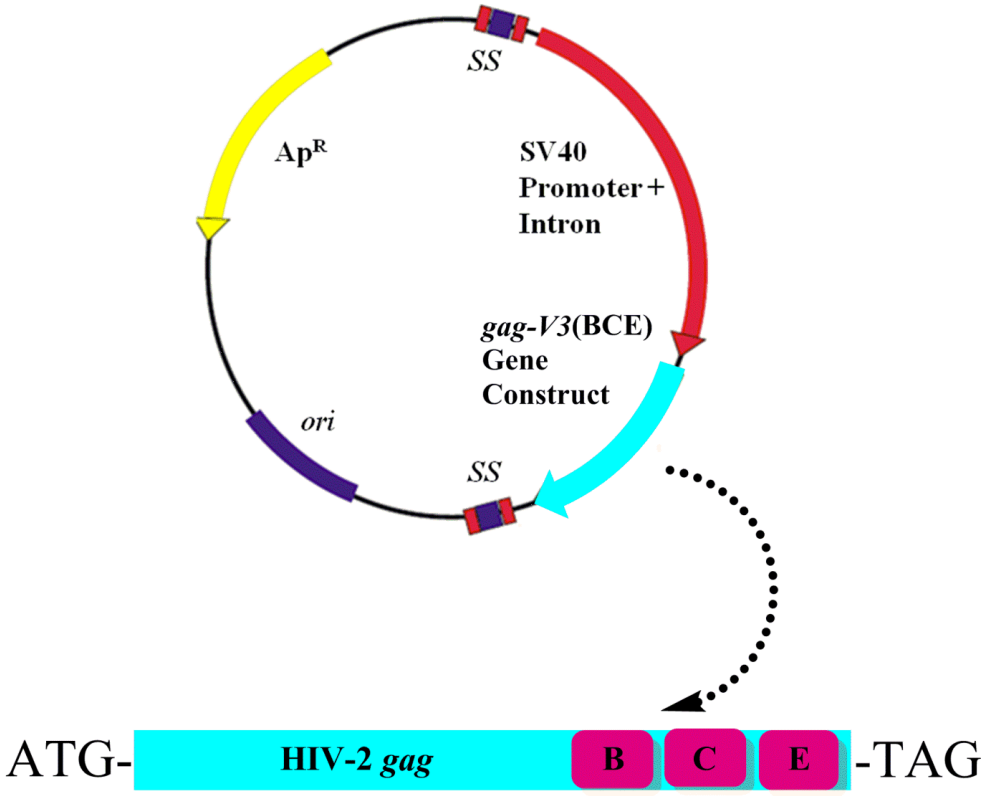

Figure 5.1 Schematic of pGagV3(BCE) Vector. Adapted from [228]**.**

5.2.2 Production of *gagV3(BCE)* LCC DNA Ministrings

The pGagV3(BCE) vector was transferred into Tel^+ W3NN cells using standard transformation techniques described in [154]. The production of *gagV3*(BCE) DNA ministrings was accomplished by batch cultivation as described in section 2.2.2. Briefly, a single colony of Tel+ W3NN [pGagV3(BCE)] was grown overnight in 5 ml LB + Ap (100 μg/ml) under repressed conditions at 30° C with aeration. Fresh cells were grown from the overnight culture (50 ml; 1:100 dilution) at 30° C with aeration to late log phase A_{600} = 0.8. Protelomerase expression was induced upon temperature upshift and incubation at 42° C for 60 min. The cultures were subjected to post-induction incubation at 37° C for 30 min prior to overnight incubation at 30° C. Cells were harvested and plasmid extracted with *E.Z.N.A.* Plasmid Mini/Maxi-Prep Kit (Omega, VWR). The production of *gagV3*(BCE) DNA ministrings was confirmed by AGE.

5.2.3 Transfection of K562 Cells

Immortalized myelogenous leukemia K562 cells, with induced surface expression of CD51/CD61 ($\alpha_v\beta_3$) integrin (K562-$\alpha_v\beta_3$) were generously provided by Dr. Scott Blystone (SUNY Upstate Medical University, Syracuse, NY, USA). K562-$\alpha_v\beta_3$ cells were cultured in Iscove's Modified Dulbecco's Medium (IMDM) supplemented with 10% FBS and Geneticin (G418) (1.2 mg/ml of IMDM) for sustained receptor expression. K562-$\alpha_v\beta_3$ cells were grown at 37° C with 5% CO_2 and were maintained at concentrations of 10^5 - 10^6 cells/ml prior to transfection. 500 μl of K562-$\alpha_v\beta_3$, corresponding to 100,000 or 500,000 cells/well, were seeded into 24-well plates and incubated at 37° C for 60 min prior to transfection.

Transfection was carried out using Lipofectamine^{TM} 2000 and 16-3-16 gemini/DOPE synthetic vectors comprised of pNN9 or *egfp* expressing DNA ministring.

For transfection with Lipofectamine, CCC pNN9 and *egfp*-expressing LCC DNA ministrings were complexed with varying amounts (2-5 µl/ 0.5 µg DNA) of 1 mg/ml Lipofectamine^{TM} 2000 (Invitrogen) according the manufacturer's protocol. Resulting lipoplexes were added drop-wise at amounts corresponding to 0.5 µg of DNA per well. Cells were subsequently incubated at 37° C for 5 h prior to the addition 500 µl of fresh IMDM (10% FBS; G418) and further incubation until 24 or 48 h post-transfection. At each respective time point, cells were collected, washed, and re-suspended in PBS. Samples were stained with propidium iodide and analyzed by fluorescence activated cell sorting (FACS) (Guava easyCyte^{TM}, Millipore) for the assessment of transfection efficiency, as determined by EGFP expression, and cell viability post-transfection. Duplicate samples were assessed, by FACS, with respect to samples measured at 24 hours post-transfection.

For 16-3-16/DOPE synthetic vectors, the transfection complexes were prepared as follows: 0.5 µg of pNN9 vector or *egfp* DNA ministrings was mixed with different aliquots of 1.5 mM 16-3-16 gemini surfactant solution to yield N^+/P^- charge ratios of 2:1, 5:1, and 10:1. After 15 minute incubation at room temperature, different aliquots of 1 mM DOPE was added to ascertain a constant gemini to DOPE ratio of 1:2.5 and the subsequent mixture was further incubated for 30 min at room temperature. The resulting lipoplexes were added drop-wise corresponding to 0.5 µg of DNA per well. Cells were subsequently incubated at 37° C for five hours prior to the addition 500 µl of fresh IMDM (10% FBS; G418) and further incubation until 24 h post-transfection. After 24 h, cells were collected, washed, and re-

suspended in PBS. The samples were stained with propidium iodide (PI) and analyzed by fluorescence activated cell sorting (FACS) for the assessment of transfection efficiency, as determined by EGFP expression, and cell viability post-transfection.

5.3 Results

5.3.1 Production of *gagV3(BCE)* LCC DNA Ministrings

The 6.56 kb pGagV3(BCE) vector consisted of the same genetic components as the 5.6 kb pNN9 plasmid with the exception of the replacement of the 717 bp *egfp* gene with the 1,647 bp *gagV3*(BCE) chimeric gene construct. As such, the resulting eukaryotic expression cassette was flanked by two SuperSequence sites, enabling the generation of LCC DNA ministrings. Functionality of the *pal* site was preserved as heat-induced expression of *tel* conferred the generation of LCC DNA products upon protelomerase processing of pGagV3(BCE) (Figure 5.2). Tel processing of pGagV3(BCE) constituted the production of parental LCC DNA (6.56 kb), LCC backbone DNA (3.2 kb), and *gagV3*(BCE) LCC DNA ministrings (3.36 kb), all of which were also present upon protelomerase processing of pNN9. The similar sizes of LCC backbone DNA and *gagV3*(BCE) LCC DNA ministrings contributed to the observed overlap in gel bands.

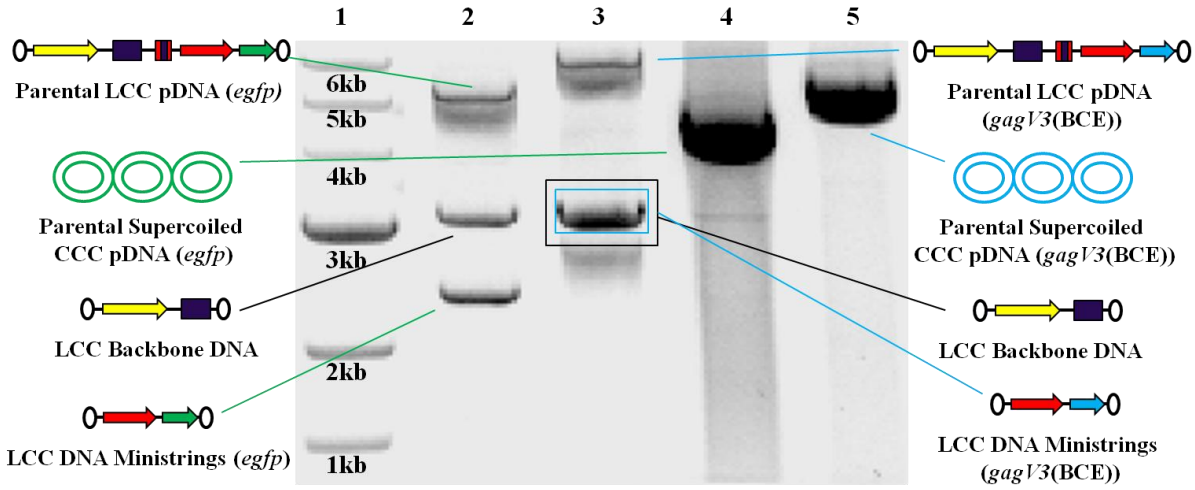

Figure 5.2 Tel-mediated processing of precursor plasmids into *egfp* and *gagV3(BCE)* LCC DNA ministrings. Representative gel image of LCC DNA ministring production for respective ministrings bearing *egfp* and *gagV3*(BCE) as the gene of interest: ladder (lane 1); W3NN [pNN9] (lane 2); W3NN [pGagV3(BCE)] (lane 3); JM109 [pNN9] (lane 4); JM109 [pGagV3(BCE)] (lane 5). Tel protelomerase processing of pGagV3(BCE) resulted in the generation of three LCC DNA products: parental LCC DNA (6.56 kb), LCC backbone DNA (3.2 kb), and *gagV3*(BCE) LCC DNA ministrings (3.36 kb). Differences in the gel profiles for W3NN [pNN9] and W3NN [pGagV3(BCE)] were due to differences in the sizes of *egfp* and *gagV3*(BCE) with overlap in the gel bands corresponding to LCC backbone DNA and *gagV3*(BCE) LCC DNA ministrings.

5.3.2 Preliminary Investigation into Optimal K562 Transfections with Lipofectamine

Variations to cell seeding and quantity of transfection reagent were assessed to ascertain optimal conditions for attaining high transfection efficiencies in K562 cells (Figure 5.3). Initial assessment of transfection efficiency with varying amounts (2-5 µl/0.5 µg DNA) of Lipofectamine denoted increasing transfection efficiencies with increasing amounts of Lipofectamine. Transfection complexes with 5 µl of Lipofectamine elicited the highest transfection efficiencies, 7.0% for CCC pNN9 and 4.6% LCC DNA ministring, in samples seeded with 100,000 cells. In comparison between transfection efficiencies of 100,000 and 500,000 seeded cells, higher transfection efficiencies were attained when seeding 500,000 cells for transfections involving CCC pNN9 (9.3%) and DNA ministrings (7.1%). Further

improvements were observed with increasing post-transfection incubation as transfection efficiencies of 13.9% and 11.1% were achieved for CCC pNN9 and LCC DNA ministring upon FACS analysis at 48 h post-transfection. Hence, transfection of 500,000 cells using diluted transfection complexes with 5 µl of Lipofectamine constituted conditions for the highest observed transfection efficiencies upon FACS analysis at 48 h post-transfection.

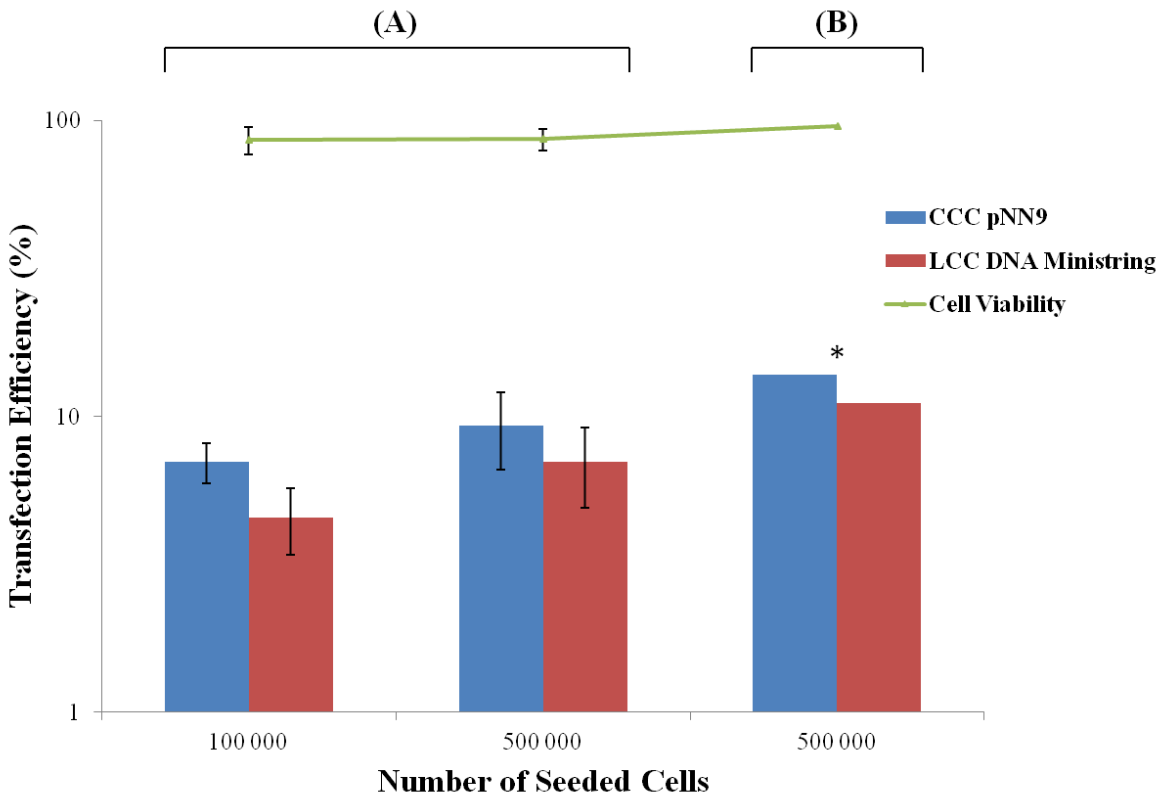

Figure 5.3 Preliminary analysis of transfection efficiencies attained from variations to cell seeding and post transfection incubation using Lipofectamine (N=1). Progressive improvements in transfection efficiencies were observed with changes to cell seeding, from 100,000 to 500,000 K562 cells, and extended post-transfection incubation, from 24 h **(A)** to 48 h **(B)**, prior to FACS analysis. High cell viabilities were observed for all tested conditions. Minimal variations to transfection efficiencies were observed in duplicate samples. **Duplicate samples not available.*

Transfection efficiencies were subsequently assessed using 16-3-16/DOPE synthetic vectors under the aforementioned optimal conditions. Initial analysis denoted a progressive increase in transfection efficiency with increasing gemini/DNA (N^+/P^-) charge ratios; however, higher transfection efficiencies came at a cost of greater cytotoxicity (Figure 5.4). Increases to transfection efficiency and cytotoxicity for DNA ministrings, were more prominent with increasing (N^+/P^-) charge ratios. In particular, the high transfection efficiencies (19.4%) attained with LCC/16-3-16/DOPE lipoplexes, at 10:1 charge ratios, corresponded to the lowest observed cell viabilities (68.7%). LCC/16-3-16/DOPE lipoplexes at 5:1 charge ratios resulted in a cell viability of 82.1% while attaining comparable transfection efficiencies to CCC pNN9/16-3-16/DOPE at 5:1 and 10:1 charge ratios.

5.4 Discussion

The LCC DNA minivector production system demonstrated high versatility as different LCC DNA ministrings may be produced to suit numerous applications. The growing AIDS pandemic and the significant prospects of the SAV001-H prophylactic vaccine prompted exploration into LCC DNA ministrings conferring the downstream development of a HIV DNA-VLP vaccine. Successes in VLP formation upon the delivery of *gagV3*(BCE) LCC DNA ministrings will demonstrate a proof of concept, highlighting the use of DNA ministrings in diverse applications.

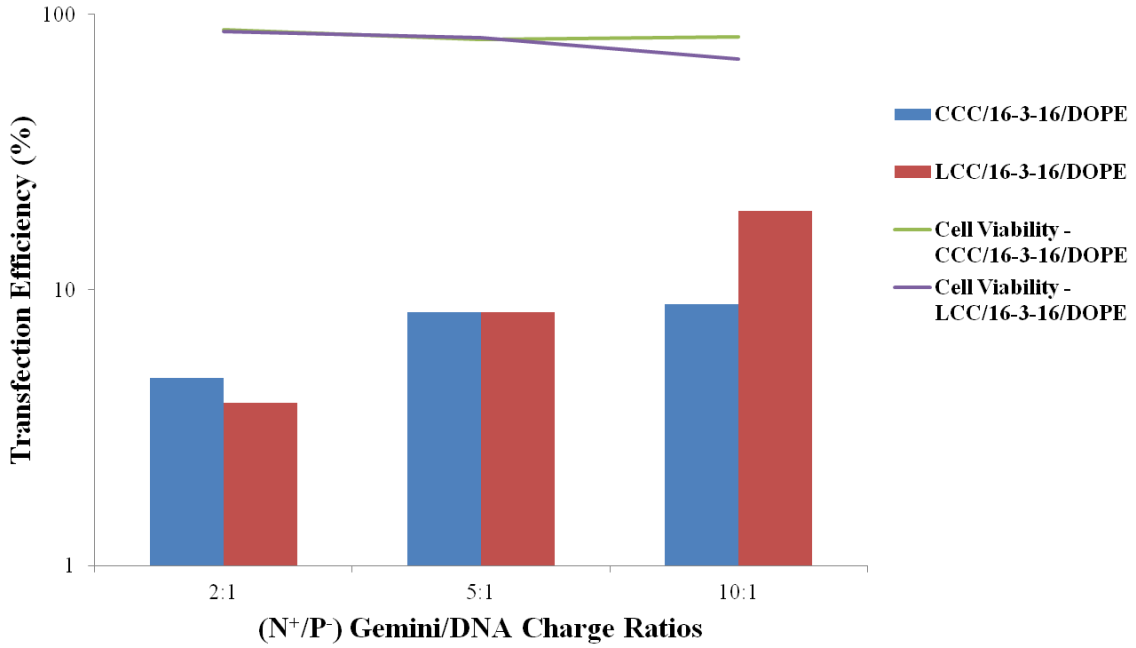

Figure 5.4 Preliminary analysis of transfection efficiencies using DNA/16-3-16/DOPE lipoplexes (N=1). Increasing charge ratios (2:1, 5:1, and 10:1) constituted increases to both transfection efficiencies and cytotoxicity. For lipoplexes at 10:1 charge ratio, LCC DNA ministrings elicited higher transfection efficiencies than pNN9, but at a cost of greater cytotoxicity.

As confirmed, the insertion of the *gagV3*(BCE) chimeric gene construct, in place of the *egfp* gene, did not alter protelomerase mediated processing of the corresponding parental pGagV3(BCE) vector into DNA ministrings. Tel processing of pGagV3(BCE) resulted in the production of the same LCC DNA products as observed in pNN9. The similar sizes of the LCC backbone DNA and *gagV3*(BCE) LCC DNA ministring may potentially interfere with complete separation and purification of the DNA ministring. However, as the DNA ministring will be utilized in the downstream development of a HIV DNA-VLP vaccine, the residual LCC backbone DNA, possessing CpG motifs, may serve as an adjuvant for immunostimmulation upon successful gene delivery. As the LCC backbone DNA is co-

administered as a separate entity, transgene silencing from backbone sequence induced, heterochromatin-associated histone modifications [115] will be avoided; thus preserving effective transgene expression and VLP formation.

The proposed HIV DNA-VLP vaccine involves targeted delivery of *gagV3*(BCE) DNA ministrings to dendritic cells. The αvβ3 integrin, also referred to as CD51/CD61 or vitronectin receptor, was selected to demonstrate targeted delivery of Arg-Gly-Asp (RGD) peptides. RGD peptides most prominently interact with the CD51 family of receptors and previous studies have demonstrated improved binding and internalization of cationic liposomes through RGD-dependent receptor mediated endocytosis [231]. In addition, αvβ3 is a receptor of dendritic cells involved in efficient and selective phagocytosis of apoptotic bodies [232]. Dendritic cells expressing high levels of CD51 were shown to express higher levels of MHC I, denoting higher cross presentation and activation of cellular immunity [233]. Selective targeting of αvβ3 contributed to improved Adenoviral serotype 5 (Ad5) transduction that initiated dendritic cell maturation and $CD8^+$ T cell responses against Ad-encoded antigens [233, 234]. The delivery of Ad5 vectors improved with greater CD51 surface expression and was impeded by competitive binding of RGD peptides; both of which demonstrate the critical role of αvβ3 in the observed improvements to Ad5 transduction. Lastly, the RGD domain of HIV Tat was shown to inhibit dendritic cell-mediated phagocytosis of apoptotic bodies. This inhibition was suspected to involve αvβ3 [235] and was speculated to contribute to HIV induced dysregulation of dendritic cells, limiting their capacity to undergo antigen presentation.

K562-αvβ3 was considered to be an appropriate model demonstrating targeted delivery of RGD-functionalized synthetic vectors. GFP-encoding λ phage, displaying high affinity αvβ3 binding protein (3JCLI4), was shown to elicit improved internalization and transgene expression in K562-αvβ3 cells when compared to the undecorated control phage [236]. Hence, K562-αvβ3 was used as a convenient, cost-effective means of assessing the efficacy of targeted delivery and the associated improvements on transfection efficiencies for RGD-functionalized lipoplexes. Actively dividing leukemia cells, grown in suspension, typically exhibit low transfection capacities. Among them, K562 cells are considered to be relatively transfection competent [237]. Using SucPG complex, composed of pH-sensitive fusogenic liposomes and DNA-bound lipoplexes, K562 cells were shown to elicit the lowest transfection efficiency (5%) among the tested cancer-derived cell lines, and transfection using Lipofectamine was less efficient than that achieved with SucPG complexes [238]. The low transfection efficiencies may be attributed to cytotoxicity as transfected K562 cells, grown in suspension, were reported to exhibit 35.1 ± 7.8 % cell death—a stark difference compared to the 2.8 ± 0.17 % cell death observed for non-transfected cells [237].

The observed transfection efficiencies with Lipofectamine, for both CCC pNN9 and LCC DNA ministrings, were comparable to previous literature results. In contrast to adherent cultures, a greater number of K562 cells must be seeded in order to elicit higher transfection efficiencies. In addition, extended post-transfection incubation, from 24 to 48 h, led to higher transfection efficiencies. Using similar transfection conditions to this study, Amini et al. [239] reached 25% transfection efficiency in K562 cells with Lipofectamine upon FACS analysis 72 h post-transfection. This was comparatively higher than the transfection

efficiencies attained in this study. Hence, further improvements to transfection efficiency may arise using their outlined transfection protocols, which involve modifications to the current protocol in terms of fresh medium supplementation and incubation pre/post transfection. With respect to transfection using DNA/16-3-16/DOPE lipoplexes, preliminary analysis indicated improved transfection efficiencies for LCC DNA ministring over CCC pNN9 DNA. Improvements in transfection efficiency for LCC/16-3-16/DOPE lipoplexes over their CCC pDNA counterparts were more apparent than previous transfections involving OVCAR-3 cells (see Figure 4.4). This was suspected to be the result of transfection with K562 cells of lower passage number (6) in contrast to the cells with high passage number (18-20) used in OVCAR-3 transfections. Further investigation will be warranted to confirm such findings.

As αvβ3 integrin is not uniquely expressed by dendritic cells, the use of ligands targeting conserved receptors of dendritic cells is proposed to further improve targeted delivery and vector endocytosis in dendritic cells. Ligands targeting CD205, a receptor highly expressed by dendritic cells, may suit such purpose as CD205 is involved in the presentation of apoptotic/necrotic cell-derived antigens to both $CD4^+$ and $CD8^+$ T-cells [240]. Immunolipoplexes functionalized with anti-CD205 antibodies was shown to improve transfection efficiency (~10%) in immature and mature dendritic cells over non-functionalized lipoplexes [241], prompting the use of such antibodies as ligands for targeted delivery.

Prospects of DNA-VLPs as a viable HIV vaccine was strengthened by DermaVir, a topical formulation consisting of a pDNA encapsulated within a shell of mannobiosylated

polyethylenimine (PEIm) for delivery into Langerhans cells [205, 242]. Advantages associated with DNA vaccines were exemplified by DermaVir as the delivered pDNA encodes a VLP, comprising 15 antigens (13 native and 2 genetically modified HIV-1 proteins), capable of presenting over 900 MHC I and 2000 MHC II epitopes to $CD8^+$ and $CD4^+$ T-cells respectively [242]. DermaVir increased HIV specific memory T-cells in individuals receiving HAART while inducing a gradual suppression of viral loads in antiretroviral-naive, HIV infected individuals [205]. Similarly, the targeted delivery of *gagV3*(BCE) DNA ministrings into dendritic cells is speculated to induce neutralizing antibodies and CTL responses, both of which are critical factors to an effective HIV vaccine. Processing of internally expressed antigens in dendritic cells will prompt MHC I presentation, inducing CTL responses. Subsequent budding of unprocessed Gag-V3 VLPs will activate exogenous uptake of antigens for MHC II presentation and the generation of neutralizing antibodies.

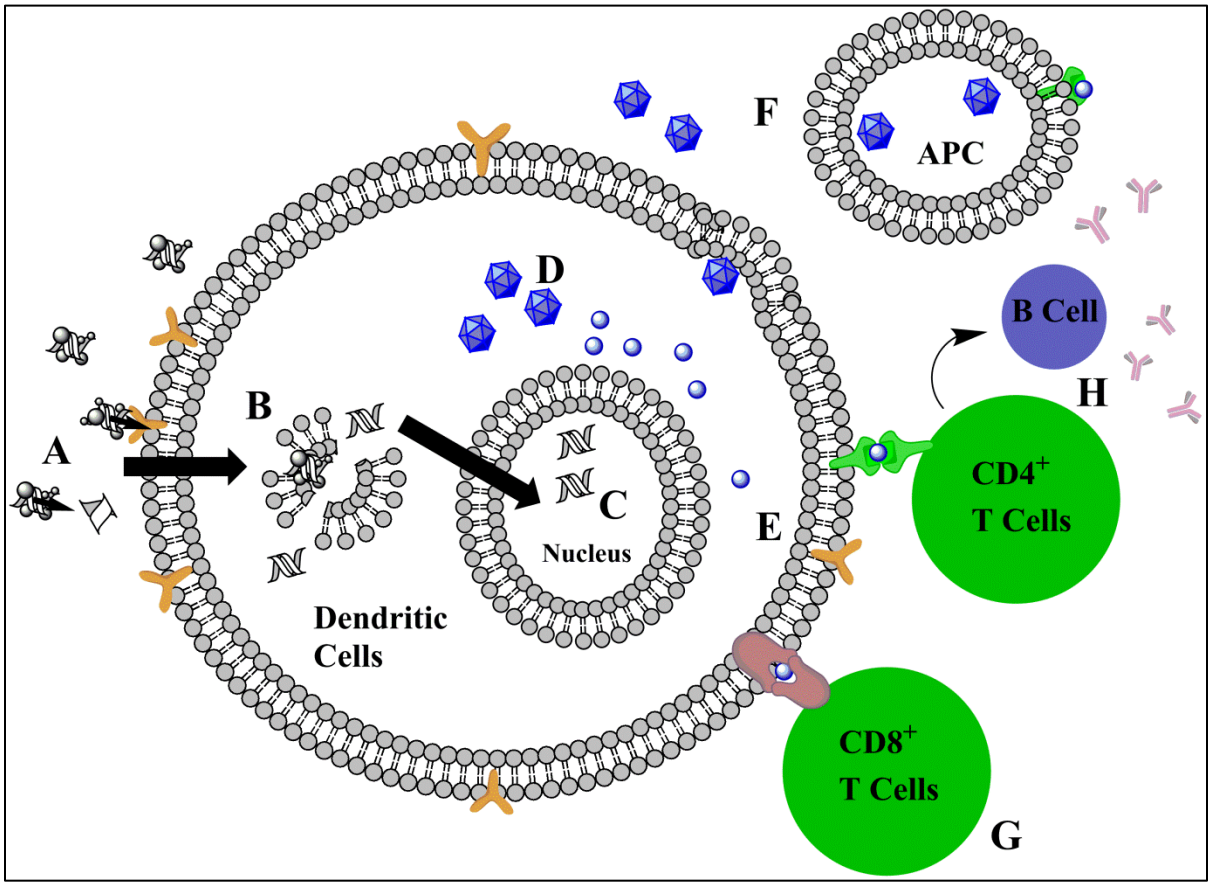

Figure 5.5 Schematic for targeted delivery of *gagV3*(BCE) DNA ministring into dendritic cells. **A)** Targeted delivery of *gagV3*(BCE) DNA ministring derived synthetic vectors into dendritic cells; **B)** Successful endosomal escape enabling the release of DNA cargo for nuclear entry; **C)** Expression of *gagV3*(BCE) results the expression of gag-V3; **D)** Formation of VLPs; **E)** Antigen processing; **F)** VLP budding and release leading to internalization by other antigen presenting cells (APC); **G)** MHC I antigen presentation to $CD8^+$ T cells for CTL response and cellular immunity; **H)** MHC II antigen presentation to $CD4^+$ helper T cells for neutralizing antibody production by B cells.

5.5 Conclusion

HIV DNA-VLPs may be excellent vaccine candidates as they possess the capacity to induce CTL responses and neutralizing antibodies, both of which are necessary for effective vaccination against HIV. Targeted delivery of *gagV3*(BCE) DNA ministrings to dendritic cells may serve to directly stimulate HIV-specific immune responses, thereby prompting

prevention and suppression of subsequent HIV challenge. Results from this study marked the early stages in the development of a HIV DNA-VLP vaccine. Synthesis of pGagV3(BCE) led to successful production of *gagV3*(BCE) LCC DNA ministrings through the LCC DNA minivector production system. Optimal transfection in K562-αvβ3 cells served as the initial step for evaluating targeted delivery using RGD peptides and this model will act as the basis for comparison in future studies involving dendritic cells.

Chapter 6
Summary

6.1 Summary

As genes are the inherent blueprint to all living organisms, gene therapy offers limitless potential for the future treatment of various diseases and genetic defects. While sound and powerful in theory, the delivery of gene therapeutics may and has induced unforeseen adverse reactions that can result in morbidity or even death. While viral vectors continue to comprise the majority of gene therapeutics, and demonstrating high efficacy with positive clinical outcomes, such safety concerns persist, thwarting the future generation of translational technologies. Non-viral delivery GT systems serve as an alternative that addresses the abovementioned safety limitations, but suffer from low transfection efficiencies that limit their efficacy and continue to pose substantial roadblocks in the promotion of such systems into clinical relevance. With respect to lipid-based synthetic vectors, extensive research has been focused on the structural composition of cationic lipids and the molecular mechanisms associated with improved delivery. In addition (though often overlooked), careful consideration must also be put into the design of the DNA cargo such that optimal transgene expression, and corresponding therapeutic effect, can take place. LCC DNA ministrings offer heightened effectiveness, while conferring an exceptional safety profile. LCC DNA ministrings are designed to offer high versatility with use toward many applications, and the implementation of the one step *in vivo* DNA minivector production

system allows rapid, simple and scalable production of both CCC and LCC DNA minivectors.

In the present study, numerous aspects pertaining to the generation of gene therapeutics with LCC DNA ministrings had been explored with relevance to both industry and clinical settings. Upon systematic assessment of induction duration, cultivation strategy, and genetic/chemical modifications for optimal production of LCC DNA ministrings in the *in vivo* system, high yields conferring ~90% production efficiency were observed. Improvements in production efficiency and ministring yields, over the current system, were observed with: a two-step continuous cultivation strategy, a Δ*hflX* host mutation background, the application of ciprofloxacin, and the introduction of slow stop *dnaB*[Ts] mutation.

Purification of LCC DNA ministrings using anion exchange membrane chromatography demonstrated rapid, scalable purification of DNA vectors as well as its potential in the separation of different DNA isoforms. The application of a hydrogel-based strong Q-anion exchange membrane, with manipulations to salt gradient, constituted effective separation of parental supercoiled CCC precursor pDNA and LCC DNA. Upon comparative analysis between synthetic vectors derived from LCC DNA ministrings and CCC pDNA, differences in DNA topology contributed to differences in particle size and protection from DNase degradation. Lastly, *gagV3*(BCE) LCC DNA ministrings were successfully produced. This paves the way for their targeted delivery into dendritic cells, conferring subsequent VLP formation and antigen presentation which serve as the basis of the HIV DNA-VLP vaccine.

6.2 Future Directions

6.2.1 Further Optimization of LCC DNA Minivector Production System for Complete pDNA Processing

Findings from the present study showed improvements to production efficiency upon individual modifications using two step continuous cultivation and through genetic modifications in the introduction of Δ*hflX* deletion and *dnaB*[Ts] slow stop mutation. Hence, two step continuous cultivation in a genetically modified *ΔhflX* strain may potentially serve to attain complete pDNA processing with dramatically higher yields of LCC DNA ministrings and is currently being investigated. While potentially additive, the addition of the *dnaB*[Ts] slow stop mutation would further compromise cell health and limit plasmid yields due to the replication deficiency, even at permissive temperatures. Such modifications can be simultaneously applied with temperature oscillations, as highlighted by Caspeta et al. [161], allowing cells to better accommodate to heat stress for improved protelomerase expression, reduced by-product accumulation, and higher DNA ministring yields.

6.2.2 Targeted Delivery into K562-αvβ3 with RGD-Functionalized Synthetic Vectors

K562-αvβ3 cells serve as an appropriate model to demonstrate targeted delivery of RGD-functionalized synthetic vectors. As such, we anticipate that transfection of K562-αvβ3 cells by LCC/16-3-16/DOPE lipoplexes functionalized with RGD peptides, *via* electrostatic interactions, should confer higher transfection efficiencies than that imparted by non-functionalized lipoplexes. Transfection of non-functionalized and RGD-functionalized lipoplexes into K562-αvβ5 cells would serve as controls, confirming enhanced transfection efficiencies in K562-αvβ3 as result of targeted delivery.

6.2.3 Targeted Delivery into Dendritic Cells and VLP Formation

The abovementioned non-functionalized and RGD-functionalized LCC/16-3-16/DOPE lipoplexes will be assessed for transfection into dendritic cells. Transfection efficiencies will be assessed by FACS for the successful delivery of *egfp* LCC DNA ministrings. Subsequently, *gagV3*(BCE) LCC DNA ministrings will be delivered into dendritic cells to assess VLP formation by electron microscopy.

Bibliography

1. Hsu, C.Y., Uludag, H., *Nucleic-acid based gene therapeutics: delivery challenges and modular design of nonviral gene carriers and expression cassettes to overcome intracellular barriers for sustained targeted expression.* J Drug Target, 2012. **20**(4): p. 301-28.
2. Ginn, S.L., Alexander, I. E., Edelstein, M. L., Abedi, M. R., Wixon, J., *Gene therapy clinical trials worldwide to 2012 - an update.* J Gene Med, 2013. **15**(2): p. 65-77.
3. Wirth, T., Parker, N., Yla-Herttuala, S., *History of gene therapy.* Gene, 2013. **525**: p. 162-169.
4. Bryant, L.M., Christopher, D. M., Giles, A. R., Hinderer, C., Rodriquez, J. L., Smith, J. B., Traxler, E. A., Tycko, J., Wojno, A. P., Wilson, J. M., *Lessons learned from the clinical development and market authorization of Glybera.* Hum Gene Ther Clin Dev, 2013. **24**(2): p. 55-64.
5. Melchiorri, D., Pani, L., Gasparini, P., Cossu, G., Ancans, J., Borg, J. J., Drai, C., Fiedor, P., Flory, E., Hudson, I., Leufkens, H. G., Müller-Berghaus, J., Narayanan, G., Neugebauer, B., Pokrotnieks, J., Robert, J. L., Salmonson, T., Schneider, C. K., *Regulatory evaluation of Glybera in Europe - two committees, one mission.* Nat Rev Drug Discov, 2013. **12**(9): p. 719.
6. Thomas, C.E., Ehrhardt, A., Kay, M. A., *Progress and problems with the use of viral vectors for gene therapy.* Nat Rev Genet, 2003. **4**(5): p. 346-58.
7. Somai, N., Verma, I. M., *Gene Therapy: trials and tribulations.* Nat Rev Genet, 2000. **1**(2): p. 91-99.
8. M., W.J., *Lessons learned from the gene therapy trial for ornithine transcarbamylase deficiency.* Molecular Genetics and Metabolism, 2009. **96**: p. 151-157.
9. Fischer, A., Hacein-Bey-Abina, S., Cavazzana-Calvo, M. , *20 years of gene therapy for SCID.* Nature Immunology, 2010. **11**(6): p. 457-460.
10. Donkuru, M., Badea, I., Wettig, S., Verrall, R., Elsabahy, M., Foldvari, M., *Advancing nonviral gene delivery: lipid- and surfactant-based nanoparticle design strategies.* Nanomedicine, 2010. **5**(7): p. 1103-1127.
11. Al-Dosari, M.S., Gao, X., *Nonviral gene delivery: principle, limitations, and recent progress.* AAPS J, 2009. **11**(4): p. 671-81.
12. Mintzer, M.A., Simanek, E. E. , *Nonviral Vectors for Gene Delivery.* Chem. Rev., 2009. **109**: p. 259-302.
13. Seow, Y., Wood, M. J., *Biological gene delivery vehicles: beyond viral vectors.* Molecular Therapy, 2009. **17**(5): p. 767-777.
14. Medina-Kauwe, L.K., Hamm-Alvarez, S. , *Intracellular trafficking of nonviral vectors.* Gene Therapy, 2005. **12**: p. 1734-1751.
15. Wettig, S.D., Verrall, R. E., Foldvari, M., *Gemini Surfactants: A New Family of Building Blocks for Non-Viral Gene Delivery Systems.* Current Gene Therapy, 2008. **8**: p. 9-23.
16. Zhang, X.X., McIntosh, T. J., Grinstaff, M. W., *Functional lipids and lipoplexes for improved gene delivery.* Biochimie, 2012. **94**(1): p. 42-58.
17. Eliyahu, H., Barenholz, Y., Domb, A. J., *Polymers for DNA Delivery.* Molecules, 2005. **10**: p. 34-64.
18. Zhang, Y., Satterlee, A., Huang, L., *In vivo gene delivery by nonviral vectors: overcoming hurdles?* Mol Ther, 2012. **20**(7): p. 1298-304.
19. Plank, C., Mechtler, K., Szoka, F. C. Jr., Wagner, E., *Activation of the complement system by synthetic DNA complexes: a potential barrier for intravenous gene delivery.* Hum Gene Ther, 1996. **7**(12): p. 1437-1446.

20. Wang, W., Li, W., Ma, N., Steinhoff, G., *Non-Viral Gene Delivery Methods.* Current Pharmaceutical Biotechnology, 2013. **14**: p. 46-60.
21. Dean, D.A., Strong, D. D., Zimmer, W. E. , *Nuclear entry of nonviral vectors.* Gene Therapy, 2005. **12**: p. 881-890.
22. Gao, X., Kim, K., Liu, D., *Nonviral gene delivery: what we know and what is next* AAPS J, 2007. **9**(1): p. E92-104.
23. Mellot, A.J., Forrest, M. L., Detamore, M. S. , *Physical non-viral gene delivery methods for tissue engineering.* Ann Biomed Eng, 2013. **41**(3): p. 446-468.
24. Jafari, M., Soltani, M., Naahidi, S., Karunaratne, D. N., Chen, P., *Nonviral Approach for Targeted Nucleic Acid Delivery.* Current Medicinal Chemistry, 2012. **19**: p. 197-208.
25. Patil, S.D., Rhodes, D. G., Burgess, D. J. , *DNA-based therapeutics and DNA delivery systems: a comprehensive review.* AAPS J, 2005. **7**(1): p. E61-77.
26. Delalande, A., Postema, M., Mignet, N., Midoux, P., Pinchon, C., *Ultrasound and microbubble-assisted gene delivery: recent advances and ongoing challenges.* Therapeutic Delivery, 2012. **3**(10): p. 1199-1215.
27. Geis, N.A., Katus, H. A., Bekeredijan, R. , *Microbubbles as a vehicle for gene and drug delivery: current clinical implications and future persepctives.* Current Pharmaceutical Design, 2012. **18**: p. 2166-2183.
28. Sirsi, S.R., Hernandex, S. L., Zielinski, L., Blomback, H., Koubaa, A., Synder, M., Homma, S., Kandel, J. J., Yamashiro, D. J., Borden, M. A., *Polyplex-microbubble hybrids for ultrasound-guided plasmid DNA delivery to solid tumors.* Journal of Controlled Release, 2012. **157**: p. 224-234.
29. Omata, D., Negishi, Y., Hagiwara, S., Yamamura, S., Endo-Takahashi, Y., Suzuki, R., Maruyama, K., Nomizu, M., Aramaki, Y., *Bubble liposomes and ultrasound promoted endosomal escape of TAT-PEG liposomes as gene delivery carriers.* Mol Pharmaceutics, 2011. **8**: p. 2416-2423.
30. Stevenson, D.J., Gunn-Moore, F. J., Campbell, P., Dholakia, K., *Single cell optical transfection.* J. R. Soc. Interface, 2010. **7**: p. 863-871.
31. Yao, C., Zhang, Z., Rahmanzadeh, R., Huettmann, G., *Laser-based gene transfection and gene therapy.* IEEE Transactions on Nanobioscience, 2008. **7**(2): p. 111-119.
32. Praveen, B.B., Stevenson, D. J., Antkowiak, M., Dholakia, K., Gunn-Moore, F. J., *Enhancement and optimization of plasmid expression in femtosecond optical transfection.* J. Biophotonics, 2011. **4**: p. 229-235.
33. Terakawa, M., Ogura, M., *Gene transfer into mammalian cells by use of a nanosecond pulsed laser-induced stress wave.* Optics Letters, 2004. **29**(11): p. 1227-1229.
34. Ogura, M., Sato, S., Nakanishi, K., Uenoyama, M., Kiyozumi, T. Saitoh, D., Ikeda, T., Ashida, H., Obara, M., *In vivo tageted gene transfer in skin by the use of laser-induced stress waves.* Lasers in Surgery and Medicine, 2004. **34**: p. 242-248.
35. Kurita, A., Matsunobu, T., Satoh, Y., Ando, T., Sato, S., Obara, M., Shiotani, A., *Targeted gene transfer into rat facial muscles by nanosecond pulsed laser-induced stress waves.* Journal of Biomedical Optics, 2011. **16**(9): p. 098002-1-5.
36. Satoh, Y., Kanda, Y., Terakawa, M., Obara, M., Mizuno, K., Watanabe, Y., Endo, S., Ooigawa, H., Nawashiro, H., Sato, S., Takishima, K., *Targeted DNA transfection into the mouse central nervous system using laser-induced stress waves.* Journal of Biomedical Optics, 2005. **10**(6): p. 060501-1-3.
37. Plank, C., Zelphati, O., Mykhaylyk, O., *Magnetically enhanced nucleic acid delivery. Ten years of magnetofection-progress and prospects.* Adv Drug Deliv Rev, 2011. **63**(14-15): p. 1300-1331.

38. Kami, D., Takeda, S., Itakura, Y., Gojo, S., Watanabe, M., Toyoda, M., *Application of magnetic nanoparticles to gene delivery.* Int. J. Mol. Sci., 2011. **12**: p. 3705-3722.
39. Kumar, A., Jena, P. K., Behera, S., Lockey, R. F., Mohapatra, S., Mohapatra, S. , *Multifunctional magnetic nanoparticles for targeted delivery.* Nanomedicine: Nanotechnology, Biology and Medicine, 2010. **6**: p. 64-69.
40. Mykhaylyk, O., Antequera, Y. S., Vlaskou, D., Plank, C., *Generation of magnetic nonviral gene transfer and magnetofection in vitro.* Nature Protocols, 2007. **2**(10).
41. Vainuska, D., Kozireva, S., Karpovs, A., Cistjakovs, M., Bariseys, M., *A novel approach for nucleic acid delivery into cancer cells.* Medicinia(Kaunas), 2012. **48**(6): p. 324-329.
42. Song, H.P., Yang, J. Y., Lo, S. L., Wang, Y., Fan, W. M., Tang, X. S., Xue, J. M., Wang, S., *Gene transfer using self assembled ternary complexes of cationic magnetic nanoparticles, plasmid DNA and cell penetrating Tat peptide.* Biomaterials, 2010. **31**: p. 769-778.
43. Maio, L., Zhang, K., Qiao, C., Jin, X., Zheng, C., Yang, B., Sun, H., *Antitumor effect of human TRAIL on adenoid cystic carcinoma using magnetic nanoparticle-mediated gene expression.* Nanomedicine, 2013. **9**(1): p. 141-150.
44. Prijic, S., Prosen, L., Cemazar, M., Scancar, J., Romih, R., Lavrencak, J., Bregar, V. B., Coer, A., Krzan, M., Znidarsic, A., Sersa, G., *Surface modified magnetic nanoparticles for immuno-gene therapy of murine mammary adenocarcinoma.* Biomaterials, 2012. **33**: p. 4379-4391.
45. Zhou, X., Liu, B., Yu, X., Zha, X., Zhang, X., Wang, X., Jin, Y., Wu, Y., Jiang, C., Chen, Y., Chen, Y., Shan, Y., Liu, J., Kong, W., Shen, J., *Using magnetic force to enhance immune response to DNA vaccine.* Small, 2007. **3**(10): p. 1707-1713.
46. Owen, J., Pankhurst, Q., Stride, E., *Magnetic targeting and ultrasound mediated drug delivery: benefits, limitations and combination.* Int. J. Hyperthermia 2012. **28**(4): p. 362-373.
47. Martin, M.E., Rice, K. G., *Peptide-guided Gene Delivery.* AAPS J, 2007. **9**(1): p. Article 3.
48. Patnaik, S., Gupta, K. C., *Novel polyethylenimine-derived nanoparticles for in vivo gene delivery.* Expert Opin. Drug Deliv., 2013. **10**(2): p. 215-228.
49. Jager, M., Schubert, S., Ochrimenko, S., Fischer, D., Schubert, U. S., *Branched and linear poly(ethylene imine)-based conjugates: synthetic modification, characterization, and application.* Chem. Soc. Rev., 2012. **41**: p. 4755-4767.
50. Elouahabi, A., Ruysschaert, J. M., *Formation and intracellular trafficking of lipoplexes and polyplexes.* Mol Ther, 2005. **11**(3): p. 336-47.
51. Sonawane, N.D., Szoka, F. C. Jr., Verkman, A. S., *Chloride accumulation and swelling in endosomes enhances DNA transfer by polyamine-DNA polyplexes.* J Biol Chem, 2003. **278**(45): p. 44826-31
52. Akinc, A., Thomas, M., Klibanov, A. M., Langer, R., *Exploring polyethylenimine-mediated DNA transfection and the proton sponge hypothesis* J Gene Med, 2005. **7**: p. 657-663.
53. Xu, Q., Wang, C., Pack, D. W., *Polymeric Carriers for Gene Delivery: Chitosan and Poly(amidoamine) Dendrimers.* Curr Pharm Des, 2010. **16**(21): p. 2350-2368.
54. Huang, M., Fong, C., Khor, E., Lim, L., *Transfection efficiency of chitosan vectors: Effect of polymer molecular weight and degree of deacetylation.* Journal of Controlled Release, 2005. **106**: p. 391-406.
55. Chen, H.H., et al., *Quantitative comparison of intracellular unpacking kinetics of polyplexes by a model constructed from quantum dot-FRET.* Mol Ther, 2008. **16**(2): p. 324-32.
56. Dutta, T., Jain, N. K., McMillan, N. A. J., Parekh, H. S., *Dendrimer nanocarriers as versatile vectors in gene delivery.* Nanomedicine: Nanotechnology, Biology and Medicine, 2010. **6**: p. 25-34.
57. Bielinska, A.U., Chen, C., Johnson, J., Baker Jr, J. R., *DNA complexing with polyamidoamine dendrimers: implications for trasfection.* Bioconjugate Chem., 1999. **10**: p. 843-850.

58. Chen, W., Turro, N. J., Tomalia, D. A., *Using Ethidium Bromide to Probe the Interactions between DNA and Dendrimers.* Langmuir, 2000. **16**: p. 15-19.
59. Wadhwa, M.S., Collard, W. T., Adami, R. C., McKenzie, D. L., Rice, K. G. , *Peptide-mediated gene delivery: influence of peptide structure on gene expression.* Bioconjug Chem, 1997. **8**(1): p. 81-88.
60. Adami, R.C., Collard, W. T., Gupta, S. A., Kwok, K. Y., Bonadio, J., Rice, K. G., *Stability of peptide-condensed plasmid DNA formulations.* J Pharm Sci, 1998. **87**(6): p. 678-683.
61. Futaki, S., Ohashi, W., Suzuki, T., Niwa, M., Tanaka, S., Ueda, K., Harashima, H., Sugiura, Y., *Steraylated arginine-rich peptides: a new class of transfection systems.* Bioconjug Chem, 2001. **12**(6): p. 1005-1011.
62. Margus, H., Padari, K., Pooga, M., *Cell-penetrating peptides as versatile vehicles for oligonucleotide delivery.* Mol Ther, 2012. **20**(3): p. 525-533.
63. Lehto, T., Kurrikoff, K., Langel, U., *Cell-penetrating peptides for the delivery of nucleic acids.* Expert Opin Drug Deliv., 2012. **9**(7): p. 823-836.
64. Lo, S.L., Wang, S., *An endoosmolytic Tat peptide produced by incorporation of hisitidine and cystein residues as nonviral vector for DNA transfection.* Biomaterials, 2008. **29**(15): p. 2408-2414.
65. Srinivas, R., Samanta, S., Chaudhuri, A., *Cationic amphiphiles: promising carriers of genetic materials in gene therapy.* Chem. Soc. Rev., 2009. **38**: p. 3326-3338.
66. Felgner, P.L., Gadek, T. R., Holm, M., Roman, R., Chan, H. W., Wenz, M., Northrop, J. P., Ringold, G. M., Danielsen, M., *Lipofection: a highly efficient, lipid-mediated DNA-transfection procedure.* Proc Natl Acad Sci U S A, 1987. **84**(21): p. 7413-7417.
67. Labas, R., Beilvert, F., Barteau, B., David, S., Chevre, R., Pitard, B., *Nature as a source of inspiration for cationic lipid synthesis.* Genetica, 2010. **138**: p. 153-168.
68. Caracciolo, G., Amenitsch, H., *Cationic liposome/DNA complexes: from structure to interactions with cellular membranes.* Eur Biophys J, 2012. **41**(10): p. 815-29.
69. Ma, B., Zhang, S., Jiang, H., Zhao, B., Lv, H., *Lipoplex morphologies and their influences on transfection efficiency in gene delivery.* J Control Release, 2007. **123**(3): p. 184-94.
70. Ewert, K.K., Ahmad, A., Evans, H. M., Safinya, C. R. , *Cationic lipid-DNA complexes for non-viral gene therapy: relating supramolecular structures to cellular pathways.* Expert Opin. Biol. Ther., 2005. **5**(1): p. 33-53.
71. Tros de Ilarduya, C., Sun, Y., Duzgunes, N., *Gene delivery by lipoplexes and polyplexes.* Eur J Pharm Sci, 2010. **40**(3): p. 159-70.
72. Even-Chen, S., Cohen, R., Barenholz, Y., *Factors affecting DNA binding and stability of association to cationic liposomes.* Chemistry and Physics of Lipids, 2012. **165**(4): p. 414-423.
73. Safinya, C.R., *Structures of lipid-DNA complexes: supramolecular assembly and gene delivery.* Current Opinions in Structural Biology, 2001. **11**: p. 440-448.
74. Nagarajan, R., *Molecular Packing Parameter and Surfactant Self-Assembly: The Neglected Role of the Surfactant Tail.* Langmuir, 2002. **18**: p. 31-38.
75. Hafez, I.M., Maurer, N., Cullis, P. R., *On the mechanism whereby cationic lipids promote intracellular delivery of polynucleic acids.* Gene Ther., 2001. **8**(15): p. 1188-1196.
76. Zuhorn, I.S., Engberts, J. B., Hoekstra, D., *Gene delivery by cationic lipid vectors: overcoming cellular barriers.* Eur Biophys J, 2007. **36**(4-5): p. 349-62.
77. Mochizuki, S., Kanegae, N., Nishina, K., Kamikawa, Y., Koiwai, K., Masunaga, H., Sakurai, K., *The role of the helper lipid dioleoylphosphatidylethanolamine (DOPE) for DNA transfection cooperating with a cationic lipid bearing ethylenediamine.* Biochim Biophys Acta, 2013. **1828**(2): p. 412-8.

78. Ziello, J.E., Huang, Y., Jovin, I. S., *Cellular endocytosis and gene delivery.* Mol Med, 2010. **16**(5-6): p. 222-9.
79. Khalil, I.A., Kogure, K., Akita, H., Harashima, H., *Uptake pathways and subsequent intracellular trafficking in nonviral gene delivery.* Pharmacol Rev, 2006. **58**(1): p. 32-45.
80. Rejman, J., Oberle, V., Zuhorn, I. S., Hoekstra, D., *Size-dependent internalization of particles via the pathways of clathrin and caveolae-mediated endocytosis.* Biochem. J., 2004. **377**: p. 159-169.
81. Parton, R.G., Simons, K., *The multiple faces of caveolae.* Nature Reviews Molecular Cell Biology, 2007. **8**: p. 185-194.
82. Lin, A.J., Slack, N. L., Ahmad, A., George, C. X., Samuel, C. E., Safinya, C. R., *Three Dimensional Imaging of Lipid Gene-Carriers: Membrane Charge Density Controls Transfection Behavior in Lamellar Cationic Liposome-DNA Complexes.* Biophysical Journal, 2003. **84**: p. 3307-3316.
83. Xu, Y., Szoka, F. C., *Mechanism of DNA Release from Cationic Liposome/DNA Complexes Used in Cell Transfection.* Biochemistry, 1996. **35**: p. 5616-5623.
84. Kamiya, H., Fujimura, Y., Matsuoka, I., Harashima, H. , *Visualization of intracellular trafficking of exogenous DNA delivered by cationic liposomes.* Biochemical and Biophysical Research Communications, 2002. **298**: p. 591-597.
85. Wang, H., Wettig, S. D., *Synthesis and aggregation properties of dissymmetric phytanyl-gemini surfactants for use as improved DNA transfection vectors.* Phys Chem Chem Phys, 2011. **13**(2): p. 637-42.
86. Ilies, M.A., Seitz, W. A., Johnson, B. H., Ezell, E. L., Miller, A. L., Thompson, E. B., Balaban, A. T., *Lipophilic pyrylium salts in the synthesis of efficient pyridinium-based cationic lipids, gemini surfactants, and lipophilic oligomers for gene delivery.* J. Med. Chem., 2006. **49**: p. 3872-3887.
87. Yang, P., Singh, J., Wettig, S., Foldvari, M., Verrall, R. E., Badea, I., *Enhanced gene expression in epithelial cells transfected with amino acid-substituted gemini nanoparticles.* Eur J Pharm Biopharm, 2010. **75**(3): p. 311-20.
88. Kumar, M., Jinturkar, K., Yadav, M. R., Misra, A., *Gemini Amphipiles: A Novel Class of Nonviral Gene Delivery Vectors.* Critical Reviews in Therapeutic Drug Carrier Systems, 2010. **27**(3): p. 237-278.
89. Mohammed-Saeid, W., Michel, D., El-Aneed, A., Verrall, R., Low, N. H., Badea, I., *Development of Lyophilized Gemini Surfactant-Based Gene Delivery Systems: Influence of Lyophilization on the Structure, Activity and Stability of Lipoplexes.* J Pharm Pharmaceut Sci, 2012. **15**(4): p. 548-567.
90. Karlsson, L., van Eijk, M. C., Soderman, O., *Compaction of DNA by gemini surfactants: effects of surfactant architecture.* J Colloid Interface Sci, 2002. **252**(2): p. 290-6.
91. Badea, I., Verrall, R., Baca-Estrada, M., Tikoo, S., Rosenberg, A., Kumar, P., Foldvari, M. , *In vivo cutaneous interferon-γ gene delivery using novel dicationic (gemini) surfactant-plasmid complexes.* The Journal of Gene Medicine, 2005. **7**: p. 1200-1214.
92. Wettig, S.D., Verrall, R. E., *Thermodynamic Studies of Aqueous m-s-m Gemini Surfactant Systems.* J Colloid Interface Sci, 2001. **235**(2): p. 310-316.
93. Wettig, S.D., Badea, I., Donkuru, M., Verrall, R. E., Foldvari, M., *Structural and transfection properties of amine-substituted gemini surfactant-based nanoparticles.* J Gene Med, 2007. **9**(8): p. 649-58.
94. Donkuru, M., Wettig, S. D., Verrall, R. E., Badea, I., Foldvari, M., *Designing pH-sensitive gemini nanoparticles for non-viral gene delivery into keratinocytes.* Journal of Materials Chemistry, 2012. **22**(13): p. 6232.

95. Badea, I., *Gemini cationic surfactant-based delivery systems for non-invasive cutaneous gene therapy.* Ph.D. Thesis, University of Saskatchewan, Saskatoon, SK, 2006.
96. Wang, H., Kaur, T., Tavakoli, N., Joseph, J., Wettig, S. , *Transfection and structural properties of phytanyl substituted gemini surfactant-based vectors for gene delivery.* Phys. Chem. Chem. Phys., 2013. **15**: p. 20510-20516.
97. Foldvari, M., Badea, I., Wettig, S., Verrall, R., Bagonluri, M. , *Structural characterization of novel micro- and nano-scale non-viral DNA delivery systems for cutaneous gene therapy.* NSTI-Nanotech, 2005. **1**: p. 128-131.
98. Foldvari, M., Wettig, S., Badea, I., Verrall, R., Bagonluri, M., *Dicationic gemini surfactant gene delivery complexes contain cubic-lamellar mixed polymorphic phase.* NSTI-Nanotech, 2006. **2**: p. 400-403.
99. Akbar, J., Tavakoli, N., Marangoni, D. G., Wettig, S. D., *Mixed aggregate formation in gemini surfactant/1,2-dialkyl-sn-glycero-3-phosphoethanolamine systems.* J Colloid Interface Sci, 2012. **377**(1): p. 237-43.
100. Heinrich, J., Schultz, J., Bosse, M., Ziegelin, G., Lanka, E., Moelling, K., *Linear closed mini DNA generated by the prokaryotic cleaving-joining enzyme TelN is functional in mammalian cells.* J Mol Med, 2002. **80**(10): p. 648-654.
101. Yew, N.S., Zhao, H., Wu, I., Song, A., Tousignant, J. D., Przybylska, M., Cheng, S. H., *Reduced Inflammatory Response to Plasmid DNA Vectors by Elimination and Inhibition of Immunostimulatory CpG Motifs.* Molecular Therapy, 2000. **1**(3): p. 255-262.
102. Takahashi, Y., Nishikawa, M., Takakura, Y., *Development of safe and effective nonviral gene therapy by eliminating CpG motifs from plasmid DNA vector.* Frontiers in Bioscience 2012. **S4**: p. 133-141.
103. Mayrhofer, P., Schleef, M., Jechlinger, W., *Use of minicircle plasmids for gene therapy.* Methods Mol Biol, 2009. **542**: p. 87-104.
104. Yew, N.S., Zhao, H., Przybylska, M., Wu, I., Tousignant, J. D., Scheule, R. K., Cheng, S. H. , *CpG-Depleted Plasmid DNA Vectors with Enhanced Safety and Long-Term Gene Expression in vivo.* Molecular Therapy, 2002. **5**(6): p. 731-738.
105. Wolf, H.K., Johansson, N., Thong, A., Snel, C. J., Mastrobattista, E., Hennink, W. E., Strom G., *Plasmid CpG Depletion Improves Degree and Duration of Tumor Gene Experession Ater Intravenous Administration of Polyplexes.* Pharmaceutical Research, 2008. **25**(7): p. 1654-1662.
106. Hyde, S.C., Pringle, I. A., Abdullah, S., Lawton, A. E., Davies, L. A., Varathalingam, A., Nunez-Alonso, G., Green, A., Bazzani, R. P., Summer-Jones, S. G., Chan, M., Li, H., Yew, N. S., Cheng, S. H., Boyd, A. C., Davies, J. C., Griesenbach, U., Porteous, D. J., Sheppard, D. N., Munkonge, F. M., Alton, E. W. F. W., Gill, D. R., *CpG-free plasmids confer reduced inflammation and sustained pulmonary gene expression.* Nature Biotechnology, 2008. **26**(5): p. 549-551.
107. Gill, D.R., Pringle, I. A., Hyde, S. C., *Progress and Prospects: The design and production of plasmid vectors.* Gene Therapy, 2009. **16**: p. 165-171.
108. Nafissi, N., Slavcev, R., *Construction and characterization of an in-vivo linear covalently closed DNA vector production system.* Microbial Cell Factories, 2012. **11**: p. 154.
109. Darquet, A.M., Cameron, B., Wils, P., Scherman, D., Crouzet, J., *A new DNA vehicle for nonviral gene delivery: supercoiled minicircle.* Gene Therapy, 1997. **4**: p. 1341-1349.
110. Groth, A.C., Calos, M. P., *Phage integrases: biology and applications.* J. Mol. Biol., 2004. **335**: p. 667-678.
111. Dong, Y., Aied, A., Li, J., Wang, Q., Hu, X., Wang, W., *An in vitro approach for production of non-scar minicircle DNA vectors.* J Biotechnol, 2013. **166**(3): p. 84-7.

112. Mayrhofer, P., Blaesen, M., Schleef, M., Jechlinger, W. , *Minicircle-DNA production by site specific recombination and protein-DNA interaction chromatography.* The Journal of Gene Medicine, 2008. **10**: p. 1253-1269.
113. Chen, Z., He, C., Ehrhardt, A., Kay, M. A., *Minicircle DNA vectors devoid of bacterial DNA result in persistent and high-level transgene expression in vivo.* Molecular Therapy, 2003. **8**(3): p. 495-500.
114. Kay, M.A., He, C., Chen, Z., *A robust system for production of minicircle DNA vectors.* Nature Biotechnology, 2010. **28**: p. 1287-1289.
115. Chen, Z.Y., Riu, E., He, C. Y., Xu, H., Kay, M. A., *Silencing of episomal transgene expression in liver by plasmid bacterial backbone DNA is independent of CpG methylation.* Mol Ther, 2008. **16**(3): p. 548-556.
116. Rodriguez, E.G., *Nonviral DNA vectors for immunization and therapy: design and methods for their obtention.* J Mol Med (Berl), 2004. **82**(8): p. 500-9.
117. Schakowski, F., Gorschluter, M., Junghans, C., Schroff, M., Buttgereit, P., Ziske, C., Schottker, B., Konig-Merediz, S. A., Sauerbruch, T., Wittig, B., Schmidt-Wolf, I. G., *A novel minimal-size vector (MIDGE) improves transgene expression in colon carcinoma cells and avoids transfection of undesired DNA.* Mol Ther, 2001. **3**(5): p. 793-800.
118. Schakowski, F., Gorschluter, M., Buttgereit, P., Marten, A., Lilienfeld-Toal, M. V., Junghans, C., Schroff, M., Konig-Merediz, S. A., Ziske, C., Strehl, J., Sauerbruch, T., Wittig, B., Schmidt-Wolf, I. G. H., *Minimal Size MIDGE Vectors Improve Transgene Expression In Vivo.* in vivo, 2007. **21**: p. 17-24.
119. Lopez-Fuertes, L., Perez-Jimenez, E., Vila-Coro, A. J., Sack, F., Moreno, S., Konig, S. A., Junghans, C., Wittig, B., Timon, M., Esteban, M., *DNA vaccination with linear minimalistic (MIDGE) vectors confers protection against Leishmania major infection in mice.* Vaccine, 2002. **21**(3-4): p. 247-257.
120. Wang, H., Chen, Z., Zhang, G., Ou, X., Yang, X., Wong, C. K. C., Giesy, J. P., Du, J., Chen, S., *A novel micro-linear vector for in vitro and in vivo gene delivery and its application for EBV positive tumors.* PLoS One, 2012. **7**(10): p. e47159.
121. Meinhardt, F., Klassen, R. , *Microbial Linear Plasmids* Microbiology Monographs, Springer, 2007: p. 142-160.
122. Ravin, N.V., *Mechanisms of replication and telomere resolution of the linear plasmid prophage N15.* FEMS Microbiology Letters, 2003. **221**(1): p. 1-6.
123. Ravin, N.V., *N15: the linear phage-plasmid.* Plasmid, 2011. **65**(2): p. 102-9.
124. Deneke, J., Ziegelin, G., Lurz, R., Lanka, E., *Phage N15 Telomere Resolution.* The Journal of Biological Chemistry, 2002. **277**(12): p. 10410-10419.
125. Hertwig, S., Klein, I., Lurz, R., Lanka, E., Appel, B., *PY54, a linear plasmid prophage of Yersinia enterocolitica with covalently closed ends.* Molecular Microbiology, 2003. **48**(4): p. 989-1003.
126. Kreiss, P., Cameron, B., Rangara, R., Mailhe, P., Aguerre-Charriol, O., Airiau, M., Scherman, D., Crouzet, J., Pitard, B., *Plasmid DNA size does not affect the physicochemical properties of lipoplexes but modulates gene transfer efficiency*. Nucleic Acids Research, 1999. **27**(19): p. 3792-3798.
127. Yin, W., Xiang, P., Li, Q., *Investigations of the effect of DNA size in transient transfection assay using dual luciferase system.* Analytical Biochemistry, 2005. **346**: p. 289-294.
128. Hsu, C.Y., Uludag, H., *Effects of size and topology of DNA molecules on intracellular delivery with non-viral gene carriers.* BMC Biotechnol, 2008. **8**: p. 23.

129. Kamiya, H., Yamazaki, J., Harashima, H., *Size and topology of exogenous DNA as determinant factors of transgene transcription in mammalian cells.* Gene Ther, 2002. **9**(22): p. 1500-7.
130. Young, J.L., Benoit, J.N., Dean, D.A., *Effect of a DNA nuclear targeting sequence on gene transfer andexpression of plasmids in the intact vasculature.* Gene Therapy, 2003. **10**: p. 1465-1470.
131. Mesika, A., Grigoreva, I., Zohar, M., Reich, Z., *A Regulated, NFkappaB-assisted Import of Plasmid DNA into Mammalian Cell Nuclei.* Mol Ther, 2001. **3**(5 Pt 1): p. 653-7.
132. Breuzard, G., Tertil, M., Goncalves, C., Cheradame, H., Geguan, P., Pichon, C., Midoux, P., *Nuclear delivery of NFkappaB-assisted DNA/polymer complexes: plasmid DNA quantitation by confocal laser scanning microscopy and evidence of nuclear polyplexes by FRET imaging.* Nucleic Acids Res, 2008. **36**(12): p. e71.
133. Dean, D.A., Dean, B. S., Muller, S., Smith, L. C., *Sequence Requirements for Plasmid Nuclear Import.* Experimental Cell Research, 1999. **253**: p. 713-722.
134. Valdez-Cruz, N.A., et al., *Production of recombinant proteins in E. coli by the heat inducible expression system based on the phage lambda pL and/or pR promoters.* Microb Cell Fact, 2010. **9**: p. 18.
135. Peleg, Y. and T. Unger, *Resolving bottlenecks for recombinant protein expression in E. coli.* Methods Mol Biol, 2012. **800**: p. 173-86.
136. Berlec, A. and B. Strukelj, *Current state and recent advances in biopharmaceutical production in Escherichia coli, yeasts and mammalian cells.* J Ind Microbiol Biotechnol, 2013. **40**(3-4): p. 257-74.
137. Baneyx, F., *Recombinant protein expression in Escherichia coli.* Current Opinions in Biotechnology, 1999. **10**: p. 411-421.
138. Baneyx, F. and M. Mujacic, *Recombinant protein folding and misfolding in Escherichia coli.* Nat Biotechnol, 2004. **22**(11): p. 1399-408.
139. Sevastsyanovich, Y.R., S.N. Alfasi, and J.A. Cole, *Sense and nonsense from a systems biology approach to microbial recombinant protein production.* Biotechnol Appl Biochem, 2010. **55**(1): p. 9-28.
140. Hoffman, F., Rinas, U., *Plasmid amplificaiton in Escherichia coli after temperature upshift is impaired by induction of recombinant protein synthesis.* Biotechnology Letters, 2001. **23**: p. 1819-1825.
141. Chou, C.P., *Engineering cell physiology to enhance recombinant protein production in Escherichia coli.* Appl Micobiol Biotechnol, 2007. **76**: p. 521-532.
142. Wegrzyn, G., Wegrzyn, A., *Stress responses and replication of plasmids in bacterial cells.* Microbial Cell Factories, 2002. **1**(2).
143. Hoffman, F.R., U., *Kinetics of Heat-Shock Response and Inclusion Body Formation During Temperature-Induced Production of Basic Fibroblast Growth Factor in High-Cell-Density Cultures of Recombinant Escherichia coli.* Biotechnol. Prog., 2000. **16**(6): p. 1000-1007.
144. Sayadi, S., et al., *Effect of temperature on the stability of plasmid pTG201 and productivity of xylE gene product in recombinant Escherichia coli: development of a two-stage chemostat with free and immobilized cells.* J Gen Microbiol, 1987. **133**(7): p. 1901-8.
145. Dong, H., Nilsson, L., Kurland, C. G., *Gratuitous overexpression of genes in Escherichia coli leads to grwoth inhibition and ribosome destruction.* J. Bacteriol., 1995. **177**(6): p. 1497-1504.
146. Baneyx, F., *Recombinant protein expression in Escherichia coli.* . Current Opinions in Biotechnology, 1999. **10**: p. 411-421.

147. Gill, R.T., J.J. Valdes, and W.E. Bentley, *A comparative study of global stress gene regulation in response to overexpression of recombinant proteins in Escherichia coli.* Metab Eng, 2000. **2**(3): p. 178-89.
148. Meyer, A.S. and T.A. Baker, *Proteolysis in the Escherichia coli heat shock response: a player at many levels.* Curr Opin Microbiol, 2011. **14**(2): p. 194-9.
149. Schrodel, A. and A. de Marco, *Characterization of the aggregates formed during recombinant protein expression in bacteria.* BMC Biochem, 2005. **6**: p. 10.
150. Hengge-Aronis, R., *Recent Insights into the General Stress Response Regulatory Network in Escherichia coli.* J. Mol. Microbiol. Biotechnol., 2002. **4**(3): p. 341-346.
151. Micevski, D. and D.A. Dougan, *Proteolytic Regulation of Stress Response Pathways in Escherichia coli.* Subcell Biochem, 2013. **66**: p. 105-28.
152. Licht, S.L., I., *Resolving Individual Steps in the Operation of ATP-Dependent Proteolytic Molecular Machines: From Conformational Changes to Substrate Translocation and Processivity.* Biochemistry, 2008. **47**(12): p. 3595-3605.
153. Baba, T., Ara, T., Hasegawa, M., Takai, Y., Okumura, Y., Baba, M., Datsenko, K. A., Tomita, M., Wanner, B. L., Mori, H., *Construction of Escherichia coli K-12 in-frame, single-gene knockout mutants: the Keio collection.* Mol Syst Biol, 2006. **2**: p. 2006 0008.
154. Sambrook, J., Russell, D. W., *Molecular Cloning: A Laboratory Manual.* 2001.
155. Slavcev, R.A., Funnell, B. E., *Identification and characterization of a novel allele of Escherichia coli dnaB helicase that compromises the stability of plasmid P1*. J Bacteriol, 2005. **187**(4): p. 1227-37.
156. Biswas, E.E., Chen, P., Biswas, S. B., *Modulation of enzymatic activities of Escherichia coli DnaB helicase by single-stranded DNA-binding proteins.* Nucl. Acids Res., 2002. **30**(13): p. 2809-2816.
157. Konieczny, I., *Strategies for helicase recruitment and loading in bacteria*. EMBO reports, 2003. **4**(1): p. 37-41.
158. Saluja, D., Godson, G. N., *Biochemical Characterization of E coli temperature sensitive dnaB mutants dnaB8 dnaB252 dnaB70 dnaB43 dnaB454*. Journal of Bacteriology, 1995. **177**(4): p. 1104-1111.
159. Hoffman, F., Rinas, U., *Stress induced by recombinant protein production in Escherichia coli.* Adv Biochem Eng/Biotechnol, 2004. **89**: p. 73-92.
160. Caspeta, L., Flores, N., Perez, N. O., Bolivar, F. Ramirez, O. T. , *The effect of heating rate on Escherichia coli metabolism, physiological stress, transcriptional response, and production of temperature-induced recombinant proteins: a scale-down study*. Biotechnology and Bioengineering, 2009. **102**(2): p. 468-482.
161. Caspeta, L.L., A. R., Perez, N. O., Flores, N., Bolivar, F., Ramirez, O. T. , *Enhancing thermo-induced recombinant protein production in Escherichia coli by temperature oscillations and post-induction nutrient feeding strategies.* Journal of Biotechnology, 2013. **167**: p. 47-55.
162. Bissonnette, S.A., et al., *The IbpA and IbpB small heat-shock proteins are substrates of the AAA+ Lon protease.* Mol Microbiol, 2010. **75**(6): p. 1539-49.
163. Akiyama, Y., *Self-processing of FtsH and its implication for the cleavage specificity of this protease.* Biochemistry, 1999. **38**(36): p. 11693-9.
164. Kihara, A., Y. Akiyama, and K. Ito, *Host regulation of lysogenic decision in bacteriophage lambda: transmembrane modulation of FtsH (HflB), the cII degrading protease, by HflKC (HflA).* Proc Natl Acad Sci U S A, 1997. **94**(11): p. 5544-9.

165. Kihara, A.A., Y.; Ito, K., *A protease complex in the Escherichia coli plasma membrane: HflKC (HflA) forms a complex with FtsH (HflB), regulating its proteolytic activity against SecY.* The EMBO Journal, 1996. **15**(22): p. 6122-6131.
166. Saikawa, N., Y. Akiyama, and K. Ito, *FtsH exists as an exceptionally large complex containing HflKC in the plasma membrane of Escherichia coli.* J Struct Biol, 2004. **146**(1-2): p. 123-9.
167. Schweder, T., Lin, H. Y., Jurgen, B., Breitenstein, A., Riemschneider, S., Khalameyzer, V., Gupta, A., Buttner, K., Neubauer, P., *Role of the general stress response during strong overexpression of a heterologous gene in Escherichia coli.* Appl. Microbiol. Biotechnol., 2002. **58**: p. 330-337.
168. Shields, M.J., J.J. Fischer, and H.J. Wieden, *Toward understanding the function of the universally conserved GTPase HflX from Escherichia coli: a kinetic approach.* Biochemistry, 2009. **48**(45): p. 10793-802.
169. Dutta, D., et al., *Properties of HflX, an enigmatic protein from Escherichia coli.* J Bacteriol, 2009. **191**(7): p. 2307-14.
170. Jain, N., et al., *E. coli HflX interacts with 50S ribosomal subunits in presence of nucleotides.* Biochem Biophys Res Commun, 2009. **379**(2): p. 201-5.
171. Fischer, J.J., et al., *The ribosome modulates the structural dynamics of the conserved GTPase HflX and triggers tight nucleotide binding.* Biochimie, 2012. **94**(8): p. 1647-59.
172. Harcum, S.W., Haddadin, F. T., *Global transcriptome response of recombinant Escherichia coli to heat-shock and dual heat-shock recombinant protein induction.* J. Ind. Microbiol. Biotechnol., 2006. **33**: p. 801-814.
173. Breidenstein, E.B., M. Bains, and R.E. Hancock, *Involvement of the lon protease in the SOS response triggered by ciprofloxacin in Pseudomonas aeruginosa PAO1.* Antimicrob Agents Chemother, 2012. **56**(6): p. 2879-87.
174. Yamaguchi, Y., et al., *Effects of disruption of heat shock genes on susceptibility of Escherichia coli to fluoroquinolones.* BMC Microbiol, 2003. **3**: p. 16.
175. Belle, J.J., Casey, A., Courcelle, C. T., Courcelle, J., *Inactivation of DnaB helicase leads to the collapse and degradation of replication fork: a comparison to UV-induced arrest.* J. Bacteriol., 2007. **189**(15): p. 5452-5462.
176. Guerrero-German, P., Prazeres, D. M., Guzman, R., Montesinos-Cisneros, R. M., Tejeda-Mansir, A., *Purification of plasmid DNA using tangential flow filtration and tandem anion-exchange membrane chromatography.* Bioprocess Biosyst Eng, 2009. **32**(5): p. 615-23.
177. Zhong, L., Scharer, J., Moo-Young, M., Fenner, D., Crossley, L., Honeyman, C. H., Suen, S. Y., Chou, C. P., *Potential application of hydrogel-based strong anion-exchange membrane for plasmid DNA purification.* J Chromatogr B Analyt Technol Biomed Life Sci, 2011. **879**(9-10): p. 564-72.
178. Guerrero-German, P., Montesinos-Cisneros, R. M., Prazeres, D. M. F., Tejeda-Mansir, A., *Purification of plasmid DNA from Escherichia coli ferments using anion exchange membrane and hydrophobic chromatography.* Biotechnol Appl Biochem, 2011. **58**(1): p. 68-74.
179. Urthaler, J., Buchinger, W., Necina, R., *Improved downstream process for the production of pDNA for gene therapy.* Acta Biochimica Polonica, 2005. **52**(3): p. 703-711.
180. Sun, B., Yu, X., Yin, Y., Liu, X., Wu, Y., Chen, Y., Zhang, X., Jiang, C., Kong, W., *Large-scale purification of pharmaceutical-grade plasmid DNA using tangential flow filtration and multi-step chromatography.* J Biosci Bioeng, 2013.
181. Prather, K.J., Sagar, S., Murphy, J., Chartrain, M., *Industrial scale production of plasmid DNA for vaccine and gene therapy: plasmid design, production, and purification.* Enzyme and Microbial Technology, 2003. **33**(7): p. 865-883.

182. Diogo, M.M., Queiroz, J. A., Prazeres, D. M. F., *Chromatography of plasmid DNA.* Journal of Chromatography A, 2005. **1069**(1): p. 3-22.
183. Eon-Duval, A. and G. Burke, *Purification of pharmaceutical-grade plasmid DNA by anion-exchange chromatography in an RNase-free process.* J Chromatogr B Analyt Technol Biomed Life Sci, 2004. **804**(2): p. 327-35.
184. Haber, C., Skupsky, J., Lee, A., Lander, R., *Membrane chromatography of DNA: conformation-induced capacity and selectivity.* Biotechnol Bioeng, 2004. **88**(1): p. 26-34.
185. Mahut, M., Gargano, A., Schuchnigg, H., Lindner, W., Lammerhofer, M., *Chemoaffinity material for plasmid DNA analysis by high-performance liquid chromatography with condition-dependent switching between isoform and topoisomer selectivity.* Anal Chem, 2013. **85**(5): p. 2913-20.
186. Prazeres, D.M.F., Schluep, T., Cooney, C. , *Preparative purification of supercoiled plasmid DNA using anion-exchange chromatography.* Journal of Chromatgraphy A, 1998. **806**: p. 31-45.
187. Smith, C.R., DePrince, R. B., Dackor, J., Weigl, D., Griffith, J., Persmark, M., *Separation of topological forms of plasmid DNA by anion-exchange HPLC: shifts in elution order of linear DNA.* J Chromatogr B Analyt Technol Biomed Life Sci, 2007. **854**(1-2): p. 121-7.
188. Hirabayashi, J., Kasai, K. I., *Effects of DNA topology, temperature and solvent viscosity on DNA retardation in slalom chromatography.* J Chromatogr A, 2000. **893**(1): p. 115-22.
189. Zhang, S., Krivosheyeva, A., Nochumson, S. , *Large scale capture and partial purification of plasmid DNA using anion-exchange membrane capsules.* Biotechnol. Appl. Biochem, 2003. **37**: p. 245-249.
190. Sousa, F., Prazeres, D. M. F., Queiroz, J. A., *Affinity chromatography approaches to overcome the challenges of purifying plasmid DNA.* Trends in Biotechnology, 2008. **26**(9): p. 518-525.
191. Ghanem, A., Healey, R., Adly, F. G., *Current trends in separation of plasmid DNA vaccines: A review.* Analytica Chimica Acta, 2013. **760**: p. 1-15.
192. Wils, P., Escriou, V., Warnery, A., Lacroix, F., Lagneaux, D., Olivier, M., Crouzet, J., Mayaux, J-F., Scherman, D., *Efficient purification of plasmid DNA for gene transfer using triple-helix affinity chromatrography.* Gene Therapy, 1997. **4**: p. 323-330.
193. Sousa, F., Cruz, C., Queiroz, J. A.,, *Amino acids-nulceotides biomolecular recognition: from biological occurrence to affinity chromatography.* J. Mol. Recognit., 2010. **23**: p. 505-518.
194. Bo, H., Wang, J., Chen, Q., Shen, H., Wu, F., Shao, H., Huang, S., *Using a single hydrophobic-interaction chromatography to purify pharmaceutical-grade supercoiled plasmid DNA from other isoforms.* Pharm Biol, 2013. **51**(1): p. 42-8.
195. Bombelli, C., Giansanti, L., Luciani, P., Mancini, G., *Gemini Surfactant Based Carriers in Gene and Drug Delivery.* Current Medicinal Chemistry, 2009. **16**: p. 171-183.
196. Badea, I., Virtanen, C., Verrall, R. E., Rosenberg, A., Foldvari, M., *Effect of topical interferon-γ gene therapy using gemini nanoparticles on pathophysiological markers of cutaneous scleroderma in Tsk/+ mice.* Gene Therapy, 2012. **19**: p. 978-987.
197. Badea, I., Wettig, S., Verrall, R., Foldvari, M., *Topical non-invasive gene delivery using gemini nanoparticles in interferon-γ-deficient mice.* Eur J Pharm Biopharm, 2007. **65**(3): p. 414-22.
198. Zana, R., *Gemini (Dimeric) surfactants in water: solubility, cmc, thermodynamics of micellization, and interaction with water soluble polymers*, in *Gemini surfactants: synthesis, interfacial and solution-phase behavior, and applications*, R. Zana, Xia, J., Editor. 2003, Marcel Dekker, Inc: New York. p. 108-138.

199. Wang, C., Li, X., Wettig, S. D., Badea, I., Foldvari, M., Verrall, R. E., *Investigation of complexes formed by interaction of cationic gemini surfactants with deoxyribonucleic acid.* Phys Chem Chem Phys, 2007. **9**(13): p. 1616-28.
200. Wettig, S.D., Deubry, R., Akbar, J., Kaur, T., Wang, H., Sheinin, T., Joseph, J. W., Slavcev, R. A., *Thermodynamic investigation of the binding of dissymmetric pyrenyl-gemini surfactants to DNA.* Phys Chem Chem Phys, 2010. **12**(18): p. 4821-6.
201. Munoz-Ubeda, M., Misra, S. K., Barran-Berdon, A. L., Aicart-Ramos, C., Sierra, M. B., Biswas, J., Kondaiah, P., Junquera, E., Bhattacharya, S., Aicart, E., *Why is less cationic lipid required to prepare lipoplexes from plasmid DNA than linear DNA in gene therapy?* J Am Chem Soc, 2011. **133**(45): p. 18014-7.
202. Munoz-Ubeda, M., Misra, S. K., Barran-Berdon, A. L., Datta, S., Aicart-Ramos, C., Castro-Hartmann, P., Kondaiah, P., Junquera, E., Bhattacharya, S., Aicart, E., *How does the spacer length of cationic gemini lipids influence the lipoplex formation with plasmid DNA? Physicochemical and biochemical characterizations and their relevance in gene therapy.* Biomacromolecules, 2012. **13**(12): p. 3926-37.
203. Girard, M.P., Osmanov, S., Assossou, O. M., Kieny, M. P., *Human immunodeficiency virus (HIV) immunopathogenesis and vaccine development: a review.* Vaccine, 2011. **29**(37): p. 6191-218.
204. Garcia, F., Leon, A., Gatell, J. M., Plana, M., Gallart, T., *Therapeutic vaccines against HIV infection.* Hum Vaccin Immunother, 2012. **8**(5): p. 569-81.
205. Lori, F., *DermaVir: a plasmid DNA-based nanomedicine therapeutic vaccine for the treatment of HIV/AIDS.* Expert Rev Vaccines, 2011. **10**(10): p. 1371-1384.
206. Koff, W.C., Russell, N. D., Walport, M., Feinberg, M. B., Shiver, J. W., Karim, S. A., Walker, B. D, McGlynn, M. G., Nweneka, C. V., Nabel, G. J., *Accelerating the development of a safe and effective HIV vaccine: HIV vaccine case study for the Decade of Vaccines.* Vaccine, 2013. **31 Suppl 2**: p. B204-8.
207. Liu, K., Nussenzweig, M. C., *Origin and development of dendritic cells.* Immunological Reviews, 2010. **234**: p. 45-54.
208. Joffre, O.P., Segura, E., Savina, A., Amigorena, S., *Cross-presentation by dendritic cells.* Nat Rev Immunol, 2012. **12**(8): p. 557-69.
209. Dresch, C., Leverrier, Y., Marvel, J., Shortman, K., *Development of antigen cross-presentation capacity in dendritic cells.* Trends Immunol, 2012. **33**(8): p. 381-8.
210. Ahmed, Z., Czubala, M., Blanchet, F., Piguet, V., *HIV impairment of immune responses in dendritic cells.* Advances in Experimental Medicine and Biology, 2013. **762**: p. 201-238.
211. Kooyk, Y.V., Geijtenbeek, T. B. H., *C-type lectins on dendritic cells: antigen receptors and modulators of immune responses*. Handbook of Dendritic Cells: Biology, Diseases, and Therapies ed. M.B. Lutz, Romani, N., Steinkasserer, A. 2008, Weinheim, Germany: Wiley. 129-140.
212. Cunningham, A.L., Wilkinson, J., Turville, S., Pope, M., *Binding and uptake of HIV by dendritic cells and transfer to T lymphocytes: implications for pathogenesis.* The Biology of Dendritic Cells and HIV Infection, 2007: p. 381-404.
213. Mellman, I., Steinman, R. M., *Dendritic cells: specialized and regulated antigen processing machines.* Cell 2001. **106**: p. 255-258.
214. Vachot, L., Turville, S. G., Trapp, S., Peretti, S., Morrow, G., Frank, I., Pope, M., *Sleeping with the enemy: the insidious relationship between dendritic cells and immunodeficiency viruses*, in *Handbook of Dendritic Cells: Biology, Diseases, and Therapies*, M.B. lutz, Romani, N., Steinkasserer, A., Editor. 2008, Wiley: Weinheim, Germany.

215. Altfeld, M., Fadda, L., Frleta, D., Bhardwaj, N., *DCs and NK cells: critical effectors in the immune response to HIV-1*. Nat Rev Immunol, 2011. **11**(3): p. 176-86.
216. Del Corno, M., Conti, L., Gauzzi, M. C., Fantuzzi, L., Gessani, S., *HIV exploitation of DC biology to subvert the host immune response.* The Biology of Dendritic Cells and HIV Infection, 2007: p. 447-484.
217. van Gils, M.J., Sanders, R. W., *Broadly neutralizing antibodies against HIV-1: templates for a vaccine.* Virology, 2013. **435**(1): p. 46-56.
218. Kwong, P.D., Mascola, J. R., Nabel, G. J., *The changing face of HIV vaccine research.* Journal of the International AIDS Society, 2012. **15**: p. 17407.
219. Gandhi, R.T., Atfeld, M., *The Quest for an HIV-1 therapeutic vaccine.* The Journal of Infectious Diseases, 2005. **192**(4): p. 556-559.
220. Loes, S.K., Hoen, B., Smith, D. E., Autran, B., Lampe, F. C., Philips, A. N., Goh, L., Andersson, J., Tsoukas, C., Sonnerborg, A., Tambussi, G., Girard, P., Bloch, M., Battegay, M., Carter, N., Habib, R. E., Theofan, G., Cooper, D. A., Perrin, L., *Impact of therapeutic immunization on HIV-1 viremia after discontinuation of antiretroviral therapy initiated during acute infection.* The Journal of Infectious Diseases, 2005. **192**(4): p. 607-617.
221. Ramirez, L.A., Arango, T., Boyer, J., *Therapeutic and prophylactic DNA vaccines for HIV-1*. Expert Opin Biol Ther, 2013. **13**(4): p. 563-573.
222. Rerks-Ngarm, S., Paris, R. M., Chunsutthiwat, S., Premsri, N., Namwat, C., Bowonwatanuwong, C., Li, S. S., Kaewkungkal, J., Trichavaroj, R., Churikanont, N., de Souza, M. S., Andrews, C., Francis, D., Adams, E., Flores, J., Gurunathan, S., Tartaglia, J., O'Connell, R.J., Eamsila, C., Nitayaphan, S., Ngauy, V., Thongcharoen, P., Kunasol, P., Michael, N. L., Robb, M. L., Gilbert, P. B., Kim, J. H. , *Evaluation of the Virologic, Immunologic and Clinical Course of Volunteers Who Acquired HIV-1 Infection in a Phase III Vaccine Trial of ALVAC-HIV and AIDSVAX B/E.* J. Infect. Dis., 2013. **207**(8): p. 1195-1205.
223. Young, K.R., McBurney, S. P., Karkhanis, L. U., Ross, T. M., *Virus-like particles: designing an effective AIDS vaccine.* Methods, 2006. **40**(1): p. 98-117.
224. Buonaguro, L., Tagliamonte, M., Visciano, M. L., Tornesello, M. L., Buonaguro, F. M., *Developments in virus-like particle-based vaccines for HIV.* Expert Rev. Vaccines, 2013. **12**(2): p. 119-127.
225. Buonaguro, L., Tornesello, M. L., Buonaguro, F. M., *Virus-Like particles as particulate vaccines.* Current HIV Research, 2010. **8**: p. 299-309.
226. Chang, M.O., Suzuki, T., Suzuki, H., Takaku, H. , *HIV-1 Gag-virus-like particles induce natural killer cell immune responses via activation and maturation of dendritic cells.* J Innate Immun, 2012. **4**: p. 187-200.
227. Kang, C.Y., Luo, L., Wainberg, M. A., Li, Y., *Development of HIV/AIDS Vaccine using chimeric gag-env virus-like particles.* Biol. Chem. , 1999. **380**: p. 353-364.
228. Kang, C.Y., Michalski, C., *HIV combination vaccine and prime boost*, 2011, The University of Western Ontario: US.
229. Luo, L., Li, Y., Chang, J., Cho, S., Kim, T., Choi, M., Cheong, H., Kim, H., Ahn, H., Min, M., Chun, B., Jung, S., Woo, S., Park, S., Kang, C. Y., *Induction of V3-Specific cytotoxic T lymphocyte responses by HIV gag particles carrying multiple immunodominant V3 epitopes of gp120.* Virology, 1998. **240**: p. 316-325.
230. Schaft, N., Dorrie, J., Nettelbeck, D. M., *Nucleic acid transfer*. Handbook of Dendritic Cells: Biology, Diseases, and Therapies, ed. M.B. Lutz, Romani, N., Steinkasserer, A. 2008, Weinheim, Germany: Wiley.

231. Smith, R.A., Giorgio, T. D., *Quantitation and kinetics of CD51 surface receptor expression: implications for targeted deliver.* Annals of Biomedical Engineering, 2004. **32**(5): p. 635-644.
232. Rubartelli, A., Poggi, A., Zocchi, M. R., *The selective engulfment of apoptotic bodies by dendritic cells is mediated by the αvβ3 integrin and requires intracellular and extracellular calcium.* Eur. J. Immunol., 1997. **27**: p. 1893-1900.
233. Harui, A., Roth, M. D., Vira, D., Sanghvi, M., Mizuguchi, H., Basak, S. K., *Adenoviral-encoded antigens are presented efficiently by a subset of dendritic cells expressing high levels of αvβ3 integrins.* Journal of Leukocyte Biology, 2006. **79**(6): p. 1271-1278.
234. Maguire, C.A., Sapinoro, R., Girgis, N., Roderiguez-Colon, S. M., Ramirez, S. H., Williams, J., Dewhurst, S., *Recombinant adenovirus type 5 vectors that target DC-SIGN, ChemR23, and αvβ3 integrin efficiently transduce human dendritic cells and enhance presentation of vectored antigens.* Vaccine, 2006. **24**: p. 671-682.
235. Zocchi, M.R., Poggi, A., Rubartelli, A., *The RGD-containing domain of exogenous HIV-1 Tat inhibits the engulfment of apoptotic bodies by dendritic cells.* AIDS, 1997. **11**: p. 1227-1235.
236. Lankes, H.A., Zanghi, C. N., Santos, K., Capella, C., Duke, C. M. P., Dewhurst, S., *In vivo gene delivery and expression by bacteriophage lambda vectors.* Journal of Applied Microbiology, 2007. **102**: p. 1337-1349.
237. Esendagli, G., Canpinar, H., Lale Dogan, A., Akkaya, M., Kansu, E., Guc, D., *Transfection of myeloid leukaemia cell lines is distinctively regulated by fibronectin substratum.* Cytotechnology, 2009. **61**(1-2): p. 45-53.
238. Sakaguchi, N., Kojima, C., Harada, A., Koiwai, K., Emi, N., Kono, K., *Effect of transferrin as a ligand of pH-sensitive fusogenic liposome-lipoplex hybrid complexes.* Bioconjugate Chem., 2008. **19**: p. 1588-1595.
239. Amini, R., Jalilian, F. A., Abdullah, S., Veerakumarasivam, A., Hosseinkhani, H., Abdulamir, A. S., Domb, A. J., Ickowicz, D., Rosli, R., *Dynamics of PEGylated-dextran-spermine nanoparticles for gene delivery to leukemic cells.* Appl Biochem Biotechnol, 2013. **170**(4): p. 841-53.
240. Shrimpton, R.E., Butler, M., Morel, A. S., Eren, E., Hue, S. S., Ritter, M. A., *CD205 (DEC-205): a recognition receptor for apoptotic and necrotic self.* Mol Immunol, 2009. **46**(6).
241. Tan, P.H., Beutelspacher, S. C., Wang, Y. H., McClure, M. O., Ritter, M. A., Lombardi, G., George, A. J., *Immunolipoplexes: an efficient, nonviral alternative for transfection of human dendritic cells with potential for clinical vaccination.* Mol Ther, 2005. **11**(5): p. 790-800.
242. Somogyi, E., Xu, J., Gudics, A., Toth, J., Kovacs, A. L., Lori, F., Lisziewicz, J., *A plasmid DNA immunogen expressing fifteen protein antigens and complex virus-like particles (VLP+) mimicking naturally occurring HIV.* Vaccine, 2011. **29**(4): p. 744-53.